Diabetes Phenotypes in Transgenic Pancreatic Cancer Mouse Models

2015

Toya Albury-Warren
University of Central Florida

DIABETES PHENOTYPES IN TRANSGENIC PANCREATIC CANCER MOUSE MODELS

by

TOYA M. ALBURY-WARREN
B.S. Oakwood College, 2005
MPH Florida International University, 2012

A dissertation submitted in partial fulfillment of the requirements
for the degree of Doctor of Philosophy
in the Department of Biomedical Sciences
in the College of Medicine
at the University of Central Florida
Orlando, Florida

Fall Term
2015

Major Professor: Deborah A. Altomare

ABSTRACT

Protein Kinase B/AKT, a serine/threonine kinase with three isoforms (AKT1-3), is downstream of phosphatidylinositol 3-kinase (PI3K), and signals through the phosphorylation and subsequent activation or inhibition of downstream substrates, such as mammalian target of rapamycin complex 1 (mTORC1) or glycogen synthase kinase 3 beta (GSK-3β), respectively. The AKT1 isoform is predominantly recognized for regulation of cell survival, growth, and proliferation, due to its constitutive activation in pancreatic cancers (e.g., islet cell carcinoma and pancreatic adenocarcinoma). The progression of pancreatic ductal adenocarcinoma (PDAC), the most lethal common cancer, is initiated by activation mutations of the KRas oncogene. This leads to additional molecular changes, such as activation of the AKT1 oncogene, which drives PDAC progression and tumor formation. By mating transgenic mice with activation of KRas (Pdx-Cre;LSL-KRasG12D) and mice with activation of AKT1 (Pdx- Tta;TetO-MyrAKT1) we were able to produce mice with two activated oncogenes ($AKT1^{Myr}$/KRasG12D) for comparative studies. Kaplan-Meier survival curves, histology, and genomic/proteomic analysis were used to characterize the incidence and frequency of histological (e.g. presence of mucin-4 in pancreatic intraepithelial neoplasms) and genetic (e.g. loss of tumor suppressors *p16Ink4a* and *p19Arf*) alterations known to commonly occur in human pancreatic cancer, as well as delineate the role of AKT1 in accelerating pancreatic tumor progression and metastasis. We determined that $AKT1^{Myr}$/KRasG12D mice, unlike other PDAC mouse models, accurately mimic the human PDAC progression molecularly, structurally, and temporally.

Interestingly, the $AKT1^{Myr}$ and $AKT1^{Myr}$/KRasG12D models both exhibit a pre-tumor, diabetic phenotype. While, AKT1 hyperactivation in various cancers has been thoroughly studied,

its role in glucose metabolism has been noted, but comparatively overlooked. As early as the 1900s a relationship between diabetes and pancreatic cancer has been proposed. With 80% of PDAC patients suffering from hyperglycemia or diabetes prior to diagnosis, one prevailing theory is that new onset diabetes is an early marker for pancreatic cancer. This is also supported by experimental and clinical studies, such as the resolution of diabetes with tumor removal and the induction of hyperglycemia with the implantation of cancer cell lines. To better understand the role of AKT1 and its hyperactivation in glucose metabolism, $AKT1^{Myr}$ mice were characterized via metabolic (e.g. glucose/insulin tolerance test) and histological (e.g. immunohistochemistry) studies. Beginning at weaning, 3 weeks of age, the glucose intolerant $AKT1^{Myr}$ mice exhibited non-fasted hyperglycemia, which progressed to fasted hyperglycemia by 5 months of age. The glucose intolerance was attributed to a fasted hyperglucagonemia, and hepatic insulin resistance detectable by reduced phosphorylation of the insulin receptor following insulin injection into the inferior vena cava. Additionally, $AKT1^{Myr}$/KRasG12D mice currently being studied, appear to display a more severe diabetic phenotype, with fasted hyperglycemia noticeable at an earlier age, fasted hyperglucagonemia, polyuria, muscle wasting, and bloating. Treatment of both models with doxycycline diet, to turn-off the transgene, caused attenuation of the non-fasted and fasted hyperglycemia, thus affirming AKT1 hyperactivation as the trigger. These newly revealed roles of AKT1, along with future studies of these mouse models, will better delineate the molecular mechanisms responsible for the individual and joint roles of AKT1 and KRas in pancreatic cancer oncogenesis, the initiation of cancer associated diabetes, and the association of these two diseases.

.

I dedicate this dissertation to the following loved ones:

My parents, Darryl and Carol Burr, who have always loved and supported me. I could not have done this without you. I love you.

My husband, Anthony Warren, who has been my sounding board and cheerleader during the hard times. I love you.

My children (Anthony, Harper, and Logan) who have made this process challenging, but have always provided the unlimited hugs and kisses I needed to stay the course. I love you.

My Heavenly Father who wipes my tears, eases my fears, and makes me strong. He is truly able. I love you.

ACKNOWLEDGMENTS

The successful completion of this work has involved many individuals and institutions. First, I wish to acknowledge my advisor, Deborah A. Altomare, Ph.D. I have greatly benefited from working in her laboratory. Dr. Altomare created an environment where I was encouraged to independently learn new techniques, perfect those techniques through trial and error, and then train others. The time spent in her laboratory has increased my competence and confidence, ultimately preparing me for a successful career in research/teaching. I would also like to thank the members of my graduate committee (Annette Khaled, Ph.D., Jihe Zhao, Ph.D., and Michal Masternak, Ph.D.) for investing their time, advice, and support into my graduate training. I would like to give a special "thank you" to Dr. Masternak for teaching me the basics of metabolic testing, sharing supplies and equipment, and providing his expertise in a field that was new to our lab.

I would like to thank the institutions which contributed financially toward the completion of this work: National Cancer Institute (grant R21 CA129302 and R01 CA77429), The Florida Ladies Auxiliary to the Veterans of Foreign Wars, the University of Central Florida (start-up funds), the American Cancer Society-Fox Chase Cancer Center (institutional funds), the Learning Institute for Elders at UCF (Gerontology Research Grant), and the Florida Education Fund (McKnight doctoral fellowship).

Lastly, I wish to acknowledge the following journals for publishing our research and allowing me to include the articles within this dissertation.

Chapter 2 (no changes were made except for figure numbering) – Albury TM, Pandey V, Gitto SB, Dominguez L, Spinel LP, Talarchek J, Klein-Szanto AJ, Testa JR, & Altomare DA 2015 Constitutive activation of Akt1 cooperates with KrasG12D to accelerate in vivo pancreatic tumor

onset and progression. *Neoplasia***17** 175-183. doi: 10.1016/j.neo.2014.12.006. Under a Creative Commons Attribution-NonCommercial-NoDerivatives License (CC BY-NC-ND 4.0).

Chapter 3 (no changes were made except for figure numbering) – Albury TM, Pandey V, Spinel LP, Masternak MM & Altomare DA 2015 Prediabetes Linked to Excess Glucagon in Transgenic Mice with Pancreatic Active AKT1. Journal of Endocrinology (accepted for publication 10/20/2015).

TABLE OF CONTENTS

LIST OF FIGURES

LIST OF TABLES

LIST OF ABBREVIATIONS

AAALAC	Association for Assessment and Accreditation of Laboratory Animal Care International
cAMP	Cellular Adenosine-3'-5'-Cyclic Monophosphate
COX	Cyclooxygenase
DNA	Deoxyribonucleic acid
Dox	Doxycycline
EDTA	Ethylenediaminetetraacetic acid
EGFR	Epidermal Growth Factor Receptor
ELISA	Enzyme-Linked Immunosorbent Assay
EMT	Epithelial to mesenchymal transition
FBS	Fetal Bovine Serum
GAPDH	Glyceraldehyde 3-phosphate dehydrogenase
GSIS	Glucose Stimulated Insulin Secretion
GSK-3β	Glycogen Synthase Kinase 3 Beta
GTT	Glucose Tolerance Test
H&E	Hematoxylin and Eosin
HOMA-IR	Homeostatic model assessment-Insulin Resistance
IGF1	Insulin-like growth factor 1
IP	Intraperitoneal
IR	Insulin Receptor
ITT	Insulin Tolerance Test

LSL	Lox Stop Lox
MMP	Matrix metalloproteinases
mTORC1	Mammalian Target of Rapamycin Complex 1
Muc	Mucin
Myr	Myristoylated
NSL	No Significant Lesion
PanIN	Pancreatic intraepithelial neoplasia
PCR	Polymerase chain reaction
PDAC	Pancreatic ductal adenocarcinoma
PDK1	3-phosphoinositide dependent protein kinase 1
Pdx1	Pancreatic duodenal homeobox-1
PHLPP	PH domain and leucine rich repeat protein phosphatase
Phospho	Phosphorylation/Phosphorylated
PI3K	Phosphatidylinositol 3-kinase
PIP2	Phosphatidylinositol (3,4)-bisphosphate
PIP3	Phosphatidylinositol (3,4,5)-trisphosphate
PKA	Protein Kinase A
PP2A	Protein Phosphatase 2A
PTEN	Phosphatase and tensin homolog
Reg	Regular
RIP	Rat Insulin Promoter
S473	Serine 473

SMA	Smooth Muscle Actin
SNP	Single Nucleotide Polymorphism
T308	Threonine 308
tetO	Tetracycline operator
tTA	Tetracycline transactivator
WT	Wild type

CHAPTER 1: GENERAL INTRODUCTION

Protein Kinase B/AKT

Protein Kinase B (AKT), a serine threonine kinase in the phosphatidylinositol 3-kinase (PI3K) signaling pathway (Figure 1), plays a vital role in cell signaling, making its abnormal loss or gain of function the epicenter of a variety of diseases, including cancer and diabetes mellitus (Manning & Cantley 2007). The activation of AKT (Figure 2), which is downstream of hormones, mitogens, cytokines and growth factors, is tightly controlled by positive and negative regulators within the pathway. Binding of a ligand, such as insulin, to its receptor leads to the phosphorylation of tyrosine residues on the intracellular domain of the receptor. PI3K binds to these phosphotyrosine residues leading to conformational changes in the catalytic domain of PI3K and subsequent activation. Activated PI3K phosphorylates membrane bound phosphatidylinositol (3,4)-bisphosphate (PIP2) to generate phosphatidylinositol (3,4,5)-trisphosphate (PIP3), which binds the PH domain of AKT recruiting it to the plasma membrane, where it is phosphorylated at the Threonine 308 (T308) residue and partially activated by Phosphoinositide-Dependent Kinase-1 (PDK1) (Alessi et al. 1997). Partial activation is sufficient to activate some downstream substrates, such as mTORC1 (Vander Haar et al. 2007), but full activation requires additional phosphorylation by mTORC2 (Sarbassov et al. 2005) or DNA-PK (Feng et al. 2004) at the Serine 473 residue (S473). AKT is negatively regulated by direct dephosphorylation of T308 and S473 by Protein Phosphatase 2A (PP2A) (Andjelković et al. 1996) and PH domain and leucine rich repeat protein phosphatases (PHLPP1/2) (Brognard et al. 2007), respectively. It is also negatively regulated by the indirect conversion of PIP3 to PIP2 by Phosphatase and Tensin Homolog (PTEN) (Stambolic et al. 1998). Once fully activated, AKT signals through the phosphorylation and

subsequent activation or inhibition of downstream substrates, allowing regulation of key cellular processes such as survival, growth, proliferation, metabolism, protein synthesis, transcription, apoptosis, and angiogenesis (Hemmings & Restuccia 2012).

AKT isoforms and function

It is believed that AKT controls such an array of diverse functions through its three isoforms: AKT1 (PKBα), AKT2 (PKBβ), and AKT3 (PKBγ). The isoforms are structurally analogous (Figure 3) consisting of: (1) a common NH2-terminal pleckstrin homology (PH) domain which allows binding and translocation to the membrane; (2) a catalytic domain which contains the threonine residue for partial activation; and (3) a carboxyl terminal extension containing the serine for full activation. AKT isoforms are encoded by three different genes on different chromosomes. They also have differential tissue expression and varying functions (Figure 4) (Hay 2011; Song et al. 2005). AKT1 is ubiquitously expressed in mammalian tissues and predominately recognized for its role in cell growth, proliferation, and survival (Cho et al. 2001). AKT2 is highly expressed in insulin responsive tissues (e.g., liver, skeletal muscle, and adipose tissues) and is therefore recognized for its role in glucose metabolism and insulin signaling (Cho et al. 2001; Garofalo et al. 2003). AKT3 is highly expressed in brain and is vital for brain development (Tschopp et al. 2005). Differences in the subcellular locations of the isoforms have also been identified with AKT1 in the cytoplasm, AKT2 at the mitochondria, and AKT3 in the nucleus (Santi & Lee 2010). Functional differences have largely been identified via single isoform knockout mouse studies. However, double AKT isoform knockout studies reveal possible compensation among the isoforms, making further examination necessary to fully understand isoform functional

specificity and to develop therapeutic treatments targeting AKT isoform-specific functions (Gonzalez & McGraw 2009).

AKT and Cancer

AKT is a well-known survival protein, blocking apoptosis in several ways, which includes but is not limited to: (1) phosphorylation of BAD (Serine 136) to inhibit its apoptotic activity (Datta et al. 1999); (2) phosphorylation and inhibition of Caspase-9 (Serine 196) (Cardone et al. 1998), and (3) transcriptional regulation of pro- and anti-apoptotic genes (Song et al. 2005). In addition to its anti-apoptotic activity elevated AKT leads to increased cell migration, reduced cellular adhesion, and promotion of epithelial to mesenchymal transition (EMT) (Enomoto et al. 2005; Grille et al. 2003; Tanno et al. 2001). Therefore, it is not surprising that the hyperactivation of AKT has been conclusively linked to the development of various human cancers (Figure 5), such as gastric, ovarian, prostate, breast, pancreatic, melanoma, and colorectal cancers (Staal 1987; Carpten et al. 2007; Cheng et al. 1996; Stahl et al. 2004; Schlieman et al. 2003; Toker 2012). AKT hyperactivation can occur due to increased growth factor stimulation, presence of oncogenic upstream regulators (e.g., PI3K), or loss of negative regulators (e.g., PTEN). Additionally, other pathways, such as the RAS/RAF/MEK/ERK pathway, can also be activated in cancers, such as pancreatic ductal adenocarcinoma (PDAC), further activating shared targets such as AKT (Gonzalez & McGraw 2009).

AKT and Pancreatic Ductal Adenocarcinoma

PDAC, the most lethal common cancer largely due to late diagnosis, develops primarily from precursor lesions, called pancreatic intraepithelial neoplasias (PanINs). PanINs are classified

based upon the increasing degree of structural abnormality in the tissue (Figure 6). PanIN1 lesions are subdivided into flat (PanIN1A) and papillary types (PanIN1B). PanIN2s have loss of polarity, nuclear crowding, cell enlargement, and increased nuclear staining. PanIN3s have severe nuclear abnormality, luminal necrosis, and epithelial cell budding into the ducts (Murphy et al. 2013). On average it takes 17 years for the PanINs to progress to the aggressive PDAC which has a survival rate of only four to six months after diagnosis (Hidalgo et al. 2015).

Activation mutations of Ras, specifically the Kristin Ras isoform (KRas), are found in PanIN1A lesions and 90% of PDACs, making it an important tumor initiating event (Löhr et al. 2005; Morris et al. 2010). KRas activation subsequently leads to additional molecular changes, such as activation of the AKT oncogene and loss of tumor suppressors, which further drives PDAC progression and tumor formation (Ryan et al. 2014). Further studies into the genetic changes that occur in early PanINs may provide an opportunity for early diagnosis and ultimately an increased survival rate. The unavailability of early-stage tissue from patients has hampered the search for such genetic biomarkers, and made the use of pancreatic cancer mouse models of upmost importance. In chapter 2 we used a PDAC mouse model, with activation of KRas and AKT1 ($AKT1^{Myr}$/KRasG12D), to characterize the incidence and frequency of histological (e.g. presence of mucin-4 in pancreatic intraepithelial neoplasms) and genetic (e.g. loss of tumor suppressors *p16Ink4a* and *p19Arf*) alterations known to commonly occur in human pancreatic cancer, as well as delineate the role of AKT1 in accelerating pancreatic tumor progression and metastasis. We determined that $AKT1^{Myr}$/KRasG12D mice, unlike other PDAC mouse models, accurately mimic the human PDAC progression molecularly, structurally, and most importantly temporally. Other PDAC models (mice with KRasG12D activation and Pten homozygous deletion) have rapid (<3

weeks) tumor development, while our model has a slower progression (~54 weeks) allowing for therapeutic studies that can block tumor progression at the PanIN or early carcinoma stage, before there is excessive tissue damage.

Glucose Metabolism

Insulin and glucagon are classified as the chief regulators of glucose homeostasis (Figure 7). Glucose homeostasis, maintaining blood glucose concentrations within a narrow range, is vital as glucose is the main fuel source for the brain, which can neither synthesize nor store glucose long term. Hypoglycemia, low blood glucose levels, can impair brain function and eventually lead to convulsions and death (Shrayyef & Gerich 2010). Whereas hyperglycemia, high blood glucose levels, can lead to cardiovascular damage, retinopathy, nephropathy, and neuropathy (Nathan 1993). Therefore it is essential to maintain stable blood glucose concentrations at all times, avoiding tissue damage and disease.

Homeostasis is maintained by balancing the rate of glucose entering the circulation and the rate of glucose leaving the circulation. During fasting, when blood glucose levels are low, glucagon is secreted by pancreatic α-cells to induce glycogenolysis and gluconeogenesis in the liver. Glycogenolysis is the breakdown of glycogen, the stored form of glucose, and gluconeogenesis is the formation of glucose from lactate and amino acids. Both processes result in the release of glucose from the liver into circulation. After a meal blood glucose levels spike and insulin is released by pancreatic β-cells to initiate glucose uptake by skeletal muscle and adipose tissue. Insulin also inhibits endogenous glucose production by suppressing glucagon secretion in the pancreas and promoting glycogenesis, conversion of glucose to glycogen, in the

liver. While this "bi-hormonal" explanation for glucose metabolism and regulation is widely accepted, it is relatively flawed, as the system is actually quite complex with many contributing parts, such as AKT (Aronoff et al. 2004).

AKT and Glucose Metabolism

AKT is predominantly recognized for its role in the regulation of cell survival, growth, and proliferation, but it also plays a role in glucose metabolism, which has been noted, but comparatively overlooked. Studies conducted in *C elegans*, *Drosophilia*, and mice have proven AKT, which is downstream of insulin and insulin-like growth factor 1 (IGF1), is involved in the coupling of extracellular signals and metabolism (Teleman 2009; Panowski & Dillin 2009; Peng et al. 2003). Activation of the insulin receptor leads to the phosphorylation and activation of AKT, which subsequently phosphorylates downstream effectors, such as FoxO and mTORC1, inhibiting hepatic glucose production (Nakae et al. 2002) and inducing insulin biosynthesis (Leibiger et al. 1998), respectively. AKT has also been shown to facilitate the insulin induced translocation of GLUT 4 to the plasma membrane of fat and muscle cells allowing glucose uptake and the lowering of postprandial blood glucose levels (Huang & Czech 2007; Katome et al. 2003).

As AKT2 is highly expressed in insulin responsive tissues it has been identified as a primary regulator of glucose metabolism. This is supported by the insulin resistance, hyperinsulinemia, and glucose intolerance observed in AKT2 knockout mice (AKT2-/-) (Cho et al. 2001; Garofalo et al. 2003). Initially AKT1 and 3 were deemed unnecessary for glucose homeostasis, as AKT1 (AKT1-/-) and AKT3 (AKT3-/-) knockout mice have normal glucose tolerance and insulin signaling, but impaired fetal/adult growth and reduced brain size,

respectively (Cho et al. 2001; Tschopp et al. 2005). However, a role for AKT1 in glucose homeostasis became evident with the metabolic analysis of compound isoform knockout mice (Figure 4). One such study revealed that haplodeficiency of AKT1 in AKT2-/- mice resulted in a more severe diabetic phenotype, characterized by fed and fasted hyperglycemia, glucose intolerance, insulin resistance, and hyperinsulinemia (Chen et al. 2009).

Although AKT1 hyperactivation has been frequently observed in pancreatic cancers (Schlieman et al. 2003; Missiaglia et al. 2010), there are limited studies regarding AKT1 hyperactivation and glucose homeostasis (Bernal-Mizrachi et al. 2001; Tuttle et al. 2001; Kushner et al. 2005; Stiles et al. 2006). In chapter three we metabolically characterize mice with myristoylated, membrane-bound and therefore activated AKT1 ($AKT1^{Myr}$). We report that this strain of mice exhibit non-fasted hyperglycemia as early as weaning and fasted hyperglycemia by 20 weeks of age, largely due to fasted hyperglucagonemia. We confirm that this pre-diabetic phenotype is due to AKT1 hyperactivation, as doxycycline treatment to turn off the transgene attenuates the elevated blood glucose levels. Collectively, this pre-diabetic model highlights a novel glucagon-mediated mechanism by which AKT1 hyperactivation, as seen in many cancers, affects glucose homeostasis, possibly shedding light on the association between pancreatic cancer and diabetes.

Pancreatic Cancer and Diabetes

As early as the 1900s a relationship between diabetes and pancreatic cancer has been proposed. Based upon experimental and clinical evidence, there are two prevailing theories: (1) long-term diabetes induces pancreatic cancer and (2) new onset diabetes is an early marker for

pancreatic cancer. The first theory, that long-term diabetes induces pancreatic cancer, is based upon evidence that high glucose levels can induce replication/proliferation (Butler et al. 2010; Brand et al. 2011; Han et al. 2011), epithelial-mesenchymal transition (Lee & Han 2010; Javle et al. 2007), and oxidative stress (Cullen et al. 2003). The second theory, that new onset diabetes is an early marker for pancreatic cancer, is based upon the following evidence: tumor removal resolves diabetes (Permert et al. 1993; Pannala et al. 2008) and implantation of cancer cell lines can induce hyperglycemia (Wang et al. 1997; Basso et al. 1995; Valerio et al. 2004). This theory is also strongly supported by the fact that 80% of PDAC patients suffer from hyperglycemia or diabetes prior to diagnosis (Wang et al. 2003). Additionally, a meta-analysis of 35 cohort studies revealed that diabetes was associated with a 94% increased risk of PDAC, which decreased with the duration of diabetes suggesting that the diabetes is caused by the cancer (Ben et al. 2011). So, while the association between diabetes and pancreatic cancer appears firm the specific mechanisms involved remain debatable.

In chapter 4 we begin to characterize the diabetic phenotype observed in AKT1^{Myr}/KRasG12D transgenic mice to better understand how the presence of two oncogenes (AKT1 and KRas) cooperate to affect glucose homeostasis. Similar to AKT1^{Myr} mice, yet more severe, AKT1^{Myr}/KRasG12D mice exhibit hyperglucagonemia induced non-fasted hyperglycemia as early as weaning and fasted hyperglycemia by 3 months of age. AKT1^{Myr}/KRasG12D mice also suffer from polyuria, muscle wasting, and bloating, which is not seen in AKT1^{Myr} mice. Once fully characterized this diabetic model will provide an avenue to better understand the molecular mechanisms behind the association of pancreatic cancer and diabetes. With 256 million adults worldwide suffering from type 2 diabetes, and projections likely to increase by 54.1% in the next

twenty years, it is vital that we understand this association, whether to prevent the formation of pancreatic cancer or to treat pancreatic cancer while it is still in the early stages (Shaw et al. 2010).

Figures and Tables

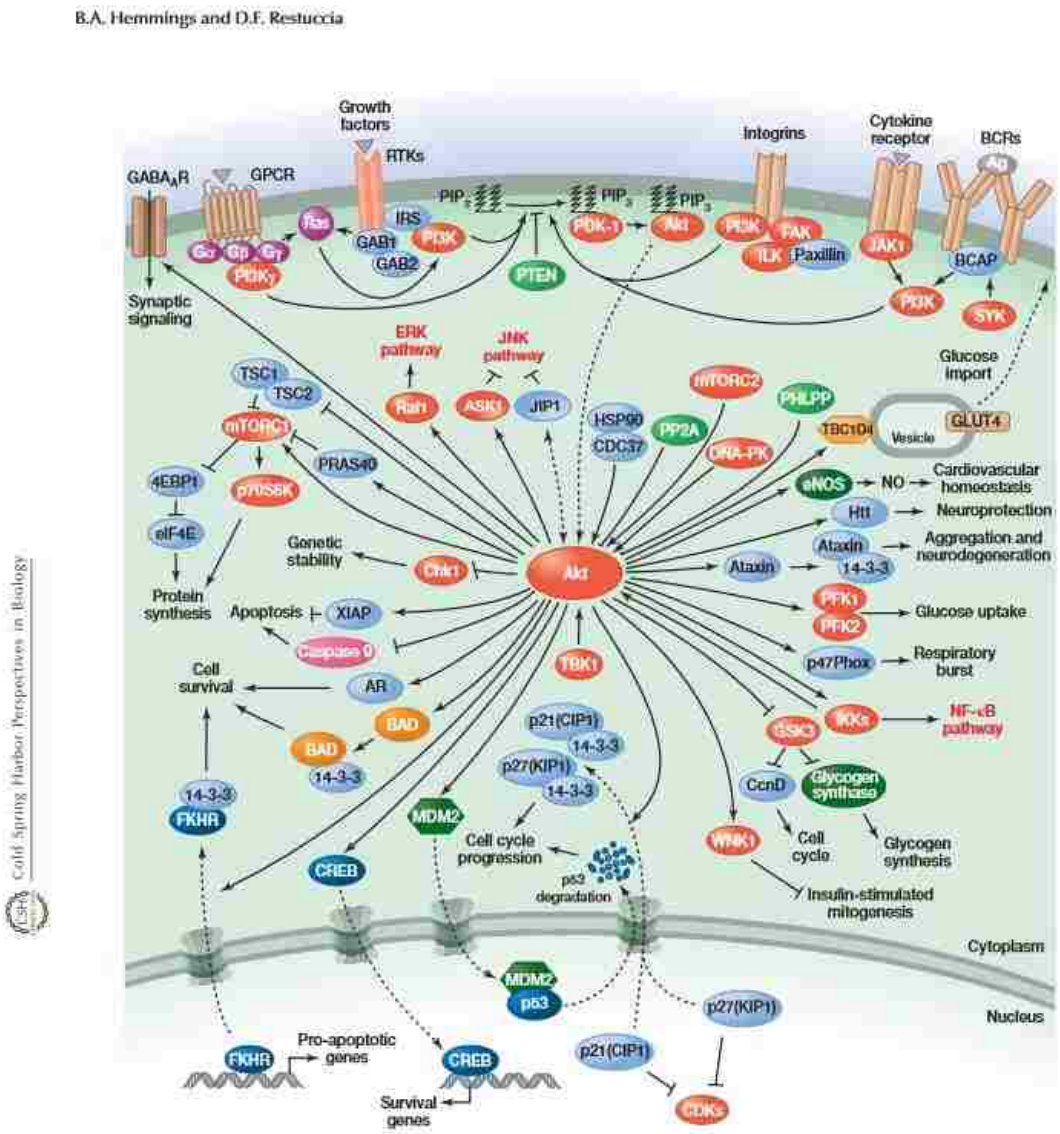

Figure 1: Signaling events activating PKB/AKT and cellular functions regulated by PKB/AKT.

Reprinted by permission: Hemmings BA & Restuccia DF 2012 PI3K-PKB/AKT pathway. Cold Spring Harb Perspect Biol 2012;4:a011189, with copyright to Cold Spring Harbor Laboratory Press.

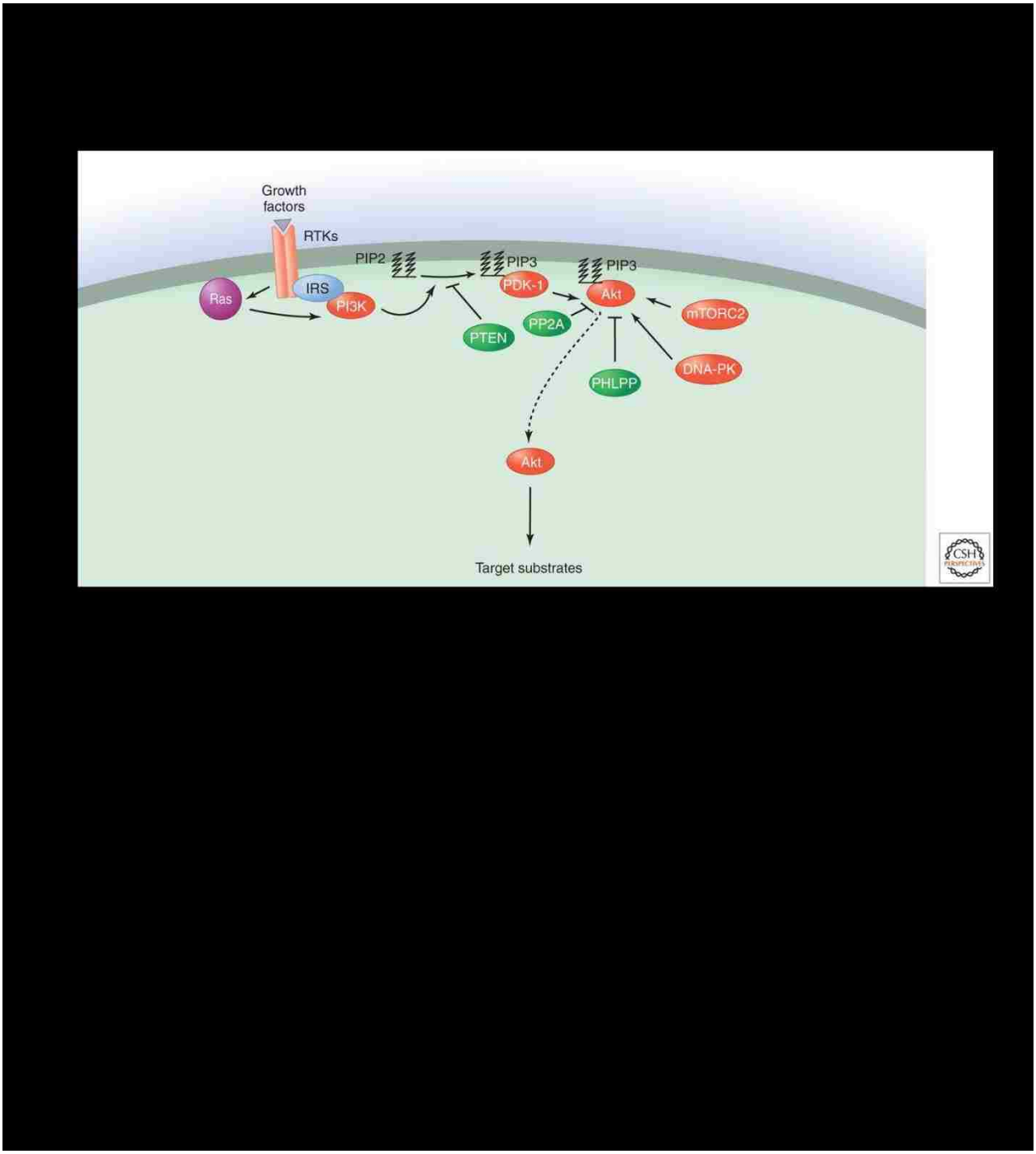

Figure 2: PKB/AKT activation downstream of RTKs via the PI3K pathway.

Reprinted by permission: Hemmings BA & Restuccia DF 2012 PI3K-PKB/AKT pathway. Cold Spring Harb Perspect Biol 2012;4:a011189, with copyright to Cold Spring Harbor Laboratory Press.

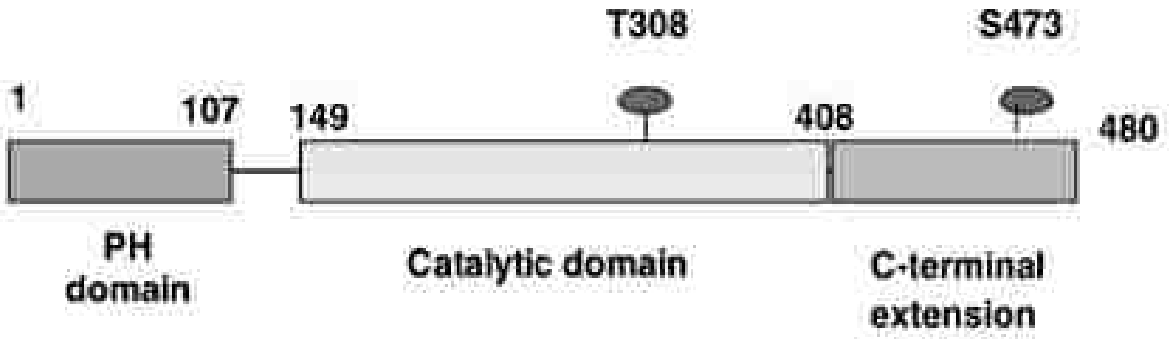

PAIR	*PH*	*LINK*	*CAT*	*EXT*
AKT1/AKT2	80	46	90	66
AKT1/AKT3	84	40	88	76
AKT2/AKT3	76	17	87	70

[a]Domain definitions using AKT1 residue numbers. PH – Pleckstrin Homology domain, AKT1 (1–107), ~30% identical to pleckstrin and other PH domains. LINK – Linker region, AKT 1(108–148), no significant homology to other proteins. CAT – Kinase Catalytic domain, AKT1 (149–408), homologous to all kinases, ~50% identical to the PKC, PKA, SGK and S6 families. EXT – C-terminal Extension, AKT1 (409–480) is only ~15% identical to the PKA family and ~35–40% identical to the rest of the AGC family members

Figure 3: AKT isoform analogous structures.

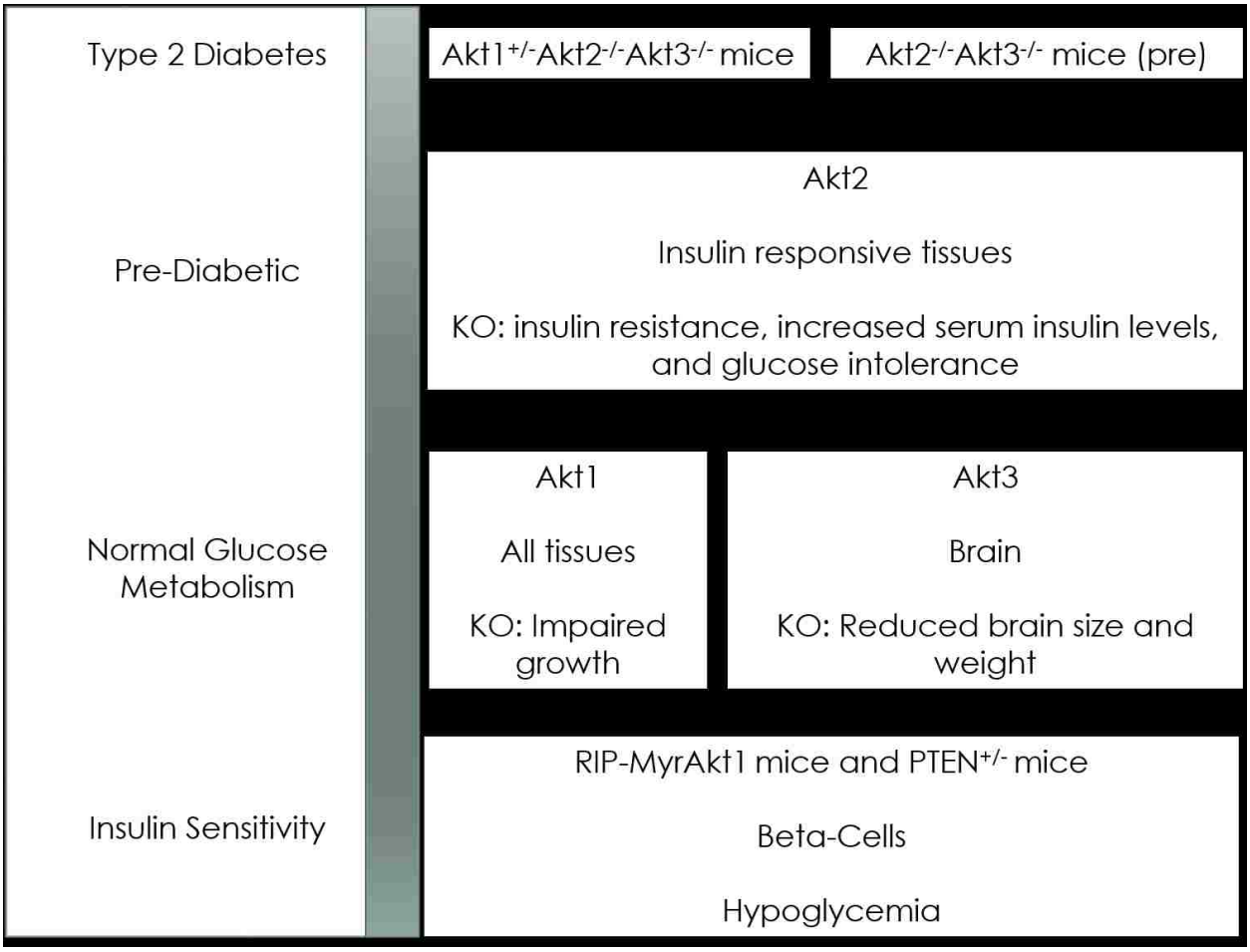

Figure 4: AKT isoform functionality knockout mice studies.

Created by author based upon articles referenced in the introduction.

Figure and tables index

Tumor type	*% Tumors with active AKT*
Glioma	~55
Thyroid carcinoma	80–100
Breast carcinoma	20–55
Small-cell lung carcinoma	~60
Non-small-cell lung carcinoma	30–75
Gastric carcinoma	~80
Gastrointestinal stromal tumors	~30
Pancreatic carcinoma	30–70
Bile duct carcinoma	~85
Ovarian carcinoma	40–70
Endometrial carcinoma	>35
Prostate carcinoma	45–55
Renal cell carcinoma	~40
Anaplastic large-cell lymphoma	100
Acute myeloid leukemia	~70
Multiple myeloma	~90
Malignant mesothelioma[a]	~65
Malignant melanoma[b]	43–67

[a] Altomare *et al.* (2005);

[b] Reviewed in Robertson (2005); remaining cancer types reviewed in Bellacosa *et al.* (2005)

Figure and tables index

Figure 5: AKT activation in human cancers.

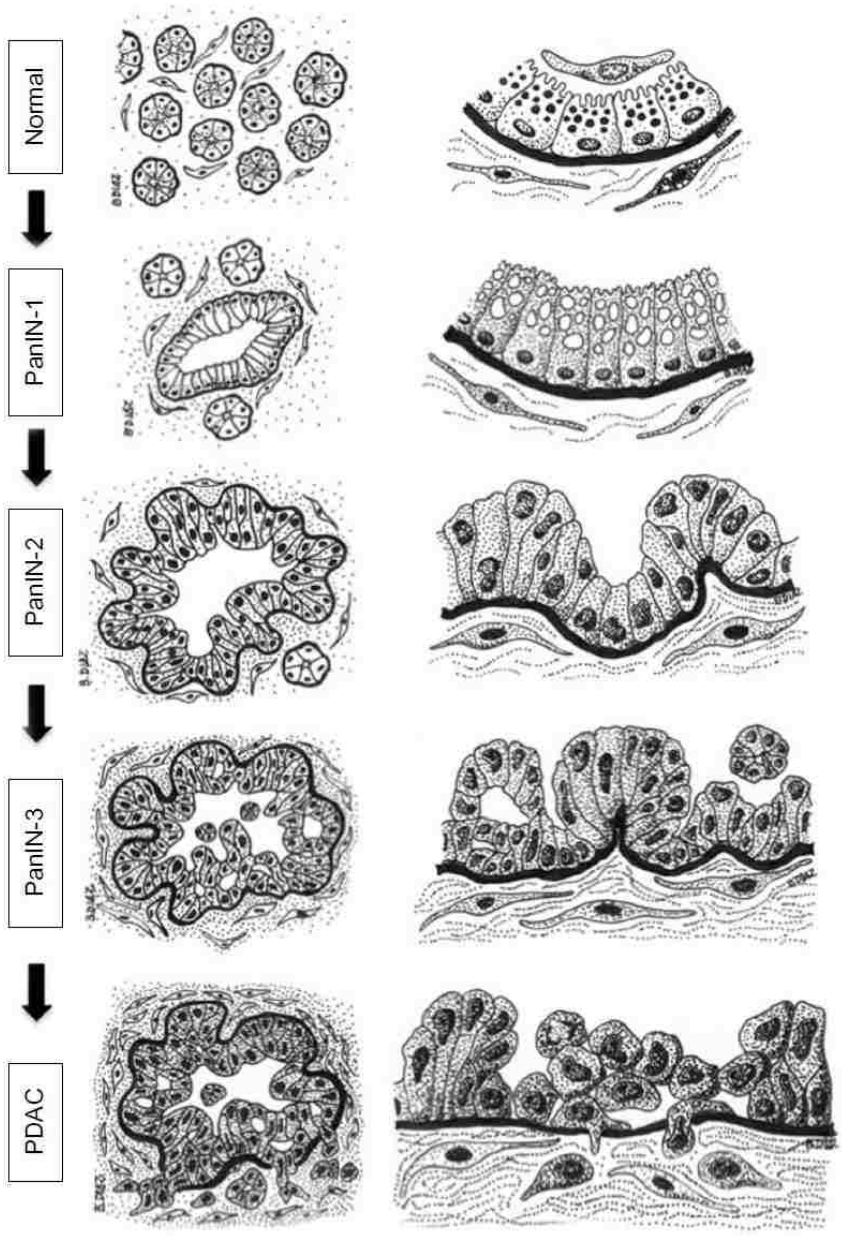

Figure 6: Diagram of the histology of precursor lesions and PDAC.

Republished with permission of [Dove Medical Press Ltd.], from [The impact of hypoxia in pancreatic cancer invasion and metastasis, Angela Yuen, Begoña Díaz, Volume 2014:2,]; permission conveyed through Copyright Clearance Center, Inc. ”

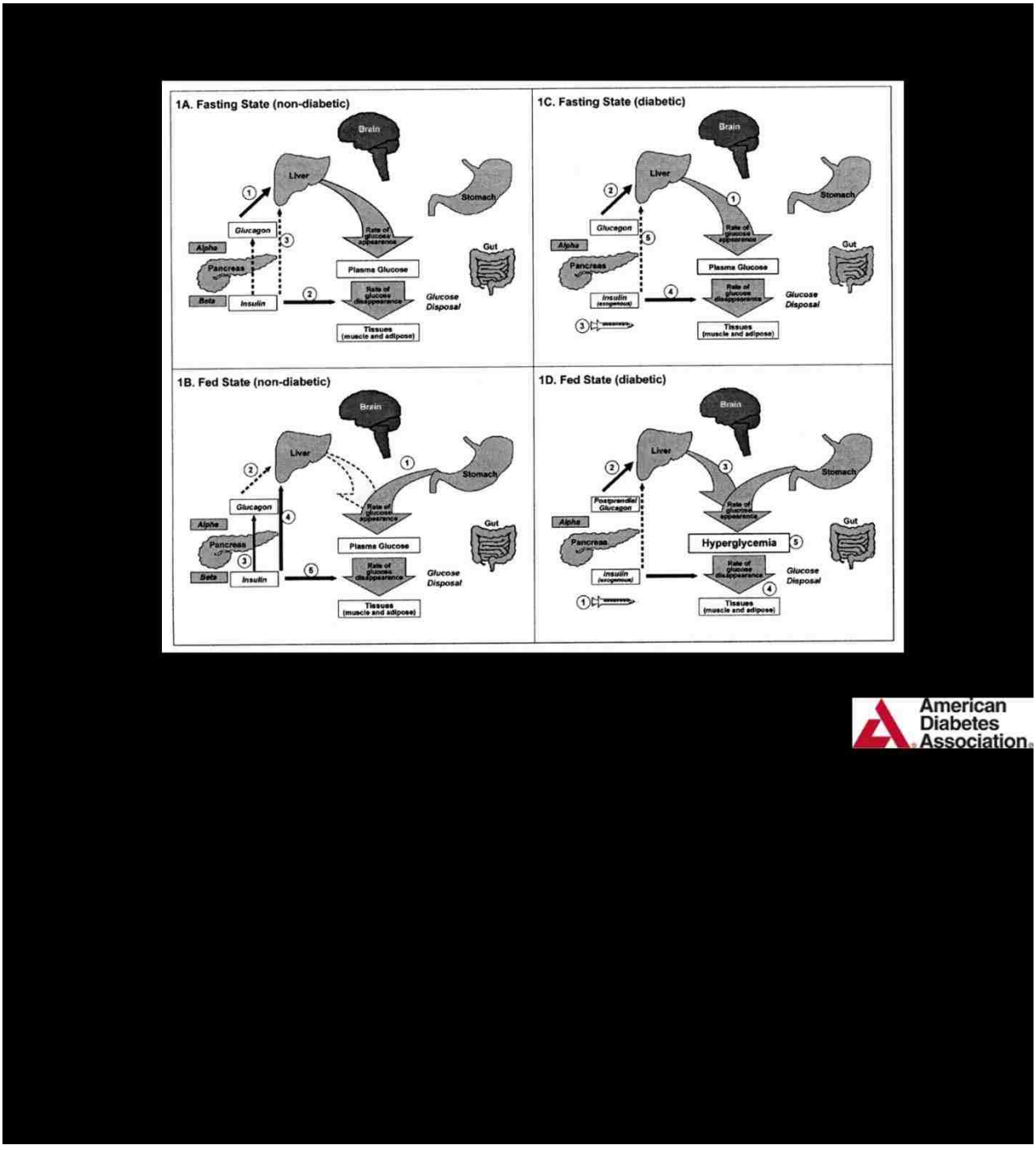

Figure 7: Glucose homeostasis – Roles of insulin and glucagon

Reprinted with permission: Aronoff SL, Berkowitz K, Shreiner B & Want L 2004 Glucose Metabolism and Regulation: Beyond Insulin and Glucagon. Diabetes Spectrum3 183-190.

List of References

Alessi DR, James SR, Downes CP, Holmes AB, Gaffney PR, Reese CB & Cohen P 1997 Characterization of a 3-phosphoinositide-dependent protein kinase which phosphorylates and activates protein kinase Balpha. *Curr Biol***7** 261-269.

Altomare DA & Testa JR 2005 Perturbations of the AKT signaling pathway in human cancer. *Oncogene***24** 7455-7464.

Andjelković M, Jakubowicz T, Cron P, Ming XF, Han JW, & Hemmings BA 1996 Activation and phosphorylation of a pleckstrin homology domain containing protein kinase (RAC-PK/PKB) promoted by serum and protein phosphatase inhibitors. *Proc Natl Acad Sci U S A***93** 5699-5704.

Aronoff SL, Berkowitz K, Shreiner B & Want L 2004 Glucose Metabolism and Regulation: Beyond Insulin and Glucagon. *Diabetes Spectrum***3** 183-190.

Basso D, Brigato L, Veronesi A, Panozzo MP, Amadori A & Plebani M 1995 The pancreatic cancer cell line MIA PaCa2 produces one or more factors able to induce hyperglycemia in SCID mice. *Anticancer Res***15** 2585-2588.

Ben Q, Xu M, Ning X, Liu J, Hong S, Huang W, Zhang H & Li Z 2011 Diabetes mellitus and risk of pancreatic cancer: A meta-analysis of cohort studies. *Eur J Cancer***47** 1928-1937.

Bernal-Mizrachi E, Wen W, Stahlhut S, Welling CM & Permutt MA 2001 Islet beta cell expression of constitutively active Akt1/PKB alpha induces striking hypertrophy, hyperplasia, and hyperinsulinemia. *J Clin Invest***108** 1631-1638.

Brand TM, Iida M, Li C & Wheeler DL 2011 The nuclear epidermal growth factor receptor signaling network and its role in cancer. *Discov Med***12** 419-432.

Brognard J, Sierecki E, Gao T & Newton AC 2007 PHLPP and a second isoform, PHLPP2, differentially attenuate the amplitude of Akt signaling by regulating distinct Akt isoforms. *Mol. Cell***25** 917-931.

Butler AE, Galasso R, Matveyenko A, Rizza RA, Dry S & Butler PC 2010 Pancreatic duct replication is increased with obesity and type 2 diabetes in humans. *Diabetologia***53** 21-26.

Carpten JD, Faber AL, Horn C, Donoho GP, Briggs SL, Robbins CM, Hostetter G, Boguslawski S, Moses TY, Savage S, et al 2007 A transforming mutation in the pleckstrin homology domain of AKT1 in cancer. *Nature***448** 439-444.

Chen WS, Peng XD, Wang Y, Xu PZ, Chen ML, Luo Y, Jeon SM, Coleman K, Haschek WM, Bass J, et al. 2009 Leptin deficiency and beta-cell dysfunction underlie type 2 diabetes in compound Akt knockout mice. *Mol Cell Biol***29** 3151-3162.

Cheng JQ, Ruggeri B, Klein WM, Sonoda G, Altomare DA, Watson DK & Testa JR 1996 Amplification of AKT2 in human pancreatic cells and inhibition of AKT2 expression and tumorigenicity by antisense RNA. *Proc Natl Acad Sci U S A***93** 3636-3641.

Cho H, Mu J, Kim JK, Thorvaldsen JL, Chu Q, Crenshaw EB, Kaestner KH, Bartolomei MS, Shulman GI & Birnbaum MJ 2001 Insulin resistance and a diabetes mellitus-like syndrome in mice lacking the protein kinase Akt2 (PKB beta). *Science***292** 1728-1731.

Cho H, Thorvaldsen JL, Chu Q, Feng F & Birnbaum MJ 2001 Akt1/PKBalpha is required for normal growth but dispensable for maintenance of glucose homeostasis in mice. *J Biol Chem***276** 38349-38352.

Cullen JJ, Weydert C, Hinkhouse MM, Ritchie J, Domann FE, Spitz D & Oberley LW 2003 The role of manganese superoxide dismutase in the growth of pancreatic adenocarcinoma. *Cancer Res***63** 1297-1303.

Datta SR, Brunet A, Greenberg ME 1999 Cellular survival: a play in three Akts. *Genes Dev***13** 2905-27.

Enomoto A, Murakami H, Asai N, Morone N, Watanabe T, Kawai K, Murakumo Y, Usukura J, Kaibuchi K & Takahashi M 2005 Akt/PKB regulates actin organization and cell motility via Girdin/APE. *Dev Cell***9** 389-402.

Feng J, Park J, Cron P, Hess D & Hemmings BA 2004 Identification of a PKB/Akt hydrophobic motif Ser-473 kinase as DNA-dependent protein kinase. *J Biol Chem***279** 41189-41196.

Garofalo RS, Orena SJ, Rafidi K, Torchia AJ, Stock JL, Hildebrandt AL, Coskran T, Black SC, Brees DJ, Wicks JR, et al. 2003 Severe diabetes, age-dependent loss of adipose tissue, and mild growth deficiency in mice lacking Akt2/PKB beta. *J Clin Invest***112** 197-208.

Grille SJ, Bellacosa A, Upson J, Klein-Szanto AJ, van Roy F, Lee-Kwon W, Donowitz M, Tsichlis PN & Larue L 2003 The protein kinase Akt induces epithelial mesenchymal transition and promotes enhanced motility and invasiveness of squamous cell carcinoma lines. *Cancer Res***63** 2172-2178.

Han L, Ma Q, Li J, Liu H, Li W, Ma G, Xu Q, Zhou S & Wu E 2011 High glucose promotes pancreatic cancer cell proliferation via the induction of EGF expression and transactivation of EGFR. *PLoS One***6** 1-7:

Hay N 2011 Akt isoforms and glucose homeostasis - the leptin connection. *Trends Endocrinol Metab***22** 66-73.

Hemmings BA & Restuccia DF 2012 PI3K-PKB/Akt pathway. *Cold Spring Harb Perspect Biol***4** 1-4.

Hidalgo M, Cascinu S, Kleeff J, Labianca R, Löhr JM, Neoptolemos J, Real FX, Van Laethem JL & Heinemann V 2015 Addressing the challenges of pancreatic cancer: future directions for improving outcomes. *Pancreatology***15** 8-18.

Huang S & Czech MP 2007 The GLUT4 glucose transporter. *Cell Metab***5** 237-252.

Javle MM, G.J., Iwata KK, Pak Y, Rutledge P, Yu J, Black JD, Tan D & Khoury T 2007 Epithelial-mesenchymal transition (EMT) and activated extracellular signal-regulated kinase (p-Erk) in surgically resected pancreatic cancer. *Ann Surg Oncol***14** 3527-3533.

Katome T, Obata T, Matsushima R, Masuyama N, Cantley LC, Gotoh Y, Kishi K, Shiota H & Ebina Y 2003 Use of RNA interference-mediated gene silencing and adenoviral overexpression to elucidate the roles of AKT/protein kinase B isoforms in insulin actions. *J Biol Chem***278** 28312-28323.

Kumar CC & Madison V 2005 AKT crystal structure and AKT-specific inhibitors. *Oncogene***24** 7493-7501.

Kushner JA, Simpson L, Wartschow LM, Guo S, Rankin MM, Parsons R & White MF 2005 Phosphatase and tensin homolog regulation of islet growth and glucose homeostasis. *J Biol Chem***280** 39388-39393.

Lee YJ & Han HJ 2010 Troglitazone ameliorates high glucose-induced EMT and dysfunction of SGLTs through PI3K/Akt, GSK-3β, Snail1, and β-catenin in renal proximal tubule cells. *Am J Physiol Renal Physiol***298** 1263-1275.

Leibiger IB, Leibiger B, Moede T & Berggren PO 1998 Exocytosis of insulin promotes insulin gene transcription via the insulin receptor/PI-3 kinase/p70 s6 kinase and CaM kinase pathways. *Mol Cell***1** 933-938.

Löhr M, Klöppel G, Maisonneuve P, Lowenfels AB & Lüttges J 2005 Frequency of K-ras mutations in pancreatic intraductal neoplasias associated with pancreatic ductal adenocarcinoma and chronic pancreatitis: a meta-analysis. *Neoplasia***7** 17-23.

Manning BD & Cantley LC 2007 AKT/PKB signaling: navigating downstream. *Cell***129** 1261-74.

Missiaglia E, Dalai I, Barbi S, Beghelli S, Falconi M, della Peruta M, Piemonti L, Capurso G, Di Florio A, delle Fave G, et al. 2010 Pancreatic endocrine tumors: expression profiling evidences a role for AKT-mTOR pathway. *J Clin Oncol***28** 245-255.

Murphy SJ, Hart SN, Lima JF, Kipp BR, Klebig M, Winters JL, Szabo C, Zhang L, Eckloff BW, Petersen GM, et al. 2013 Genetic alterations associated with progression from pancreatic intraepithelial neoplasia to invasive pancreatic tumor. *Gastroenterology***145** 1098-1109.

Nakae J, Biggs WH 3rd, Kitamura T, Cavenee WK, Wright CV, Arden KC & Accili D 2002 Regulation of insulin action and pancreatic beta-cell function by mutated alleles of the gene encoding forkhead transcription factor Foxo1. *Nat Genet***32** 245-253.

Nathan DM 1993 Long-term complications of diabetes mellitus. *N Engl J Med***328** 1676-1685.

Ocana A, Vera-Badillo F, Al-Mubarak M, Templeton AJ, Corrales-Sanchez V, Diez-Gonzalez L, Cuenca-Lopez MD, Seruga B, Pandiella A & Amir E 2014 Activation of the PI3K/mTOR/AKT pathway and survival in solid tumors: systematic review and meta-analysis. *PLoS One***9** 1-4.

Pannala R, Bamlet WR, Basu A, Petersen GM & Chari ST 2008 Prevalence and clinical profile of pancreatic cancer-associated diabetes mellitus. *Gastroenterology***134** 981-987.

Panowski SH & Dillin A 2009 Signals of youth: endocrine regulation of aging in Caenorhabditis elegans. *Trends Endocrinol Metab***20** 259-264.

Peng XD, Xu PZ, Chen ML, Hahn-Windgassen A, Skeen J, Jacobs J, Sundararajan D, Chen WS, Crawford SE, Coleman KG et al. 2003 Dwarfism, impaired skin development, skeletal muscle atrophy, delayed bone development, and impeded adipogenesis in mice lacking Akt1 and Akt2. *Genes Dev***17** 1352-1365.

Permert J, Jorfeldt L, von Schenck H, Arnquist HJ & Larsson J 1993 Improved glucose metabolism after subtotal pancreatectomy for pancreatic cancer. *Br J Surg***80** 1047-1050.

Ryan DP, Hong TS & Bardeesy N 2014 Pancreatic adenocarcinoma. *N Engl J Med***371** 1039-1049.

Santi SA & Lee H 2010 The Akt isoforms are present at distinct subcellular locations. *Am J Physiol Cell Physiol***298** 580-591.

Sarbassov DD, Guertin DA, Ali SM & Sabatini DM 2005 Phosphorylation and regulation of Akt/PKB by the rictor-mTOR complex. *Science***307** 1098-1101.

Schlieman MG, Fahy BN, Ramsamooj R, Beckett L & Bold RJ 2003 Incidence, mechanism and prognostic value of activated AKT in pancreas cancer. *Br J Cancer***89** 2110-2115.

Shaw JE, Sicree RA & Zimmet PZ 2010 Global estimates of the prevalence of diabetes for 2010 and 2030. *Diabetes Res Clin Pract***87** 4-14.

Shrayyef MZ & Gerich JE 2010 Normal Glucose Homeostasis. In: Poretsky L (ed.). Principles of Diabetes Mellitus. Springer: US, 2010, pp. 19–36.

Song G, Ouyang G & Bao S 2005 The activation of Akt/PKB signaling pathway and cell survival. *J Cell Mol Med***9** 59-71.

Staal SP 1987 Molecular cloning of the akt oncogene and its human homologues AKT1 and AKT2: amplification of AKT1 in a primary human gastric adenocarcinoma. *Proc Natl Acad Sci U S A***84** 5034-5037.

Stahl JM, Sharma A, Cheung M, Zimmerman M, Cheng JQ, Bosenberg MW, Kester M, Sandirasegarane L & Robertson GP 2004 Deregulated Akt3 activity promotes development of malignant melanoma. *Cancer Res***64** 7002-7010.

Stambolic V, Suzuki A, de la Pompa JL, Brothers GM, Mirtsos C, Sasaki T, Ruland J, Penninger JM, Siderovski DP & Mak TW 1998 Negative regulation of PKB/Akt-dependent cell survival by the tumor suppressor PTEN. *Cell***95** 29-39.

Stiles BL, Kuralwalla-Martinez C, Guo W, Gregorian C, Wang Y, Tian J, Magnuson MA & Wu H 2006 Selective deletion of Pten in pancreatic beta cells leads to increased islet mass and resistance to STZ-induced diabetes. *Mol Cell Biol***26** 2772-2781.

Tanno S, Tanno S, Mitsuuchi Y, Altomare DA, Xiao GH & Testa JR 2001 AKT activation up-regulates insulin-like growth factor I receptor expression and promotes invasiveness of human pancreatic cancer cells. *Cancer Res***61** 589-93.

Teleman AA 2009 Molecular mechanisms of metabolic regulation by insulin in Drosophila. *Biochem J***425** 13-26.

Toker A 2012 Achieving specificity in Akt signaling in cancer. *Adv Biol Regul***52** 78-87.

Tschopp O, Yang ZZ, Brodbeck D, Dummler BA, Hemmings-Mieszczak M, Watanabe T, Michaelis T, Frahm J, & Hemmings BA 2005 Essential role of protein kinase B gamma

(PKB gamma/Akt3) in postnatal brain development but not in glucose homeostasis. *Development***132** 2943-2954.

Tuttle RL, Gill NS, Pugh W, Lee JP, Koeberlein B, Furth EE, Polonsky KS, Naji A & Birnbaum MJ 2001 Regulation of pancreatic beta-cell growth and survival by the serine/threonine protein kinase Akt1/PKBalpha. *Nat Med***7** 5-14.

Valerio A, Basso D, Fogar P, Falconi M, Greco E, Bassi C, Seraglia R, Abu-Hilal M, Navaglia F, Zambon CF, et al. 2004 Maldi-TOF analysis of portal sera of pancreatic cancer patients: identification of diabetogenic and antidiabetogenic peptides. *Clin Chim Acta***343** 119-27.

Vander Haar E, Lee SI, Bandhakavi S, Griffin TJ & Kim DH 2007 Insulin signalling to mTOR mediated by the Akt/PKB substrate PRAS40. *Nat Cell Biol***9** 316-323.

Wang F, Abdiu A, Gasslander T, Westermark P, Adrian TE & Permert J 1997 Dissociated secretion of islet amyloid polypeptide and insulin in serum-free culture media conditioned by human pancreatic adenocarcinoma cell lines. *Int J Pancreatol***21** 157-164.

Yuen A & Díaz B 2014 The impact of hypoxia in pancreatic cancer invasion and metastasis. *Hypoxia***2** 91-106.

CHAPTER 2:
CONSTITUTIVELY ACTIVE AKT1 COOPERATES WITH KRAS(G12D) TO ACCELERATE IN VIVO PANCREATIC TUMOR ONSET AND PROGRESSION

Introduction

Activating KRAS mutations are present in virtually all human pancreatic adenocarcinomas and occur with increasing frequency in later stage pancreatic intraepithelial neoplasia (PanIN) lesions (Hruban et al. 2000; Hansel et al. 2003). To date, the model that most faithfully recapitulates human PanIN development and its early progression is a mouse model that expresses a Cre-activated KRas allele knocked into the endogenous KRas locus (Jackson et al. 2001) when crossed with mice expressing a Pdx1-Cre recombinase transgene promoter (Gu et al. 2002). Oncogenic KRasG12D in the progeny of the Cre matings developed PanINs within a few months, with activation of the Notch pathway and overexpression of COX-2 and MMP-7 (Hingorani et al. 2003). This model thus offered the first recapitulation of human PanIN lesions, with low incidence of progression to pancreatic adenocarcinoma (Hingorani et al. 2003).

In comparison, Pdx-Cre;Ptenlox/lox mice with pancreatic knockout of Pten display rapid progression of pancreatic ductal metaplasia, development of PanINs, and low frequency of malignant transformation (Stanger et al. 2005). Under normal conditions, mouse and human PTEN functions as a dual-specificity protein phosphatase and a lipid phosphatase. Because PTEN modulates phosphatidylinositol 3-kinase (PI3K)–AKT signaling, loss of PTEN tumor suppressor function in pancreatic tumor progression further implicates the importance of AKT signaling in pancreatic pathogenesis.

Other mouse models of pancreatic cancer have been developed to study components of the PI3K/PTEN/AKT signaling pathway. A previous study analyzed constitutively active mutant AKT1 under control of Pdx-Cre, elastase-Cre, and rat insulin promoter-2–Cre expression (Elghazi et al. 2009). Interestingly, premalignant lesions and acinar tumors were observed when expression was driven by Pdx-Cre. Constitutively active myristoylated (Myr) AKT1 under rat insulin promoter-2 was also shown to result in malignant transformation of islet cells to develop islet cell carcinomas (Alliouachene et al. 2008). Most recently, a mouse model with a constitutively activated catalytic subunit of PI3K was used to study the importance of PI3K signaling in KRas-driven pancreatic ductal adenocarcinoma (PDAC) initiation and maintenance (Eser et al. 2013) and the requirement of 3-phosphoinositide dependent protein kinase 1 (PDK1) signaling for KRas pancreatic cell plasticity and cancer. Of relevance to human pancreatic cancer, earlier reports showed amplification and protein overexpression of AKT2 in human pancreatic cell lines (Cheng et al. 1996), and both AKT1 and AKT2 were found in human PDACs and in metastases (Altomare et al. 2003). AKT alterations are among the most commonly activated oncogenic changes in solid tumors and activation of AKT isoforms is frequently attributed to down-regulation of PTEN tumor suppressor or activation of upstream signaling components (activating PI3K mutations or activating growth factor receptors). A prior study, using immunohistochemistry and tissue microarrays, revealed that 34 of 133 (~ 25%) stage II PDACs exhibited loss of PTEN expression (Foo et al. 2013). Haplo-insufficiency and occasional homozygous loss of PTEN have also been found in human PDACs (Altomare et al. 2003). Overall, the data support a dosage-dependent role for mouse and human PTEN and in the activation of downstream AKT (Hill et al. 2010).

Herein, we report the first evidence describing the contribution of constitutively active myristoylated AKT1 in vivo to pancreatic ductal tumor progression using genetically defined transgenic models to delineate potential cooperation with Pdx-regulated expression of KRasG12D. Collectively, these studies provide insights regarding the pathogenic implication of AKT perturbations in combination with KRas oncogenic mutations to accelerate pancreatic progression toward the development of invasive PDAC. In addition, we propose that this dual oncogene model may offer long-term preclinical utility for testing of novel therapeutic strategies against pancreatic tumor progression and an opportunity to intervene before extensive desmoplastic fibrosis and irreversible tissue remodeling, which is a confounding problem in the treatment of late-stage pancreatic disease.

Materials and Methods

Genetically Engineered Mice

Animal care and use was at Association for Assessment and Accreditation of Laboratory Animal Care International (AAALAC)-accredited facilities. Protocols were approved by Institutional Animal Care and Use Committees at each respective institution and were compliant with NIH guidelines. Pdx-tTA mice in an FVB/n background (Holland et al. 2002) were mated with TetO-MyrAKT1 mice in a C57Bl/6 to generate Pdx-tTA;TetO-MyrAKT1 mice (Figure 12). LSL-KRasG12D (Jackson et al. 2001) in a 129Sv/J background and Pdx-Cre (Gu et al. 2002) mice in a C57Bl/6 were mated to generate Pdx-Cre;LSL-KRasG12D mice. The progeny were mated to generate litters that were genotyped using DNA extracted from tail snips (Wizard Genomic DNA Kit; Promega, Madison, WI) and were monitored for the tumor latency study. In total, 29 Pdx-

Cre;LSL-KRasG12D (designated KRasG12D mice) and 30 Pdx-tTA;TetO-MyrAKT1 (designated AKT1^{Myr}/KRasG12D mice) were followed. Animals were housed until times outlined and then killed in accordance with American Veterinary Medical Association guidelines. Single Nucleotide Polymorphism (SNP) analysis performed by Charles River Laboratories International (Wilmington, MA) on randomly selected mice that were re-derived for the < 1 year analysis revealed that the background of AKT1^{Myr}/KRasG12D mutant mice was ~ 60% C57Bl/6N.

Genotype Analysis

Reactions were assembled using JumpStart REDTaq ReadyMix (Sigma, St Louis, MO). Primers for polymerase chain reaction (PCR) detected presence of Pdx-Cre (5′-ATCGCTGATTTGTGTAGTCGGT-3′; 5′-CAACAGTTGCGCAGCCTGAATG-3′), mutant or non-recombined LSL-KRasG12D (5′-GTCGACAAGCTCATGCGGGTG-3′; 5′-AGCTAGCC-ACCATGGCTTGAGTACGTCTGCA-3′; 5′-CCTTTACAAGCGCACGCA-GACTGTAGA-3′), heterozygous knock-in for tTA into the endogenous Pdx gene (5′-ACCATGAACAGTGAGGAGCAGTAC-3′; 5′-GCGGGTTTCAGAGGAATTTGT-3′; 5′-TAGAAGGGGAAAGCTGGCAAG-3′; 5′-TCCAGATCGAAATCGTCTAGCG-3′), or presence of TetO-MyrAKT1 (5′-CTGGACTACTTGCACTCCGAGAAG-3′; 5′-CTGTGTAGGGTCCTTCTTGAGCAG-3′).

Histologic Analysis

Specimens were fixed in 10% neutral buffered formalin (Surgipath Leica, Buffalo Grove, IL) and paraffin embedded. Five-micrometer sections were cut with a rotary microtome (Leica). Histologic staining used SelecTech hematoxylin and eosin (H&E) reagents (Surgipath). Staining

with Alcian Blue or Trichrome (both from American MasterTech, Lodi, CA) was performed as per manufacturers' instructions.

Antigen retrieval for immunohistochemistry was optimized with sodium citrate (pH 6.0) or EDTA (pH 9.0; Leica). Primary antibodies were against phospho-AKT Ser473 (GeneTex, Irvine, CA), phospho-mTor Ser2448 (Cell Signaling Technology, Danvers, MA), phospho-p70S6K Thr389 (Upstate Cell Signaling, Temecula, CA or LifeSpan BioSciences, Seattle, WA), and phospho-p70S6K Thr389 (Cell Signaling Technology), mucin-4 (Muc-4; LifeSpan BioSciences), α-2 smooth muscle actin (α-SMA; Novus, Littleton, CO), cytokeratin 17/19 (Cell Signaling Technology), and Ki67 (Abcam, Cambridge, MA). Detection used Polymer Refine Detection reagents (Leica). A Bond-Max Immunostainer and Polymer Refine Detection reagents (Leica) were used.

Cell Culture

Primary cells were collected following the killing of mice, and cells were derived from phosphate-buffered saline–washed peritoneum and cultured using Dulbecco's modified Eagle's medium (Cellgro Mediatech, Manassas, VA) supplemented with 15% FBS, 2 mM l-glutamine, and 2 mM penicillin-streptomycin. Murine pancreatic cell cultures were maintained in Dulbecco's modified Eagle's medium/10% FBS supplemented with 2 mM l-glutamine and penicillin-streptomycin. Human cell lines were from American Type Culture Collection (Manassas, VA) and grown as recommended.

Genomic PCR

Genomic DNA was extracted (Wizard Genomic DNA Isolation Kit; Promega), and PCRs were performed with GoTaq Green Master Mix (Promega). Primers for PCR detected presence of Tp53 (5′-CTTGACACCTGATCGTTACTC-3′ and 5′-CAGTCCTAACCCCACAGGCGG-3′), p16Ink4a (5′-TGGTCACACGACTGGGCGATTG-3′ and 5′-GAATCGGGGTACGACCGAAAG-3′), p19Arf (5′-AGCATGGGTCGCAGGTTCTTGG-3′ and 5′-TTGAGGAGGACCGTGAAGCCGA-3′), and control glyceraldehyde 3-phosphate dehydrogenase or Gapdh (5′-AGGCCGGTGCTGAGTATGTC-3′ and 5′-TGCCTGCTTCACCACCTTCT-3′).

Western Blots

Whole-cell extracts were harvested from low passage cell cultures with 1 × cell lysis buffer (Cell Signaling Technology) for protein, 1 mM phenylmethylsulfonyl fluoride (Sigma), and 2 mM Halt protease and phosphatase inhibitor cocktail (Thermo, Waltham, MA). Protein was quantified using the Bradford method. For Western blot analysis, 60 μg of each protein extract was combined with Laemmli's sodium dodecyl sulfate sample buffer (final 1 ×) and denatured in a boiling water bath for 5 minutes. Precision Plus (Bio-Rad Laboratories, Hercules, CA) protein standard and total protein were separated on 12% sodium dodecyl sulfate–polyacrylamide gel electrophoresis gels using a Mini-Protean Tetra Cell (Bio-Rad) unit set for 15 minutes at 20 mA and then 1 hour at 40 mA constant current. Proteins were transferred to Hybond ECL Nitrocellulose (GE Healthcare Amersham, Pittsburgh, PA) at 25 V at 4°C for 2 hours using an XCell II Blot Module (Invitrogen Life Technologies, Grand Island, NY). Antibodies for Western blots were against total AKT,

phospho-AKT Ser473, and p53 (all from Cell Signaling Technology), mouse p16Ink4a (Santa Cruz Biotechnology, Santa Cruz, CA), mouse p19Arf (Abcam), and actin (Millipore, Billerica, MA). Secondary antibodies were anti-mouse (DyLight, Thermo) and anti-rabbit (IR Dye; LI-COR Biosciences, Lincoln, NE), and signals were visualized using an Odyssey Infrared Imaging System (LI-COR).

Results

Accelerated Frequency of PDACs in Double Mutant Mice Compared to Single Mutant Mice

The pancreatic tumor model uses the Pdx1 pancreas promoter to drive expression of myristoylated, membrane-targeted, and therefore activated AKT. Specifically, it uses a dual transgenic system with tetracycline operator (TetO) sequences fused to MyrAKT1 (Kovacic et al. 2003; Shiojima et al. 2005; Mukai et al. 2006), and then the progeny were crossed with Pdx-TetA (Pdx-tTA) knock-in mice expressing tTA in the pancreas (Holland et al. 2002). Resultant Pdx-tTA;TetO-MyrAKT1 transgenic mice were identified by genotyping (Figure 12).

Transgenic Lox-Stop-Lox (LSL) KRasG12D (Jackson et al. 2001) and Pdx-Cre (Gu et al. 2002) mice were expanded, and these parental mice were mated to obtain compound mice expressing Pdx-Cre–activated KRasG12D. Resultant Pdx-Cre;LSL-KRasG12D were then mated to Pdx-tTA;TetO-MyrAKT1 mice to generate pancreatic-specific active mutant KRasG12D, active $AKT1^{Myr}$, compound mutant $AKT1^{Myr}$/KRasG12D mice or non-mutant littermates. The progeny were genotyped and littermates were followed phenotypically to determine if there is cooperation between mutant active KRasG12D and $AKT1^{Myr}$ to accelerate malignancy and/or

metastasis and to establish a potentially clinically relevant pancreatic tumor model useful for future preclinical studies to test novel targeted therapies.

Figure 8 shows age in weeks when a carcinoma was detected in mice with compound AKT1^{Myr}/KRasG12D relative to mice with KRasG12D mutant alone. Kaplan-Meier curves (GraphPad Prism 5, San Diego, CA) were used to calculate median tumor detection at 54 weeks in AKT1^{Myr}/KRasG12D mice compared to 74 weeks in KRasG12D mice. At the median 54-week time point for AKT1^{Myr}/KRasG12D mice, 11 of 22 mice examined had developed early to full pancreatic carcinoma. In comparison, only one early carcinoma and one PDAC were found in seven age-matched KRasG12D mice, and tumor progression to PDAC was significantly delayed in a subset of KRasG12D mice until approximately 15 months of age. Overall, the number of mice found with early carcinoma to PDAC was 14 of 30 AKT1^{Myr}/KRasG12D and 13 of 29 KRasG12D mice, even though AKT1^{Myr}/KRasG12D mice declined in health earlier and could not be aged as far as KRasG12D mice. Four metastatic tumors were found in AKT1^{Myr}/KRasG12D mice at 8 to 12 months of age compared to 0 metastatic tumors in KRasG12D (Table 1). In contrast, littermates that were AKT1^{Myr} mice had a tendency to develop islet carcinomas (Figure 13), rather than ductal carcinomas, at a mean latency of 75 weeks in 6 of 24 mice. Because of the predominant islet carcinoma lineage in the AKT1^{Myr} subset, these mice were not characterized further in the context of this PDAC study.

Double AKT1^{Myr}/KRasG12D Mice at $\leq$ 1 Year of Age Exhibit PanINs and PDACs

In a separate experiment, compound mutant AKT1^{Myr}/KRasG12D mice were then studied within 12 months for the frequency of PanINs and metastatic PDACs. Nearly 77% of compound

AKT1^{Myr}/KRasG12D mice aged ≤ 1 year exhibited high-grade PanINs and or PDACs (Table 2). Four of 17 mice developed PDACs. This is consistent with the results from the Kaplan-Meier study, which showed median histologic detection of malignant tumor progression at 54 weeks in AKT1^{Myr}/KRasG12D mice (Figure 8).

AKT Pathway Effector Proteins Are Activated in Early PanINs and Metastatic PDACs

Immunohistochemistry using phosphorylation-specific antibodies depicted abundant AKT pathway signaling in PanINs and metastatic PDACs (Figure 9). Pathway markers, including phospho-AKT, phospho-mTor, and phospho-p70S6 kinase were found in the pancreas of both AKT1^{Myr}/KRasG12D (Figure 9A) and KRasG12D mice (Figure 9B). A possible mechanism may be increased proliferation, as detected by Ki67 staining, in the PanINs shown in Figure 9A (see Figure 14). Metastatic PDACs in AKT1^{Myr}/KRasG12D mice exhibited ascites and metastasis to liver or other abdominal sites, with abundant levels of phospho-AKT and elevated levels of phospho-mTor and phospho-p70S6 kinase at the metastatic sites (Figure 9C).

Markers of Tissue Remodeling in the Pancreas of Mice Undergoing Progression to PDAC

Alcian Blue and Muc-4 staining, markers of mucin expression, were evident in the pancreatic ducts found in proximity to PDACs. Importantly, Muc-4 is a mucin that has been implicated as a marker of pancreatic ductal tissue transformation in human PanINs and PDACs (Swartz et al. 2002). In mice, Muc-4 has also been shown to correlate with the progression of pancreatic cancer from PanIN lesions to PDAC (Rachagani et al. 2012). Staining for Muc-4 was found in ductal regions, as well as some acinar regions of AKT1^{Myr}/KRasG12D mice with PDAC (Figure 10).

Similarly, activation of pancreatic stellate cells near centroacinar cells has been implicated as contributing to desmoplastic or fibrotic areas in PDACs and frequently expresses α-SMA (Yen et al. 2002). Recurrent staining for trichrome and α-SMA was found around the acinar regions of pancreatic tissue with PDAC and PanIN lesions in AKT1^{Myr}/KRasG12D mice (Figure 10A, representative age 7 months) and KRasG12D mice (Figure 10B, representative age 12 months). Trichrome stain revealed mild to moderate fibrosis, reminiscent of desmoplasia. Intensity of trichrome stain was variable, as depicted by green-blue staining (Figure 15) in a 12-month-old AKT1^{Myr}/KRasG12D mouse. α-SMA staining was frequently detected in pancreatic acini exhibiting a myoepithelial distribution pattern.

Tumor Cells from Double Mutant Mice Exhibit High AKT Phosphorylation and Loss of Tumor Suppressors Known to be Important in Human Pancreatic Tumor Progression

Cell cultures were derived from three KRasG12D mice diagnosed with PanINs at age 10 to 11 months and also three AKT1^{Myr}/KRasG12D mice with preneoplastic lesions and/or PDACs at age 7 to 11 months of age. Western blot analysis revealed high levels of phosphorylated AKT in low passage cell cultures from AKT1^{Myr}/KRasG12D mice, relative to cells from KRasG12D mice and two human PDAC cell lines (Figure 11A). For mouse tumors cells, p53 tumor suppressor protein was retained in all cases. Tumor suppressor p16Ink4a protein expression was frequently downregulated in the cell cultures, with complete loss of p16Ink4a in one of the AKT1^{Myr}/KRasG12D PDAC cell cultures. P19Arf protein expression was also difficult to detect, and p19Arf protein was absent in the same PDAC cell culture with loss of p16Ink4a. Genomic PCR confirmed biallelic loss of the overlapping genes p16Ink4a and p19Arf, which reside at the Cdk2na locus, in tumor cells from an AKT1^{Myr}/KRasG12D mouse that developed PDAC (Figure

11B). Such homozygous losses of CDNK2A are common in human PDACs. Moreover, a tumorigenicity study with this same PDAC tumor cell culture revealed that it was capable of forming tumors in syngeneic mice without the mutant alleles at ~ 3 weeks after the orthotopic injection of 1×10^6 cells into mouse pancreas (Figure 16).

Discussion

Pancreatic mouse models targeting genes known to be mapped to the histologic and genetic profile of PDACs have been used to test cooperativity with KRas mutations, as reviewed elsewhere (Herreros-Villanueva et al. 2012). In most cases, the combination of the predisposing KRas mutation with loss of tumor suppressors, such as p16Ink4a or p53, greatly accelerates malignancy such that mice frequently die within a few months. In humans, according to 2014 American Cancer Society projections, the median age of pancreatic cancer detection is 71 years old and increases with age (http://www.cancer.org/acs/groups/content/@research/documents/document/acspc-038828.pdf). Moreover, in humans, the progression of PanINs to PDAC probably takes more than a decade to develop (Yachida et al. 2010). Thus, the rapid onset of pancreatic disease in compound KRas/tumor suppressor knockout mice has limited utility for studies relevant to disease in the elderly and with other non-genetic factors that contribute to disease and treatment. The overall objective of the current in vivo study was to combine two oncogenic changes important for cancer progression to accelerate tumorigenesis, while maintaining a time frame that would align more closely with the physiological progression observed in the human disease.

Recently, E17K mutations in the AKT1 pleckstrin homology domain have been found in human pancreatic intraductal papillary mucinous neoplasms (3 of 36), along with activating

mutations in PI3K or loss of PTEN (Garcia-Carracedo et al. 2013). AKT1 E17K mutations were not found in a previous study of PDACs (Bleeker et al. 2008), although the number of cases examined (12) was small. Thus, the role of the AKT1 E17K mutation is still being defined and may be context dependent. As proof of principle, we used an AKT1 construct with an N-terminal myristoylation sequence (MyrAKT1), one of the oldest known constitutively active mutants of AKT1 (Andjelković et al. 1997), to directly test the experimental in vivo role of constitutively active $AKT1^{Myr}$ in the progression from PanINs to PDAC. In contrast to the E17K mutation, the myristoylation sequence is well documented as directing AKT to the plasma membrane and facilitating constitutive activation (Kohn et al. 1996), which in turn has been shown to be important for oncogenic transformation (Sun et al. 2001).

In addition to active mutant AKT1, loss of the PTEN tumor suppressor protein or constitutive activation of receptor-mediated or upstream PI3K signaling is another means for constitutive activation of AKT isoforms (She et al. 2005; She et al. 2008). Moreover, it has been suggested that loss of PTEN function and active mutations of KRas may converge to facilitate tumor growth (Ogawa et al. 2005). In terms of previous mouse models of pancreatic cancer, it has been suggested that variations in phenotypes between Pdx-Cre–activated KRasG12D and Pdx-Cre;Ptenlox/lox mice may be attributed to differences in the relative expression of KRas and Pten within centroacinar and duct cells. Previously, it was shown that all mice with KRasG12D activation and Pten homozygous deletion succumb to cancer by 3 weeks of age, and compound mutant mice for KRasG12D and heterozygous for Ptenlox/+ show accelerated acinar-to-ductal metaplasia, PanINs, and PDAC within a year (Hill et al. 2010). The high levels of phosphorylated effectors downstream in the Pten/AKT signaling cascade may be a mechanism to facilitate the

ductal pancreatic tumor progression. In addition, Pdx-Cre;Pten−/− pancreatic knockout mice were shown to display progressive replacement of the acinar cells, with ductal structures that expressed mucins.

In the AKT1^{Myr}/KRasG12D model presented here, tumor onset was accelerated compared to that observed in the KRasG12D model. The first Kaplan-Meier analysis showed that AKT1^{Myr}/KRasG12D mice aged 8 to 16 months had the greatest incidence of early or late carcinomas (12/23 or 52% of the mice in this age group), with 4 metastatic tumors, compared to only 5 of 14 (35%) of the KRasG12D mice (Figure 8 and Table 1). Overall, only two KRasG12D mice with metastasis were found at > 16 months of age when more tumors were found in the KRasG12D group and at an age when only one AKT1^{Myr}/KRasG12D could be analyzed. The second AKT1^{Myr}/KRasG12D study used re-derived mice when the colony was transferred to a new institution. It focused on mice aged to 1 year (Table 2) and was consistent with the Kaplan-Meier analysis in finding PanINs and PDAC, some with metastasis at less than 1 year of age. We cannot rule out other factors that may contribute to the decline of health in the AKT1^{Myr}/KRasG12D mice, and these factors may come to light as we start analyzing the role of the AKT1^{Myr} construct in facilitating tissue changes by using the doxycycline-off inducible AKT1^{Myr} construct in future studies.

Here, we report that PDAC formation in the compound transgenic AKT1^{Myr}/KRasG12D mice mimicked a subset of histologic alterations found in human pancreatic tumor progression, KRasG12D and perhaps KRasG12D/Ptenlox/+ deficient mice. Consistently, we found phosphorylation of AKT and downstream mTor kinase and p70S6 kinase in AKT1^{Myr}/KRasG12D mice, both in early lesions and in metastatic PDACs (Figure 9). There also was extensive

remodeling of both ductal and acinar components, as evident by increased mucin, α-SMA, and nearby fibrosis. Similar to other reports implicating Muc-4 as a marker of pancreatic ductal tissue transformation in human PanINs and PDACs (Swartz et al. 2002), Muc-4 expression and overall Alcian Blue for both neural and acidic mucins was increased in the ductal components in PanINs and in focal regions of the PDACs in these mice (Figure 10). Similarly, moderate to abundant collagen in the stroma was evident in disrupted acinar regions and around abnormal ducts.

To examine common genetic changes that are known to be important in the pancreatic tumor progression cascade, tumor cells were derived from the mice predisposed to pancreatic tumor progression and examined for down-regulation or occasional biallelic loss of tumor suppressor genes commonly implicated in PDAC. Overall, the establishment of cell cultures from the KRasG12D mice was challenging, perhaps in part due to the inefficiency of developing full PDACs until mice had reached an advanced age. A limited number of primary cultures from AKT1^{Myr}/KRasG12D PDACs were established. Similar to human pancreatic tumors, genomic PCR and Western blot analysis confirmed biallelic loss of p16Ink4a and p19Arf tumor suppressor gene expression in representative PDAC cells from an AKT1^{Myr}/KRasG12D mouse (Figure 11). Moreover, staining for H&E and immunohistochemistry against cytokeratin 17/19 detected tumors from AKT1^{Myr}/KRasG12D PDAC cells when they were orthotopically re-injected into the pancreas of a syngeneic mouse to show tumorigenic potential (Figure 16).

Collectively, compound AKT1^{Myr}/KRasG12D mice exhibited accelerated PDAC development compared with KRasG12D mice, and the tumors in AKT1^{Myr}/KRasG12D mice showed histologic and genetic alterations that recapitulate those found in human pancreatic progression. Thus, this mouse model is likely to be of importance for preclinical testing of novel

therapeutics targeting KRas and/or PI3K/AKT signaling in pancreatic cancer. Future analysis of the AKT1^{Myr}/KRasG12D mouse model is expected to elucidate in vivo contexts in which AKT1 and KRas oncogenes interact in the pancreatic microenvironment to better facilitate treatment and overcome poor patient prognosis currently associated with this deadly disease. In particular, we suggest that the model may have added value for chemoprevention studies to block tumor progression at the PanIN or early carcinoma stage, perhaps before a stage where there is excessive desmoplastic damage and fibrosis.

Figures and Tables

Table 1: Mice with Pancreatic Carcinomas for Kaplan-Meier Analysis

	<8 months	8 to 16 months	>16 months	Total
$AKT1^{Myr}$/KRasG12D	1/6 mice*	12/23 mice (four metastases)	1/1 mouse (0 metastasis)	14/30
KRasG12D		5/14 mice (0 metastasis)	8/15 mice (two metastases)	13/29†

* $AKT1^{Myr}$/KRasG12D mice were collected at < 8 months primarily because of weight loss, although KRasG12D mice did not exhibit comparable issues.
†Other pathologies in aged KRasG12D mice ≥ 12 months of age included lymphomas, hepatocellular carcinoma, and lung adenocarcinoma; a lung adenocarcinoma was found in an aged-matched $AKT1^{Myr}$/KRasG12D mouse.

Table 2: Representative Histology of AKT1^{Myr}/KRasG12D Mice up to 1 Year of Age

Mouse ID	Genotype	Age (Wks)	PanIN Low Grade	PanIN High Grade	PDAC
173	Akt/Ras	13.6	X	X	
524	Akt/Ras	20.6	X		
179	Akt/Ras	27.7	X	X	X$^{\Theta}$
505	Akt/Ras	29.1	X		
547	Akt/Ras	29.4	X	X	
192	Akt/Ras	31.1	X	X	
195(562)	Akt/Ras	31.1	X	X	X$^{\Theta}$
160	Akt/Ras	31.9	X		
161	Akt/Ras	31.9	X	X	
165	Akt/Ras	31.9	X	X	
139	Akt/Ras	38.4	X		
157	Akt/Ras	46.4		X	
533	Akt/Ras	43.1		X	X*†
9C	Akt/Ras	46.4		X	X*
167	Akt/Ras	48.4		X	
106	Akt/Ras	50.9	X	X	
177-2	Akt/Ras	52.9		X	
			12 of 17	13 of 17	4 of 17

Fibroadenomatous lesions are also found in 173, 524, 547, 160, 161, 165, 157, 106, and 177-2. Cystic papillary lesion, early cystoadenoma, and intraductal papillary tumor are found in 524, 192, and 167, respectively. (* metastasis, †carcinomatosis, $^{\Theta}$papillary)

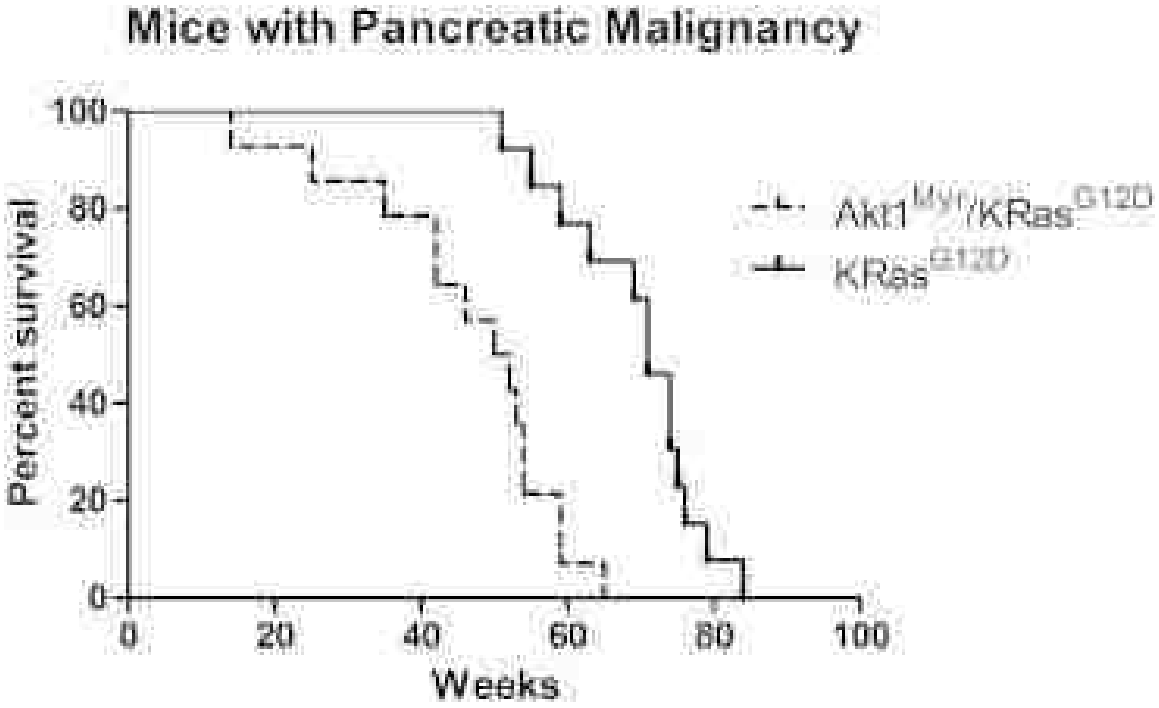

Figure 8: Tumor Latency in AKT1^{Myr}/KRasG12D versus KRasG12D mice.*

AKT1^{Myr}/KRasG12D mice (broken line) developed pancreatic tumors (PDACs) at a faster rate than KRasG12D mice (solid line). Curves were significantly different with a *P* value < .0001 by log rank (Mantel-Cox) or Gehan-Breslow-Wilcoxon tests (GraphPad Prism 5).

*Figure assembled by corresponding author, Dr. Deborah D Altomare, and pathologist, Dr. Andres Klein-Szanto, at Fox Chase Cancer Center.

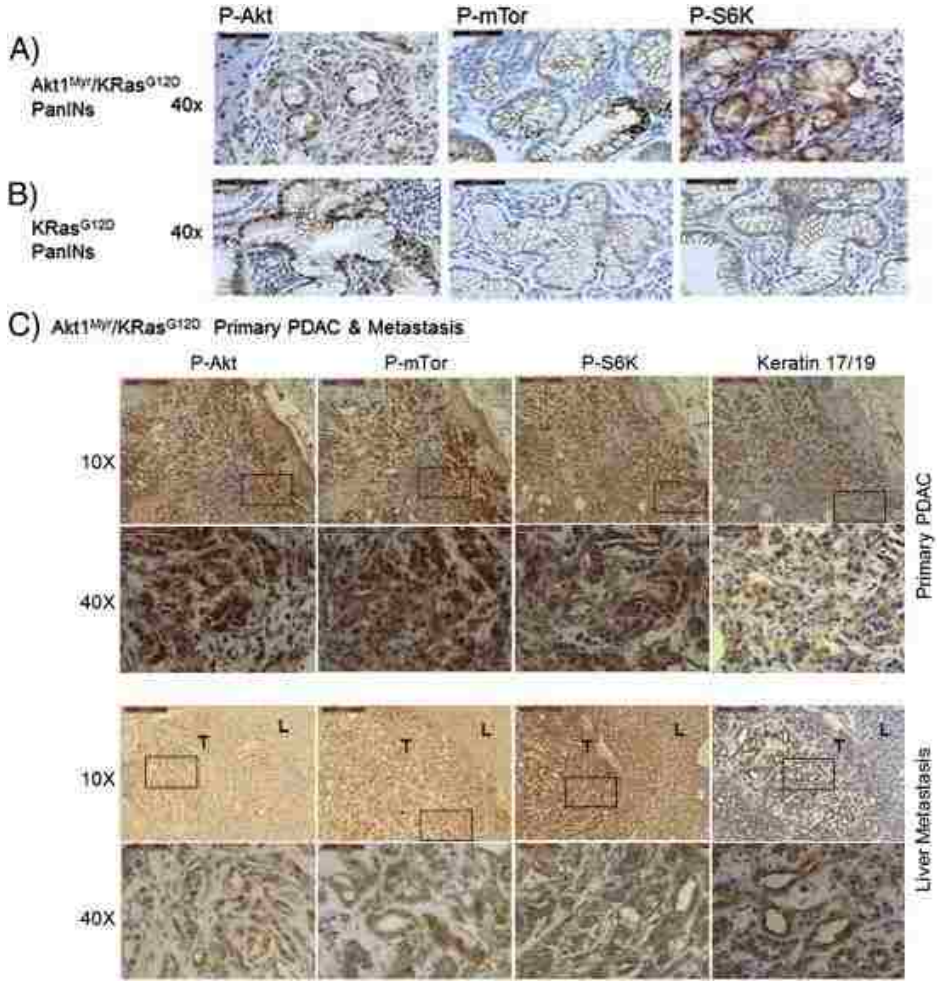

Figure 9: Activation of the AKT/mTor/S6K Pathway in Pancreatic Tumor Progression.*

The panels show representative early ductal pancreatic lesions, similar to human low-grade PanINs, with strong activation (brown DAB stain) for phospho-AKT, phospho-mTor, and phospho-p70S6 kinase in PanINs of (A) AKT1^{Myr}/KRasG12D and (B) KRasG12D mice (40 × objective). (C) Immunohistochemical staining of primary PDAC and metastatic specimens from a ~ 43-week-old AKT1^{Myr}/KRasG12D mouse for phospho-AKT, phospho-mTor, and phospho-p70S6 kinase and cytokeratin 17/19; a set of panels corresponding to PDAC metastasis to liver (10 × objective and a scale bar corresponding to 200 μm, with boxed-in close ups from the 40 × objective and a scale bar of 50 μm). In the metastasis panels, L = liver and T = tumor. Images were acquired using a Leica DM 2000 microscope with a digital DFC 295 camera.

*Figure assembled by co-first authors, Toya Albury-Warren and Veethika Pandey.

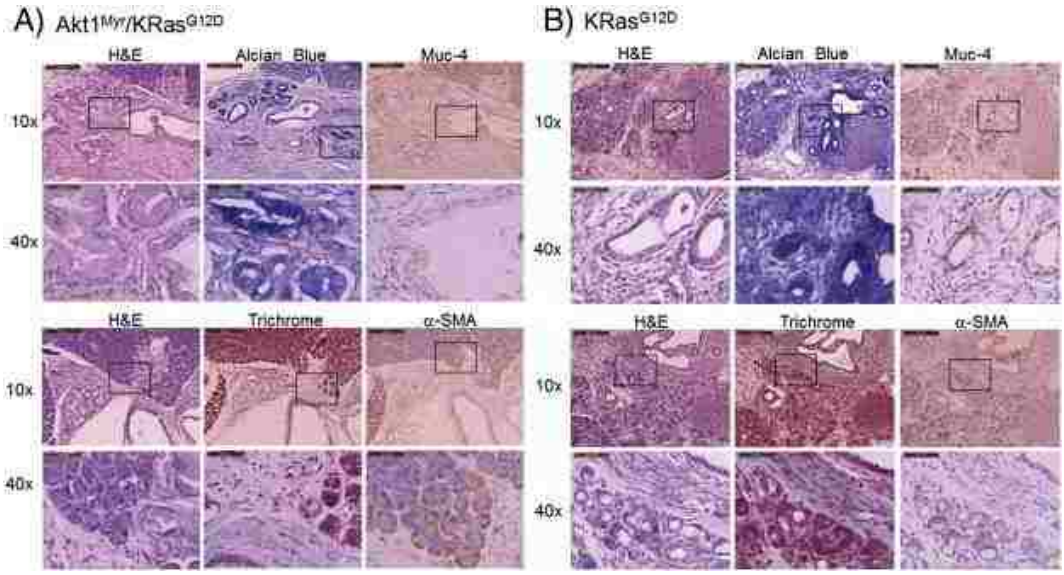

Figure 10: Pancreatic histologic alterations in AKT1^{Myr}/KRasG12D and KRasG12D mice.*

The panels from (A) AKT1^{Myr}/KRasG12D and (B) KRasG12D mice show staining of representative pancreatic tissues. Sections showed staining for H&E, Alcian Blue staining of ducts for detection of mucin (dark blue), Muc-4 (brown color) in areas of ducts, trichrome stain of red acinar cells, and green-blue collagen-rich fibrotic areas of the PDAC tumor and α-SMA marker (brown color) in areas of acinar cells near fibrotic regions. Boxed-in highlighted areas (10 × objective, scale bar of 200 μm) were magnified for a focal view with the 40 × objective (scale bar of 50 μm).

*Figure assembled by co-first author, Sarah Gitto.

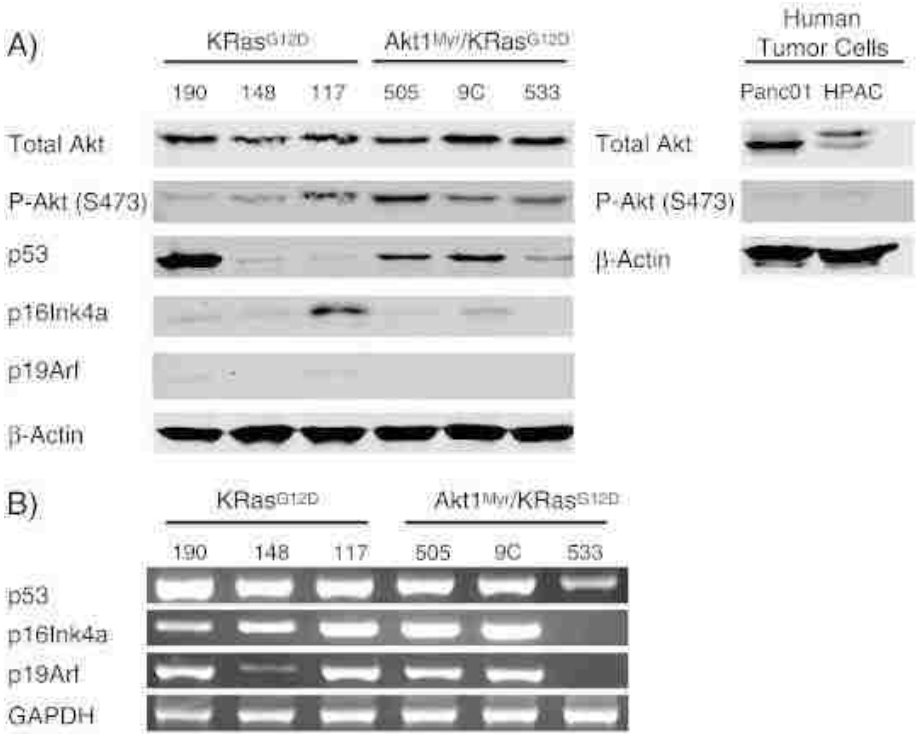

Figure 11: Phospho-AKT and tumor suppressors in mouse and human pancreatic tumor cells.*

(A) (Left) Representative Western blots from each of three KRasG12D (mouse numbers 190, 148, and 117) and three AKT1^{Myr}/KRasG12D (mouse numbers 505, 9C, and 533) tumor cell cultures analyzed for expression of total AKT, phospho-AKT (Ser473), and tumor suppressor genes *p53*, *p16Ink4a*, and *p19Arf*. Actin is a loading control. (Right) Representative human pancreatic tumor cell lines run adjacent to mouse tumor cells showing relative amount of total AKT, phospho-AKT (Ser473), and actin. (B) Genomic DNA PCR showing retention or loss of *Tp53*, *p16Ink4a*, or *p19Arf*.

*Figure assembled by co-first author, Veethika Pandey, and author Lina Spinel.

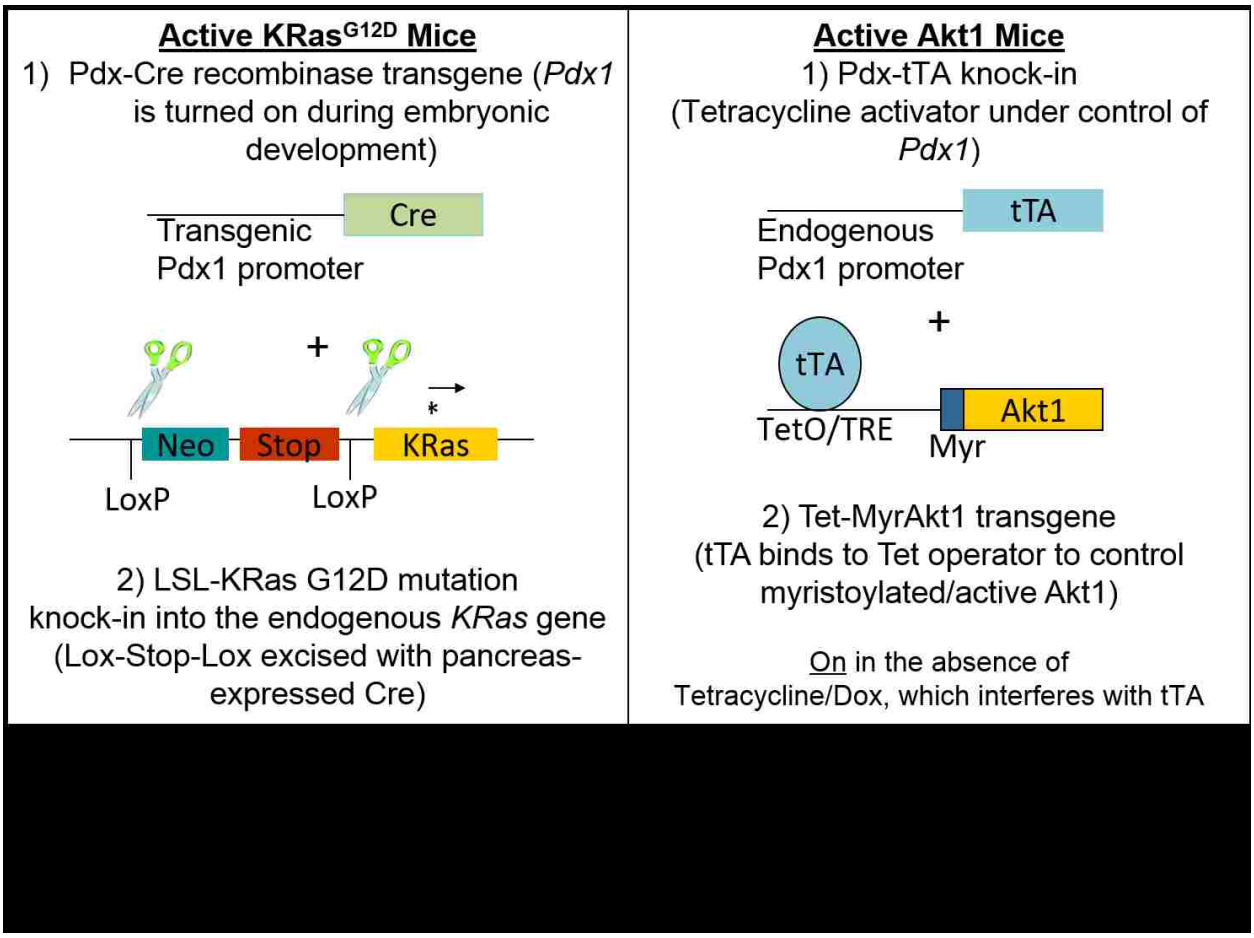

Figure 12: General construct scheme for generating genetically engineered mice.

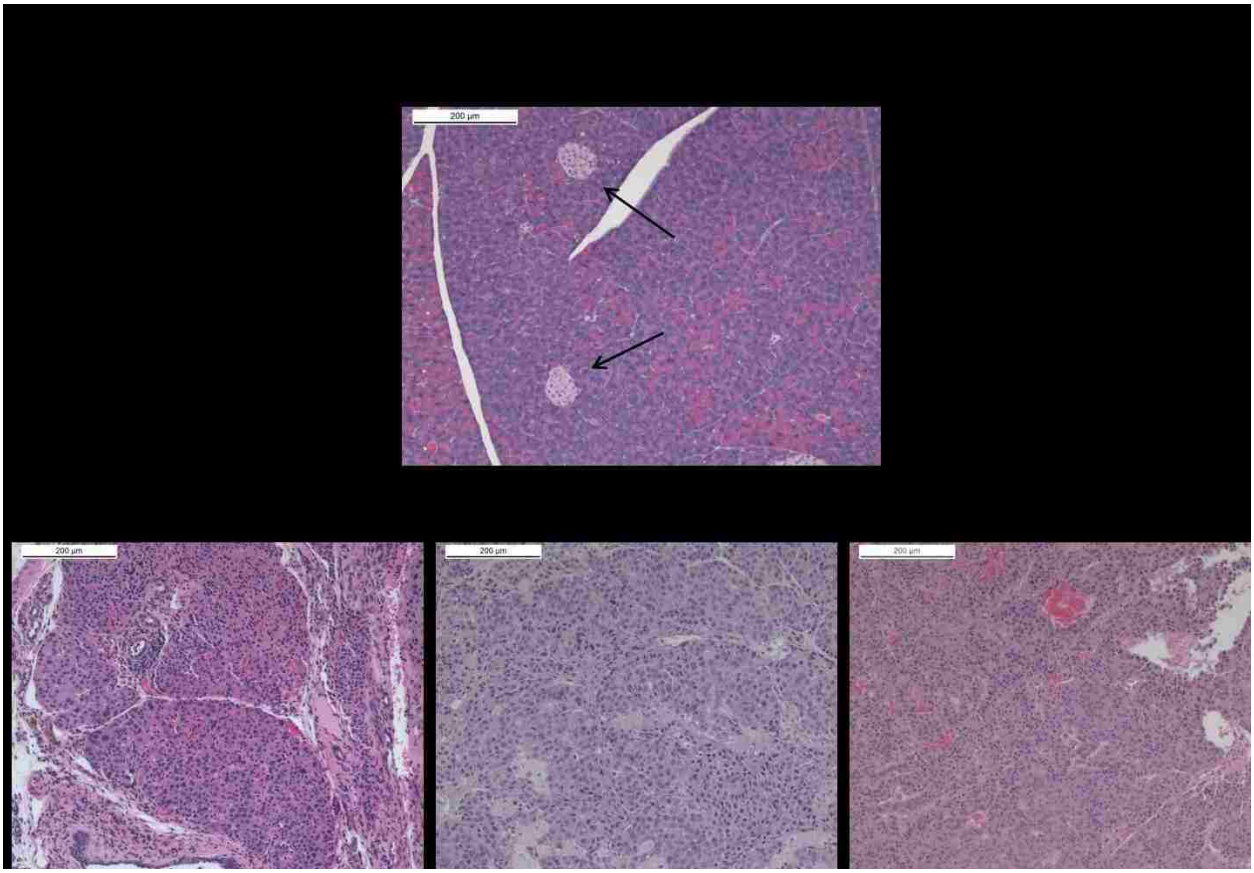

Figure 13: Representative islet carcinomas from aged AKT1^{Myr} mice.

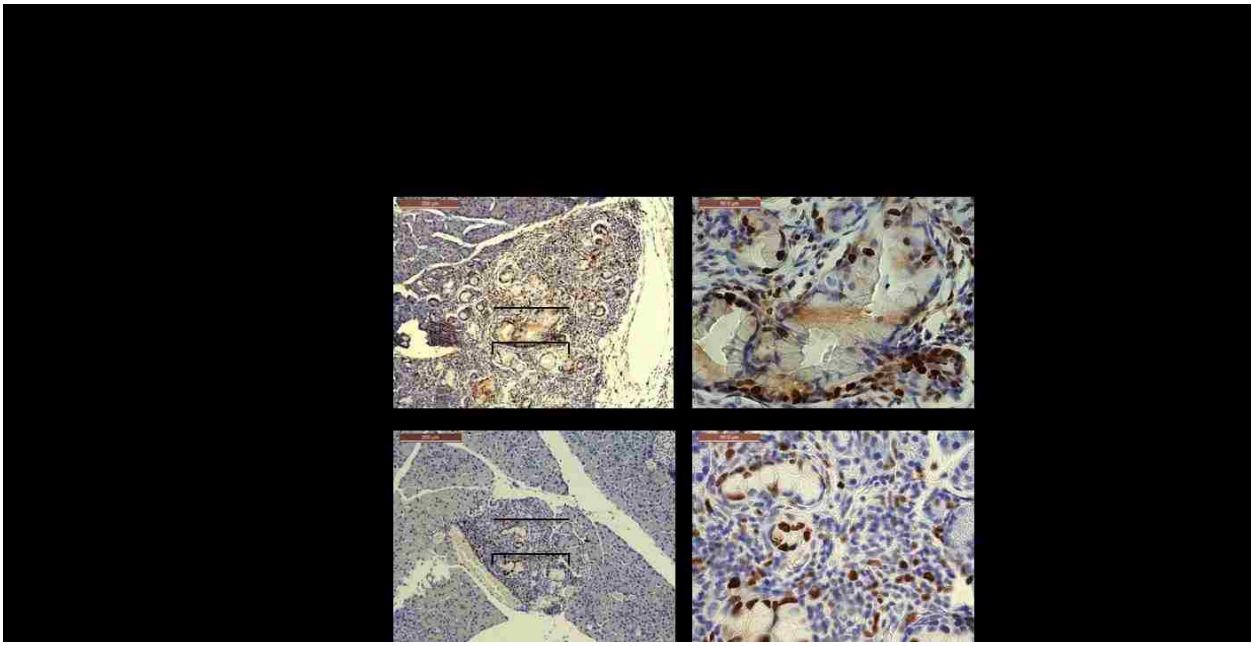

Figure 14: Ki67 immunohistochemistry for representative PanINs shown in Figure 2, *A* and *B*.

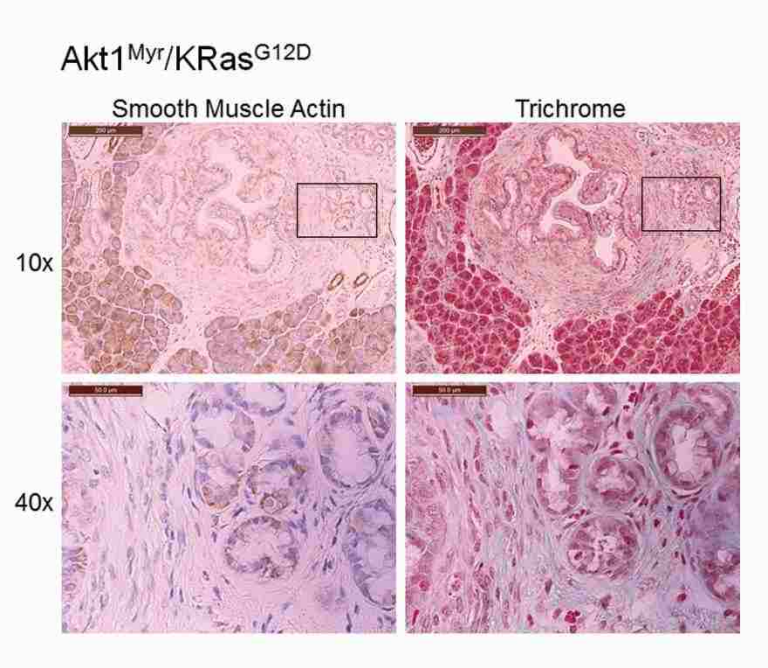

Figure 15: Representative α-SMA and trichrome staining of pancreas from a 12-month-old AKT1^{Myr}/KRasG12D mouse.

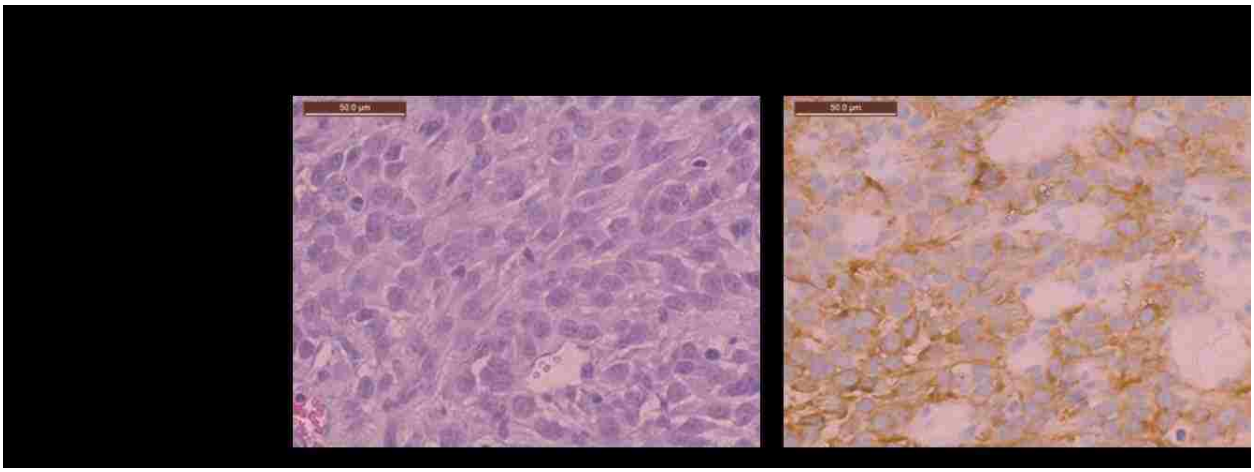

Figure 16: Representative H&E and cytokeratin 17/19 of orthotopically injected AKT1^{Myr}/KRasG12D PDAC cells (from mouse 533) into a syngeneic mouse that lacked corresponding mutant alleles.

Primary cell culture derived from a representative AKT1^{Myr}/KRasG12D mouse (histology shown in Fig 2c) was tested for tumorigenicity. One million cells suspended in 50μL PBS were orthotopically injected into the head of the pancreas of wild-type syngeneic mice using 28 ½ G syringes. Tumor growth was monitored by ultrasound imaging and detectable tumor growth was seen 1 week post tumor cell inoculation. The representative tumor was collected at 3 weeks.

List of References

Alliouachene S, Tuttle RL, Boumard S, Lapointe T, Berissi S, Germain S, Jaubert F, Tosh D, Birnbaum MJ, & Pende M 2008 Constitutively active Akt1 expression in mouse pancreas requires S6 kinase 1 for insulinoma formation. *J Clin Invest***118** 3629–3638.

Altomare DA, Tanno S, De Rienzo A, Klein-Szanto A, Skele KL, Hoffman JP, & Testa JR 2003 Frequent activation of AKT2 kinase in human pancreatic carcinomas. *J Cell Biochem***87** 470–476.

Andjelković M, Alessi DR, Meier R, Fernandez A, Lamb NJ, Frech M, Cron P, Cohen P, Lucocq JM, & Hemmings BA 1997 Role of translocation in the activation and function of protein kinase B. *J Biol Chem***272** 31515–31524.

Bleeker FE, Felicioni L, Buttitta F, Lamba S, Cardone L, Rodolfo M, Scarpa A, Leenstra S, Frattini M, & Barbareschi M 2008 AKT1(E17K) in human solid tumours. *Oncogene***27** 5648–5650.

Cheng JQ, Ruggeri B, Klein WM, Sonoda G, Altomare DA, Watson DK, & Testa JR 1996 Amplification of AKT2 in human pancreatic cells and inhibition of AKT2 expression and tumorigenicity by antisense RNA. *Proc Natl Acad Sci U S A***93** 3636–3641.

Elghazi L, Weiss AJ, Barker DJ, Callaghan J, Staloch L, Sandgren EP, Gannon M, Adsay VN, Bernal-Mizrachi E 2009 Regulation of pancreas plasticity and malignant transformation by Akt signaling. *Gastroenterology***136** 1091–1103.

Eser S, Reiff N, Messer M, Seidler B, Gottschalk K, Dobler M, Hieber M, Arbeiter A, Klein S, & Kong B 2013 Selective requirement of PI3K/PDK1 signaling for Kras oncogene-driven pancreatic cell plasticity and cancer. *Cancer Cell***23** 406–420.

Foo WC, Rashid A, Wang H, Katz MH, Lee JE, Pisters PW, Wolff RA, Abbruzzese JL, Fleming JB, & Wang H 2013 Loss of PTEN Expression Is Associated with Recurrence and Poor Prognosis in Patients with Pancreatic Ductal Adenocarcinoma. *Hum Pathol***44** 1024–1030.

Garcia-Carracedo D, Turk AT, Fine SA, Akhavan N, Tweel BC, Parsons R, Chabot JA, Allendorf JD, Genkinger JM, & Remotti HE 2013 Loss of PTEN expression is associated with poor prognosis in patients with intraductal papillary mucinous neoplasms of the pancreas. *Clin Cancer Res***19** 6830–6841.

Gu G, Dubauskaite J, & Melton DA 2002 Direct evidence for the pancreatic lineage: NGN3 + cells are islet progenitors and are distinct from duct progenitors. *Development***129** 2447–2457.

Hansel DE, Kern SE, & Hruban RH 2003 Molecular pathogenesis of pancreatic cancer. *Annu Rev Genomics Hum Genet***4** 237–256.

Herreros-Villanueva M, Hijona E, Cosme A, & Bujanda L 2012 Mouse models of pancreatic cancer. *World J Gastroenterol***18** 1286–1294.

Hill R, Calvopina JH, Kim C, Wang Y, Dawson DW, Donahue TR, Dry S, & Wu H 2010 PTEN loss accelerates KrasG12D-induced pancreatic cancer development. *Cancer Res***70** 7114–7124.

Hingorani SR, Petricoin EF, Maitra A, Rajapakse V, King C, Jacobetz MA, Ross S, Conrads TP, Veenstra TD, & Hitt BA 2003 Preinvasive and invasive ductal pancreatic cancer and its early detection in the mouse. *Cancer Cell***4** 437–450.

Holland AM, Hale MA, Kagami H, Hammer RE, & MacDonald RJ 2002 Experimental control of pancreatic development and maintenance. *Proc Natl Acad Sci U S A***99** 12236–12241.

Hruban RH, Wilentz RE, & Kern SE 2000 Genetic progression in the pancreatic ducts. *Am J Pathol***156** 1821–1825.

Jackson EL, Willis N, Mercer K, Bronson RT, Crowley D, Montoya R, Jacks T, & Tuveson DA 2001 Analysis of lung tumor initiation and progression using conditional expression of oncogenic K-ras. *Genes Dev***15** 3243–3248.

Kohn AD, Summers SA, Birnbaum MJ, & Roth RA 1996 Expression of a constitutively active Akt Ser/Thr kinase in 3 T3-L1 adipocytes stimulates glucose uptake and glucose transporter 4 translocation. *J Biol Chem***271** 31372–31378.

Kovacic S, Soltys CLM, Barr AJ, Shiojima I, Walsh K, & Dyck JR 2003 Akt activity negatively regulates phosphorylation of AMP-activated protein kinase in the heart. *J Biol Chem***278** 39422–39427.

Mukai Y, Rikitake Y, Shiojima I, Wolfrum S, Satoh M, Takeshita K, Hiroi Y, Salomone S, Kim HH, & Benjamin LE 2006 Decreased vascular lesion formation in mice with inducible endothelial-specific expression of protein kinase Akt. *J Clin Invest***116** 334–343.

Ogawa K, Sun C, & Horii A 2005 Exploration of genetic alterations in human endometrial cancer and melanoma: distinct tumorigenic pathways that share a frequent abnormal PI3K/AKT cascade. *Oncol Rep***14** 1481–1485.

Rachagani S, Torres MP, Kumar S, Haridas D, Baine M, Macha MA, Kaur S, Ponnusamy MP, Dey P, & Seshacharyulu P 2012 Mucin (Muc) expression during pancreatic cancer progression in spontaneous mouse model: potential implications for diagnosis and therapy. *J Hematol Oncol***5** 68.

She QB, Chandarlapaty S, Ye Q, Lobo J, Haskell KM, Leander KR, DeFeo-Jones D, Huber HE, & Rosen N 2008 Breast tumor cells with PI3K mutation or HER2 amplification are selectively addicted to Akt signaling. *PLoS One***3** 3065.

She QB, Solit DB, Ye Q, O'Reilly KE, Lobo J, & Rosen N 2005 The BAD protein integrates survival signaling by EGFR/MAPK and PI3K/Akt kinase pathways in PTEN-deficient tumor cells. *Cancer Cell***8** 287–297.

Shiojima I, Sato K, Izumiya Y, Schiekofer S, Ito M, Liao R, Colucci WS, & Walsh K 2005 Disruption of coordinated cardiac hypertrophy and angiogenesis contributes to the transition to heart failure. *J Clin Invest***115** 2108–2918.

Stanger BZ, Stiles B, Lauwers GY, Bardeesy N, Mendoza M, Wang Y, Greenwood A, Cheng KH, McLaughlin M, & Brown D 2005 Pten constrains centroacinar cell expansion and malignant transformation in the pancreas. *Cancer Cell***8** 185–195.

Sun M, Wang G, Paciga JE, Feldman RI, Yuan ZQ, Ma XL, Shelley SA, Jove R, Tsichlis PN, & Nicosia SV 2001 AKT1/PKBalpha kinase is frequently elevated in human cancers and its constitutive activation is required for oncogenic transformation in NIH3T3 cells. *Am J Pathol***159** 431–437.

Swartz MJ, Batra SK, Varshney GC, Hollingsworth MA, Yeo CJ, Cameron JL, Wilentz RE, Hruban RH, & Argani P 2002 MUC4 expression increases progressively in pancreatic intraepithelial neoplasia. *Am J Clin Pathol***117** 791–796.

Yachida S, Jones S, Bozic I, Antal T, Leary R, Fu B, Kamiyama M, Hruban RH, Eshleman JR, & Nowak MA 2010 Distant metastasis occurs late during the genetic evolution of pancreatic cancer. *Nature***467** 1114–1117.

Yen TW, Aardal NP, Bronner MP, Thorning DR, Savard CE, Lee SP, & Bell RH, Jr 2002 Myofibroblasts are responsible for the desmoplastic reaction surrounding human pancreatic carcinomas. *Surgery***131** 129–134.

CHAPTER 3:
PREDIABETES LINKED TO EXCESS GLUCAGON IN TRANSGENIC MICE WITH PANCREATIC ACTIVE AKT1

Introduction

AKT, a serine/threonine kinase, is downstream of phosphatidylinositol 3-kinase (PI3K) and growth factor receptors (e.g., epidermal growth factor receptor, EGFR), and is a hallmark signaling protein predominantly recognized for regulation of cell survival, growth, and proliferation. AKT signals through the phosphorylation and subsequent activation or inhibition of downstream substrates, such as mammalian target of rapamycin complex 1 (mTORC1) or glycogen synthase kinase 3 beta (GSK-3β), respectively (Hemmings & Restuccia 2012). AKT hyperactivation in various cancers has been studied (Altomare & Testa 2005; Cheung & Testa 2013), while its role in glucose metabolism has been noted, but comparatively overlooked until analysis of AKT isoform knockout mice.

Although analogous in structure, AKT isoforms (AKT1, AKT2, and AKT3) are encoded by three different genes, which are differentially expressed in tissues and have varying functions (Hay 2011). While AKT1 is ubiquitously expressed in mammalian tissues, it was initially deemed unnecessary for glucose homeostasis as AKT1 knockout mice (AKT1-/-) have impaired fetal and adulthood growth, but normal glucose tolerance and insulin signaling (Cho et al. 2001). AKT3 is primarily expressed in the brain and was also reported unnecessary for glucose homeostasis with AKT3-/- mice exhibiting reduced brain size and weight, but normal glucose regulation (Tschopp et al. 2005). In contrast, AKT2 is highly expressed in insulin responsive tissues and has been identified as a primary regulator of glucose metabolism, as AKT2 knockout mice (AKT2-/-) are

prediabetic with insulin resistance, hyperinsulinemia, and glucose intolerance (Cho et al. 2001; Garofalo et al. 2003).

A role for AKT1 in glucose homeostasis became evident with the metabolic analysis of compound isoform knockout mice (Chen et al. 2009). Similar to $AKT2^{-/-}$ mice, $AKT1^{+/+}AKT2^{-/-}AKT3^{-/-}$ mice were mildly diabetic suggesting that the loss of AKT3 was inconsequential. Conversely, haplodeficiency of AKT1 in $AKT2^{-/-}$ mice resulted in a more severe diabetic phenotype, characterized by fed and fasted hyperglycemia, glucose intolerance, insulin resistance, and hyperinsulinemia. Additional crosses of $AKT1^{+/-}AKT2^{-/-}$ mice with mice haplodeficient for tumor suppressor phosphatase and tensin homolog (PTEN+/-), an upstream regulator of AKT activation, significantly improved glucose homeostasis, and demonstrated the compensatory nature and importance of AKT1, contrary to previous reports (Cho et al. 2001). Although AKT1 hyperactivation has been frequently observed in pancreatic cancers (Schlieman et al. 2003; Missiaglia et al. 2010), there are limited studies regarding AKT1 hyperactivation and glucose homeostasis, except for attempts to improve the success rates of human islet transplantation therapy for diabetic patients (Bernal-Mizrachi et al. 2001; Tuttle et al. 2001; Kushner et al. 2005; Stiles et al. 2006;). Hyperactivation of AKT1 in pancreatic β–cells, via PTEN deletion (Kushner et al. 2005; Stiles et al. 2006) or in mice with a myristoylated AKT1 (Bernal-Mizrachi et al. 2001; Tuttle et al. 2001) under expression of a rat insulin promoter (RIP) led to hypoglycemia, hyperinsulinemia, and improved glucose tolerance, due to increased β–cell mass, size, and proliferation.

We recently characterized aged mice with myristoylated, membrane-bound AKT1 ($AKT1^{Myr}$) expressed using the Pdx promoter (Albury et al. 2015) and found that ~25% of mice

developed islet cell carcinomas after one year of age. Here we report that this strain of mice exhibit non-fasted hyperglycemia as early as weaning and fasted hyperglycemia by 20 weeks of age, thus presenting a potentially unique opportunity to study the mechanistic cross-talk between diabetes and cancer. We show that the pre-diabetic phenotype can be attributed to the $AKT1^{Myr}$ transgene, as it is tetracycline-regulatable, and down regulation of the $AKT1^{Myr}$ transgene reduced the non-fasted and fasted hyperglycemia to wild type levels. Collectively, metabolic characterization of the $AKT1^{Myr}$ mice revealed a novel glucagon-mediated mechanism by which AKT1 hyperactivation affects glucose homeostasis.

Materials and Methods

Genetically Engineered Mice

All mice were housed and handled according to protocols approved by the University of Central Florida (UCF) Institutional Animal Care and Use Committee at the AAALAC accredited UCF Lake Nona Animal Facility. Transgenic mice with activation of AKT1 (Pdx-tTA;TetO-MyrAKT1) were mated as previously described (Albury et al. 2015). At 3 weeks, the pups were weaned and tail snipped for DNA extraction and genotyping, as previously described (Albury et al. 2015). Mice with TetO-MyrAKT1, but lacking the knock-in Pdx-tTA, were classified as normal or wild-type litter mates. Mice with Pdx-tTA and TetO-MyrAKT1 were classified as $AKT1^{Myr}$ mice having constitutively active AKT1 in the pancreas. Litters were placed on a standard control diet or a doxycycline diet (BioServ, Frenchtown, NJ), which shuts off $AKT1^{Myr}$ transgene expression. All mice were euthanized according to American Veterinary Medical Association guidelines.

Genotyping Analysis

Primers for polymerase chain reactions (PCR) for $AKT1^{Myr}$ mice were previously described (Albury et al. 2015). AKT2KO mice were obtained from J. R. Testa (Fox Chase Cancer Center, Philadelphia, PA), and PCR primers detected the presence of wild-type or knockout AKT2 (5'-GATGAACTTCAGGGTCAGCTT-3'; 5'-AGAGCTTCAGTGGATAGCCTA-3'; 5'-TCTCTGTCACCTCCCCATGAG-3').

Histological Analysis

Pancreatic tissue was fixed in 10% neutral buffered formalin (Surgipath Leica, Buffalo Grove, IL) and embedded in paraffin for sectioning and processing as previously described (Albury et al. 2015). Slides were stained for hematoxylin and eosin (Surgipath) or immunohistochemistry using the Polymer Refine Detection reagents (Leica) on the Bond-Max immunostainer (Leica). Antigen retrieval was optimized using sodium citrate (pH 6) or EDTA (pH 9) buffers (Leica). The following antibodies were used: phospho-AKT Ser473 (GeneTex, Irvine, CA), also phospho-mTor Ser2448, phospho-S6 Ser235/236, glucagon, and insulin (all from Cell Signaling Technology, Danvers, MA). All slides processed on the immunostainer were run with a negative control, which was treated with antibody diluent instead of the primary antibody, to ensure antibody specificity. Images were taken using a Leica DM 2000 microscope with 5X, 10X, or 40X objectives. Islet size was measured in the whole pancreas of three mice per genotype. The mice selected had no significant lesions (NSL) at the time of necropsy, as described by a pathologist. The pancreas was sectioned into 5μm sections and every 25th section was H&E stained. A total of 50 islets from three sections were analyzed per mouse. Islet diameter was

determined using measuring tools available on an Axio Imaging System (Zeiss, Oberkochen, Germany).

Blood Glucose Measurement

Blood glucose levels were measured using a Contour glucometer (Bayer, Mississauga, Ontario, Canada) at weaning, 5-, 7-, 9-, and 12 weeks. Weaning was at 3 weeks of age. Blood glucose levels were measured randomly, between 9 AM and 10 AM, or after an overnight fast.

Glucose Tolerance Test

Mice were fasted overnight, weighed (g), intraperitoneal (IP) injected with 2g/kg D-glucose (Fisher, Waltham, MA) and blood glucose tested with a glucometer before injection, 15-, 30-, 45-, 60-, and 120 minutes after injection. Blood glucose (mg/dL) versus time (minutes) was plotted and the area under the curve was calculated using Graph Pad Prism 5 (Graph Pad Software, La Jolla, CA). Blood was collected, via cheek bleeds, into serum collection tubes at 0 and 45 minutes after injection. The serum was separated and stored at -80°C until analysis with Mercodia Glucagon and Ultrasensitive Mouse Insulin ELISAs (Mercodia, Uppsala, Sweden). The HOMA-IR [(fasted glucose x fasted insulin)/405] was calculated using the fasted blood glucose and fasted serum insulin levels acquired during the glucose tolerance test (Grote et al. 2013).

Insulin Tolerance Test

Mice were fasted for 2 hours, weighed (g), IP injected with 2 IU/kg porcine insulin (Sigma, Milwaukee, WI), and blood glucose tested with a glucometer before injection, 15-, 30-, 45-, and 60 minutes

after injection. Blood glucose (mg/dL) versus time (minutes) was plotted and the area under the curve was calculated (GraphPad).

Insulin Stimulation

Mice were fasted overnight, weighed (g), anesthetized using isoflurane, and injected with porcine insulin (10 IU/kg) (Sigma) or saline via the inferior vena cava. After two minutes mice were euthanized and the following tissues were snap frozen in liquid nitrogen: pancreas, liver, perigonadal adipose tissue, and skeletal muscle. Tissues were homogenized using 15 mg Zirconium oxide beads (1.0 mm for skeletal muscle and 0.5 mm for adipose, liver, and pancreas) with the Bullet Blender Homogenizer BBX24 (Next Advance, Averill Park, NY, USA). Proteins were extracted for ELISA analysis for AKT, AKT (pS473), Insulin Receptor (IR), and IR (pY1158) (all from Invitrogen, Camarillo, CA). Data was analyzed using a four parameter algorithm to construct the best fitting curve.

Statistical Analysis

Results are reported as mean ± SEM. Comparisons were made between two and more than two groups using unpaired or paired student's t-tests and two-way Anova followed by student's t-tests within groups, respectively. All analysis used Graph Pad Prism 5 with significance accepted at a P value of <0.05. Letters were used to illustrate significance as multiple groups are being compared. Groups that do not share the same letter display a statistical significance of $p<0.05$.

Results

AKT1^{Myr} transgenic mice have tetracycline-regulatable AKT/mTOR pathway activation in the pancreas.

The AKT1^{Myr} construct uses the Pdx1 promoter, which is important for pancreas development in utero and postnatal β-cell maintenance (Holland et al. 2002), to drive the expression of myristoylated, and therefore active AKT1 within different pancreatic cell lineages. Expression of the AKT1^{Myr} transgene is inhibited in the presence of the tetracycline analogue doxycycline. Immunohistochemistry (Figure 17A), using phospho-specific antibodies, validated increased phosphorylated or active AKT1, along with its downstream substrates mTORC1 and S6, in the islets of AKT1^{Myr} mice given standard feed, as compared to wild-type mice on standard feed and doxycycline fed AKT1^{Myr} mice. To quantify this result, protein was extracted from insulin-stimulated pancreatic tissue and measured via ELISA (Figure 17B), confirming significantly elevated ($p<0.001$) AKT1 phosphorylation (Ser 473), and thus activation in AKT1^{Myr} mice versus wild type mice. Pancreatic levels of phosphorylated AKT1 (Ser 473) were eight times greater in AKT1^{Myr} mice than wild type mice, while phosphorylated AKT1 levels in doxycycline fed AKT1^{Myr} mice were equal to those of wild type mice, confirming the ability of doxycycline to turn off the transgene. Doxycycline treatment began at weaning and continued for 2 weeks, which was sufficient to decrease the activation of the AKT/mTOR pathway to wild-type levels. There was no significant difference in total AKT between groups.

Reversible, non-fasted and fasted hyperglycemia in AKT1^{Myr} transgenic mice

At weaning, mice were tail snipped for genotyping and blood glucose tested. AKT1^{Myr} mice ($n=10$), regardless of sex (Figure 18G), had significantly higher ($p<0.0001$) non-fasted blood

glucose levels at weaning than wild-type littermates (Figure 18A). Non-fasted blood glucose levels were monitored biweekly for 9 weeks following weaning, and similarly, $AKT1^{Myr}$ mice had significantly higher ($p=0.0031$) non-fasted blood glucose levels at 12 weeks of age compared to wild-type mice (Figure 18A).

To confirm that the non-fasted hyperglycemia was due to the $AKT1^{Myr}$ transgene expression, doxycycline was administered to mice in order to turn off the transgene. Mating cages were arranged with half receiving standard feed and half receiving doxycycline feed for in utero exposure. Feeding regimens were continued at weaning and non-fasted blood glucose levels were monitored biweekly for 9 weeks. At weaning, the non-fasted blood glucose levels for $AKT1^{Myr}$ mice on a standard diet were significantly higher ($p<0.02$) than all other treatment groups. There was no significant difference between the $AKT1^{Myr}$ mice on doxycycline and the wild type mice on either diet, and the same pattern was observed at 12 weeks (Figure 18B). With regard to overnight fasting, 12-week $AKT1^{Myr}$ mice exhibited no significant difference in fasted glucose levels (Figure 18C). However, aged $AKT1^{Myr}$ exhibited fasted hyperglycemia, a more severe diabetic phenotype, by 5 months of age (Figure 18D), which was also attenuated by doxycycline treatment. Weight (Figure 18E) and food intake (Figure 18F) did not differ among genotypes.

Glucose intolerance in $AKT1^{Myr}$ transgenic mice due to insulin-glucagon imbalance.

Glucose tolerance testing (GTT) was performed at 12 weeks (n=5 males) to analyze the ability of $AKT1^{Myr}$ mice to clear glucose from the blood. $AKT1^{Myr}$ mice had a significantly higher ($p=0.0049$) area under the curve (Figure 19B) compared to wild-type mice. The significantly

elevated blood glucose levels began at 30-minutes post injection and continued for the duration of the test, signifying glucose intolerance (Figure 19A).

Glucose intolerance in AKT1^{Myr} mice was compared and found to be similar to the well-established, prediabetic AKT2 null mouse model (AKT2KO) (Figure 19C). However, serum insulin and glucagon levels, collected via cheek bleeding, revealed significant differences between AKT1^{Myr} and AKT2KO mice. AKT2KO mice had significantly ($p<0.02$) elevated insulin levels, which were evident before the glucose injection (0 min) and 45 minutes after the injection (Figure 19D/Table 3). When compared to wild type mice, AKT1^{Myr} mice did not initially (0 min) have elevated insulin levels. However, insulin levels were significantly ($p=0.009$) higher 45 minutes after the injection. Serum glucagon levels in AKT2KO mice were similar to wild type mice (Figure 19E/Table 3). However, AKT1^{Myr} mice had significantly ($p<0.05$) elevated fasted glucagon levels (0 min), which returned to wild type levels by the 45-minute time point. In addition to functional differences in pancreatic α–cells, AKT1^{Myr} mice had an altered distribution of α–cells throughout the pancreatic islets (Figure 19F), typical of several diabetic murine models (Bates et al. 2008; Cummings et al. 2008).

Insulin resistance in the liver of AKT1^{Myr} transgenic mice

One week following the GTT, an insulin tolerance test (n=5 males) was performed to analyze the sensitivity of insulin-responsive tissues in AKT1^{Myr} mice. Area under the curve was calculated (Figure 20A), blood glucose versus time, and was not significantly different when comparing AKT1^{Myr} mice and wild type mice. However, at the 15 minute time point the AKT1^{Myr} mice had significantly higher ($p=0.035$) blood glucose levels than the wild-type mice (Figure 20B).

To further analyze insulin signaling, mice were injected with 10 IU/kg porcine insulin (n=5 males) or saline (n=5 males) via the inferior vena cava. Analysis of liver tissue revealed significantly decreased insulin receptor (IR) phosphorylation (Figure 20C) in AKT1^{Myr} mice, compared to wild type mice, despite no significant difference in insulin receptor levels. There were no differences in IR phosphorylation in adipose or muscle tissue (Figure 20D & 20E). Calculation of the homeostatic model assessment for insulin resistance (HOMA-IR) confirmed insulin resistance in AKT1^{Myr} mice, as compared to wild type mice (Figure 20F).

Decreased pancreas and islet size, with aging, in AKT1^{Myr} mice.

Pancreas size was measured upon euthanization and dissection using a digital scale (n=5) in 12 week (Figure 21A) and 16 month (Figure 21B) old mice. The pancreas size in the young AKT1^{Myr} mice was not significantly different. However, the pancreas size in the aged 16 month old AKT1^{Myr} mice was significantly smaller ($p=0.0049$) than wild type mice. Islet size (n=50 islets) was also measured at 12 weeks (Figure 21C) and 16 months (Figure 21D). Islet diameter was not significantly different in 12 week old mice, but significantly decreased ($p=0.008$) in 16 month old mice.

Discussion

In this study we characterized the early onset, prediabetic phenotype observed in AKT1^{Myr} mice and highlighted a novel mechanism by which AKT1 hyperactivation affects glucose homeostasis. AKT1^{Myr} mice, previously described for their aged onset islet cell carcinomas (Albury et al. 2015), have bicistronic regulation of myristoylated AKT1 through a Pdx1-TetA and TetO-MyrAKT1 system. This allows the expression of myristoylated, membrane-bound and thus

activated, AKT1 in the pancreas except in the presence of doxycycline, a tetracycline analogue. The Pdx1 promoter, which is important for pancreas development in utero and postnatal β-cell maintenance (Holland et al. 2002), drives expression within the pancreatic progenitor cells, which eventually give rise to the endocrine cells (islets of Langerhans), exocrine cells (acini cells), and ductal cells of the pancreas (Hale et al. 2005). The hyperactivation of AKT1 throughout all cell types of the pancreas distinguishes this model from other constitutively active AKT1 mouse models, which use a rat insulin promoter (RIP) to drive expression in the β-cells (Bernal-Mizrachi et al. 2001; Tuttle et al. 2001). Additionally, the use of different tissue specific promoters highlights the important role of expression patterns and cellular localization for AKT function.

The novelty of the glucose deregulation in $AKT1^{Myr}$ mice is further elucidated when compared to the known, prediabetic AKT2 null mouse model (AKT2KO). As previously reported, AKT2KO mice have fasted and fed hyperglycemia beginning at 5- and 10 weeks in males and females respectively (Garofalo et al. 2003). Male mice progress to a severe form of diabetes by 5 months of age and females remain prediabetic until 12 months of age (Cho H et al. 2001). Conversely, $AKT1^{Myr}$ mice, regardless of sex, exhibited nonfasted hyperglycemia at weaning. There was an increase in severity with time as fasted hyperglycemia was not detectable until 5 months of age. To confirm that the hyperglycemia was due to the $AKT1^{Myr}$ transgene expression, doxycycline was administered to the mice to turn off the transgene. Doxycycline treatment reduced $AKT1^{Myr}$ blood glucose to wild type levels, confirming that the fasted and non-fasted hyperglycemia in $AKT1^{Myr}$ mice was due to AKT1 hyperactivation. Other possible contributing factors, such as weight and food intake, were ruled out further distinguishing the $AKT1^{Myr}$ mice

from the lighter AKT2KO mice (Garofalo et al. 2003) and heavier obese diabetic mouse models (i.e. db/db, NZO, and TALLYHO mice) (Coleman 1982; Herberg et al. 1970; Kim et al. 2006).

Glucose tolerance testing was performed at 12 weeks to analyze the ability of $AKT1^{Myr}$ mice to clear glucose from the blood. While both models exhibited glucose intolerance, serum insulin and glucagon levels measured during the GTT revealed that the molecular mechanisms driving the deregulations were different. As previously reported (Cho et al. 2001; Garofalo et al. 2003), AKT2KO mice had hyperinsulinemia which was evident before the glucose injection and 45 minutes after the injection. Ultimately, the AKT2KO mice model a classic, insulin-based deregulation, in which early insulin resistance leads to compensatory hyperinsulinemia, and eventually late insulin deficiency (Matthaei et al. 2000). When compared to wild type mice, $AKT1^{Myr}$ mice did not have elevated fasted insulin levels. However, insulin levels were significantly higher 45 minutes after the injection. This increase in insulin secretion may be β-cell compensation and occurred in response to the hyperglycemia also observed at this time point. This suggests that the elevated blood glucose levels were not due to a lack of insulin production or secretion, but reduced insulin sensitivity (Weir & Bonner-Weir 2004).

While insulin deregulations are well studied, glucagon deregulations have been acknowledged but relatively ignored. Glucagon, which is secreted by pancreatic α–cells when blood glucose levels are low, is known as the antagonist to insulin. When glucagon binds to its receptor it activates cellular adenosine-3'-5'-cyclic monophosphate (cAMP) and protein kinase A (PKA) signaling to induce hepatic gluconeogenesis and glycogenolysis restoring glucose homeostasis during fasting (Moon & Won 2015). Increased PKA activity impairs glucose stimulated insulin secretion (GSIS), which is needed to prevent the immediate secretion and

glucose disposing action of insulin (Song et al. 2014). Serum glucagon levels in AKT2KO mice were similar to wild type mice. However, $AKT1^{Myr}$ mice had significantly elevated fasted glucagon levels, which returned to wild type levels by the 45-minute time point, most likely due to the surge in insulin secretion.

Fasted hyperglucagonemia, as seen in $AKT1^{Myr}$ mice, has been observed in diabetic patients (Baron et al. 1987; Reaven et al. 1987; Unger et al. 1970), and linked to the manifestation of fasted hyperglycemia and glucose intolerance. The mechanisms behind hyperglucagonemia are still relatively unclear, but it has been shown to result from the inadequate response of α–cells to elevated blood glucose levels (Rizza 2010). This α–cell dysfunction leads to hepatic insulin resistance (Basu et al. 2004), causing non-fasted hyperglycemia by preventing the suppression of endogenous glucose production during a meal, and fasted hyperglycemia via chronically elevated endogenous glucose production (Basu et al. 2000; Firth et al. 1986). The hyperglucagonemia induced hepatic insulin resistance also significantly decreases hepatic glucose uptake and disposal due to impaired glucokinase activity (Caro et al. 1995; Wajngot et al. 1991). This impaired hepatic glucose metabolism has been identified in mild and severe diabetes patients making it an early contributing event in the pathogenesis of diabetes, and not simply an effect (Basu et al. 2004; Bock et al. 2007).

One week following the GTT, an insulin tolerance test was performed to analyze the sensitivity of insulin-responsive tissues in $AKT1^{Myr}$ mice. $AKT1^{Myr}$ mice and wild type mice were not significantly different when comparing area under the curve, suggesting an absence of insulin resistance. However, at the 15 minute time point the $AKT1^{Myr}$ mice had significantly higher blood glucose levels than the wild-type mice, suggesting there may be altered insulin signaling causing

this delay in insulin response. Further analysis of liver tissue revealed significantly decreased insulin receptor (IR) phosphorylation in AKT1^{Myr} mice, compared to wild type mice, despite no significant difference in insulin receptor levels. This decrease in IR activation explains the delay in insulin response seen early in the ITT and the inability of AKT1^{Myr} mice to aptly clear glucose from the blood. Further calculation of the HOMA-IR confirmed insulin resistance in AKT1^{Myr} mice, as compared to wild type mice. However, at 12 weeks, this resistance is not as severe as the resistance seen in AKT2KO mice.

Additional longevity studies must be performed to determine whether the insulin resistance worsens with age, but analysis of pancreas and islet size suggests a gradual loss of β-cell mass. This loss of β-cell mass, evident by a decrease in total pancreas size and islet diameter, is typically indicative of long term insulin resistance and β-cell failure due to chronic hyperinsulinemia and hyperglycemia (Prentki & Nolan 2006). There also appears to be an age induced increase in islet diameter of wild type mice. This is most likely due to naturally occurring beta-cell compensation or the presence of islet adenomas which also develop naturally in about 33% of our aged wild type mice.

In this study we characterized the pre-tumor, prediabetic phenotype of AKT1^{Myr} mice, which exhibit non-fasted hyperglycemia as early as weaning and fasted hyperglycemia by 5 months of age, regardless of sex. Based upon previous findings, this hyperglycemia is likely due to α-cell dysfunction, specifically hyperglucagonemia. Although the mechanisms behind hyperglucagonemia are still relatively unclear, we are proposing that AKT1^{Myr} mice, with fasted hyperglucagonemia, have impaired GSIS, resulting in glucose intolerance despite increased compensatory insulin secretion. Hepatic insulin resistance, an additional factor, may exacerbate

the problem, preventing normoglycemia via increased hepatic glucose production and decreased hepatic glucose storage. As the fasted and non-fasted hyperglycemias are reversible when the $AKT1^{Myr}$ transgene is suppressed we have attributed this diabetic phenotype to the constitutive activation of AKT1 in the pancreas of this mouse model. Collectively, this pre-diabetic model highlights a novel glucagon-mediated mechanism by which AKT1 hyperactivation affects glucose homeostasis, and provides a means to better delineate molecular mechanisms contributing to diabetes mellitus, and perhaps future association between diabetes and a subset of pancreatic cancers.

Figures and Tables

Table 3: The average insulin and glucagon serum levels in wild type, MYR AKT1, and AKT2 KO mice during the glucose tolerance test.

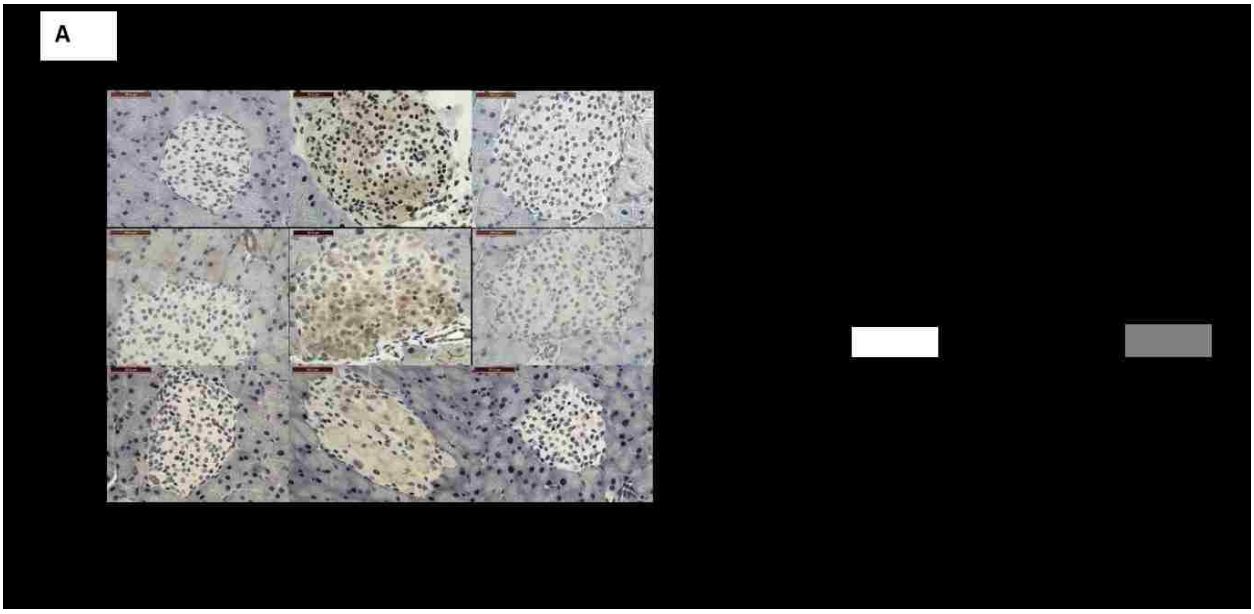

Figure 17: AKT1^{Myr} mice have doxycycline-regulatable AKT/mTOR pathway activation in the pancreas.

Hyperactivation and decreased activation of the AKT/mTOR pathway in AKT1^{Myr} mice on regular chow diet and AKT1^{Myr} mice on doxycycline diet, respectively, confirmed with: (A) immunostaining of representative pancreatic tissue using phospho-AKT (Ser 473), phospho-mTOR (Ser 2448), and phospho-S6 (Ser 235/236) antibodies (40X objective; Scale bar-50μm); and (B) analysis of protein from pancreatic tissue using a phospho-AKT1 (Ser 473) ELISA. Two-way ANOVA followed by student's t-tests within groups were used to analyze the data. Data represented as mean ± SEM (n=5). All phospho-AKT1 measurements were normalized to their total AKT measurements. Abbreviations: WT – wild type mice; Reg-regular chow diet; Dox - doxycycline diet. Letters were used to illustrate significance as multiple groups are being compared (see materials and methods for explanation).

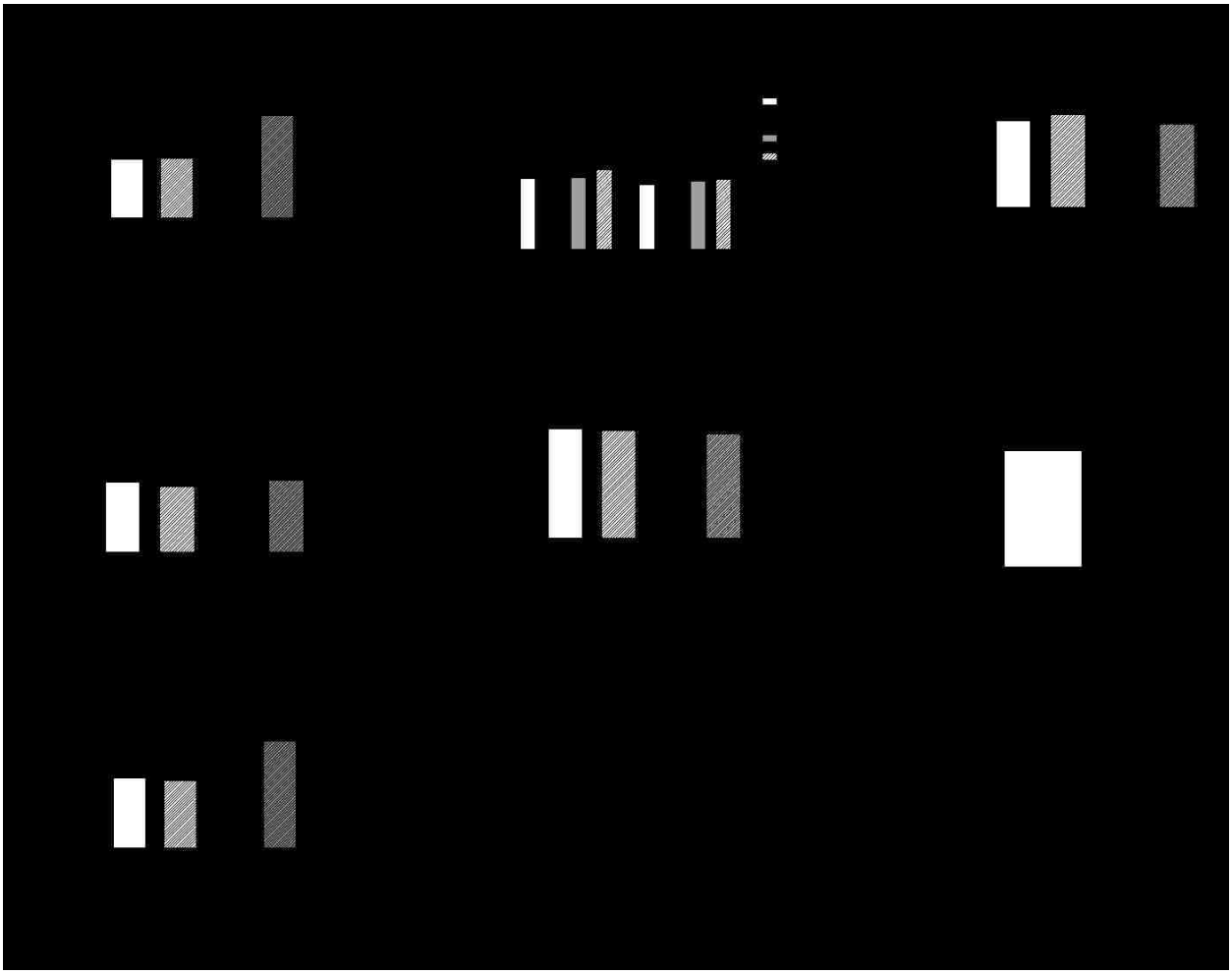

Figure 18: AKT1^{Myr} mice have a reversible, fasted and non-fasted hyperglycemia.

Blood glucose levels were measured with a glucometer (A) at weaning ($p<0.0001$) and at 12 weeks ($p=0.0031$). Weaning occurred at 3 weeks of age. To determine if the hyperglycemia exhibited at weaning was reversible, breeder mice were placed on a doxycycline diet to expose the pups in utero. Blood glucose levels were then measured (B) at weaning ($p<0.02$) and at 12 weeks ($p\leq0.003$). Mice were fasted overnight (16 hours) to determine fasted blood glucose levels (C) at 12 weeks and (D) at 20 weeks ($p<0.005$). (E) Weight was measured at weaning. At 12 weeks, mice were housed individually and (F) food intake was measured daily for four days by weighing the food in the cage. Blood glucose levels, measured at weaning, were used to identify (G) sex differences. Two-way ANOVA followed by student's t-tests within groups were used to analyze the data for figures A-E and G. Unpaired student's t-test was used for figure F. N=10 for figures A-G except D (n=5). Abbreviations: Wks - week. Letters were used to illustrate significance as multiple groups are being compared (see materials and methods for explanation).

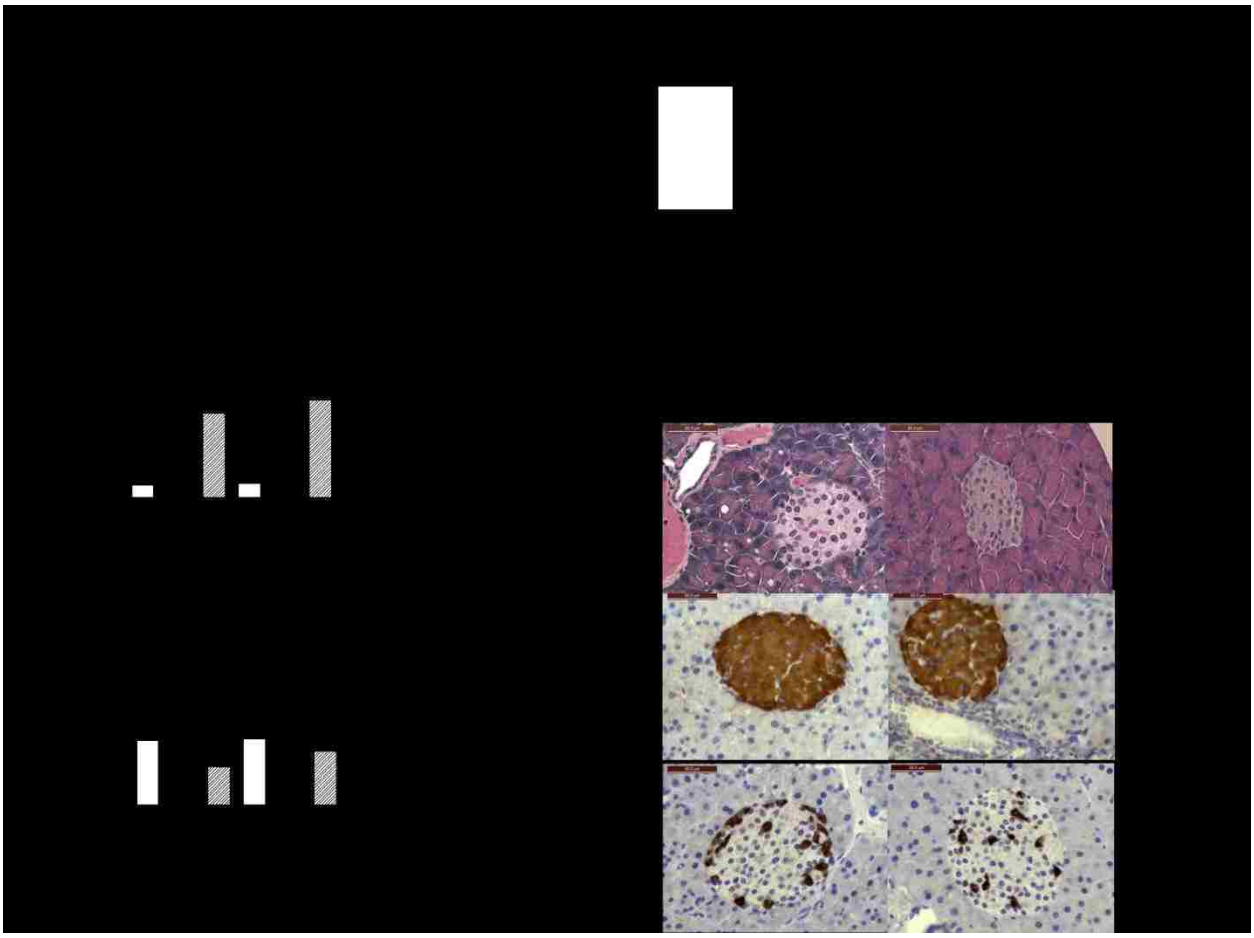

Figure 19: Glucose intolerance in AKT1^{Myr} mice due to insulin-glucagon imbalance.

Glucose tolerance testing (n=5) was performed at 12 weeks comparing: (A) wild type (WT) and AKT1^{Myr} (MYR AKT1) mice and (C) WT, MYR AKT1, and AKT2$^{-/-}$ (AKT2 KO) mice (* indicates $p<0.05$). (B) Area under the curve. Data represented as mean ± SEM ($p=0.0049$). Blood was collected, via cheek bleeds, at the 0- and 45-minute time points to analyze serum (D) insulin and (E) glucagon levels using ELISAs. Insulin and glucagon values are also provided in Table 3. (F) Immunostaining of pancreatic tissue using insulin and glucagon antibodies (Objective 40X; Scale bar-50μm). Unpaired student's t-tests were used to analyze differences in area under the curve and the glucose tolerance test time points. Two-way ANOVA followed by student's t-tests within groups were used to analyze the data for figures D-E. Letters were used to illustrate significance as multiple groups are being compared (see materials and methods for explanation).

:

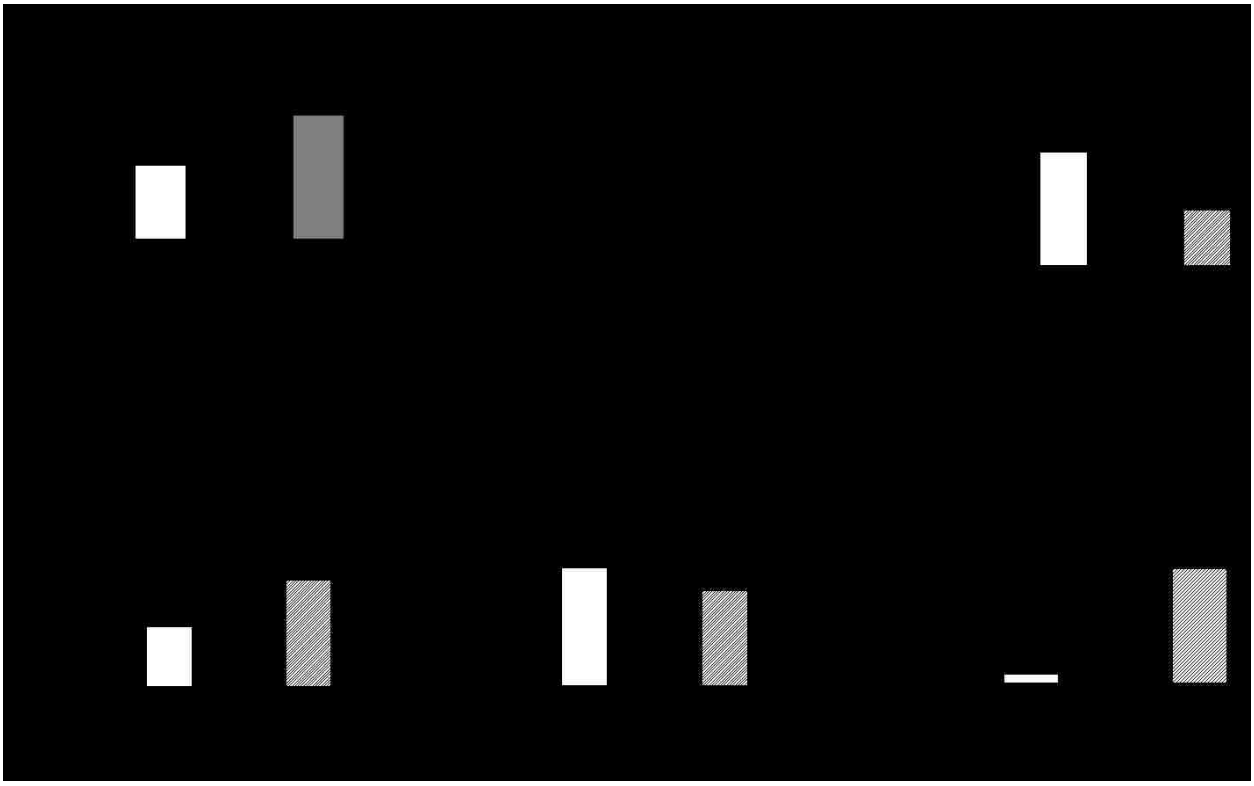

Figure 20: Insulin resistance in the liver of AKT1^{Myr} mice.

One week following the GTT, (B) an insulin tolerance test was performed (n=5). (A) Area under the curve. Data represented as mean ± SEM ($p<0.04$). To analyze insulin signaling, mice were insulin stimulated. Two minutes after injection the mice were euthanized and the pancreas, (C) liver, (D) adipose tissue, and (E) skeletal muscle were collected, protein extracted, and analyzed with insulin receptor (IR) Total and IR (pY1158) ELISAs. All phospho-IR measurements were normalized to their total IR measurements. (F) Homeostatic model assessment for insulin resistance (HOMA-IR) was calculated using the following measurements from the GTT: (fasted glucose x fasted insulin)/405. Data represented as mean ± SEM. Unpaired student's t-tests were used to analyze differences in the insulin tolerance tests time points. One-way ANOVA followed by student's t-tests within groups were used to analyze the data for figures A and C-F. Letters were used to illustrate significance as multiple groups are being compared (see materials and methods for explanation).

Figure 21: Decreased pancreas and islet size, with aging, in AKT1^{Myr} mice.

Pancreas size was measured upon euthanization and dissection using a digital scale (n=5) in (A) 12 week and (B) 16 month (p=0.0049) old mice. Islet size (n=50 islets) was also measured at (C) 12 weeks and (D) 16 months (p=0.008). Islet diameter was determined analyzing H&E stained sections through Axio Imaging Software. Unpaired student's t-tests were used to analyze figures A-D. Data represented as mean ± SEM. Letters were used to illustrate significance as multiple groups are being compared (see materials and methods for explanation).

List of References

Albury TM, Pandey V, Gitto SB, Dominguez L, Spinel LP, Talarchek J, Klein-Szanto AJ, Testa JR, & Altomare DA 2015 Constitutive activation of Akt1 cooperates with KRasG12D to accelerate in vivo pancreatic tumor onset and progression. *Neoplasia***17** 175-183.

Altomare DA & Testa JR 2005 Perturbations of the AKT signaling pathway in human cancer. *Oncogene***24** 7455-7464.

Baron AD, Schaeffer L, Shragg P & Kolterman OG 1987 Role of hyperglucagonemia in maintenance of increased rates of hepatic glucose output in type II diabetics. *Diabetes***36** 274-283.

Basu A, Basu R, Shah P, Vella A, Johnson CM, Nair KS, Jensen MD, Schwenk WF & Rizza RA 2000 Effects of type 2 diabetes on the ability of insulin and glucose to regulate splanchnic and muscle glucose metabolism: evidence for a defect in hepatic glucokinase activity. *Diabetes***49** 272-283.

Basu R, Basu A, Johnson CM, Schwenk WF & Rizza RA 2004 Insulin dose-response curves for stimulation of splanchnic glucose uptake and suppression of endogenous glucose production differ in nondiabetic humans and are abnormal in people with type 2 diabetes. *Diabetes***53** 2042-2050.

Basu R, Schwenk WF & Rizza RA 2004 Both fasting glucose production and disappearance are abnormal in people with "mild" and "severe" type 2 diabetes. *Am J Physiol Endocrinol Metab***287** E55-E62.

Bates H, Sirek A, Kiraly M, Yue J, Riddell M, Matthews S & Vranic M 2008 Adaptation to intermittent stress promotes maintenance of beta-cell compensation: comparison with food restriction. *Am J Physiol Endocrinol Metab***295** E947-58.

Bernal-Mizrachi E, Wen W, Stahlhut S, Welling CM & Permutt MA 2001 Islet beta cell expression of constitutively active Akt1/PKB alpha induces striking hypertrophy, hyperplasia, and hyperinsulinemia. *J Clin Invest***108** 1631-1638.

Bock G, Chittilapilly E, Basu R, Toffolo G, Cobelli C, Chandramouli V, Landau BR & Rizza RA 2007 Contribution of hepatic and extrahepatic insulin resistance to the pathogenesis of impaired fasting glucose: role of increased rates of gluconeogenesis. *Diabetes***56** 1703-1711.

Caro JF, Triester S, Patel VK, Tapscott EB, Frazier NL & Dohm GL 1995 Liver glucokinase: decreased activity in patients with type II diabetes. *Horm Metab Res***27** 19-22.

Chan CH, Jo U, Kohrman A, Rezaeian AH, Chou PC, Logothetis C & Lin HK 2014 Posttranslational regulation of Akt in human cancer. *Cell Biosci***4** 1-9.

Chen WS, Peng XD, Wang Y, Xu PZ, Chen ML, Luo Y, Jeon SM, Coleman K, Haschek WM, Bass J, et al. 2009 Leptin deficiency and beta-cell dysfunction underlie type 2 diabetes in compound Akt knockout mice. *Mol Cell Biol***29** 3151-3162.

Cheung M & Testa JR 2013 Diverse mechanisms of AKT pathway activation in human malignancy. *Curr Cancer Drug Targets***13** 234-244.

Cho H, Mu J, Kim JK, Thorvaldsen JL, Chu Q, Crenshaw EB, Kaestner KH, Bartolomei MS, Shulman GI & Birnbaum MJ 2001 Insulin resistance and a diabetes mellitus-like syndrome in mice lacking the protein kinase Akt2 (PKB beta). *Science***292** 1728-1731.

Cho H, Thorvaldsen JL, Chu Q, Feng F & Birnbaum MJ 2001 Akt1/PKBalpha is required for normal growth but dispensable for maintenance of glucose homeostasis in mice. *J Biol Chem***276** 38349-38352.

Coleman DL 1982 Diabetes-obesity syndromes in mice. *Diabetes***31** 1-6.

Cummings B, Digitale E, Stanhope K, Graham J, Baskin D, Reed B, Sweet I, Griffen S & Havel PJ 2008 Development and characterization of a novel rat model of type 2 diabetes mellitus: the UC Davis type 2 diabetes mellitus UCD-T2DM rat. *Am J Physiol Regul Integr Comp Physiol***295** 1782-1793.

Firth RG, Bell PM, Marsh HM, Hansen I & Rizza RA 1986 Postprandial hyperglycemia in patients with noninsulin-dependent diabetes mellitus. Role of hepatic and extrahepatic tissues. *J Clin Invest***77** 1525-1532.

Garofalo RS, Orena SJ, Rafidi K, Torchia AJ, Stock JL, Hildebrandt AL, Coskran T, Black SC, Brees DJ, Wicks JR, et al. 2003 Severe diabetes, age-dependent loss of adipose tissue, and mild growth deficiency in mice lacking Akt2/PKB beta. *J Clin Invest***112** 197-208.

Grote CW, Groover AL, Ryals JM, Geiger PC, Feldman EL & Wright DE 2013 Peripheral nervous system insulin resistance in ob/ob mice. *Acta Neuropathol Commun***1** 1-11.

Hale MA, Kagami H, Shi L, Holland AM, Elsässer HP, Hammer RE & MacDonald RJ 2005 The homeodomain protein PDX1 is required at mid-pancreatic development for the formation of the exocrine pancreas. *Dev Biol***286** 225-237.

Hay N 2011 Akt isoforms and glucose homeostasis - the leptin connection. *Trends Endocrinol Metab***22** 66-73.

Hemmings BA & Restuccia DF 2012 PI3K-PKB/Akt pathway. *Cold Spring Harb Perspect Bio***l4** 1-3.

Herberg L, Major E, Hennigs U, Grüneklee D, Freytag G & Gries FA 1970 Differences in the development of the obese-hyperglycemic syndrome in obob and NZO mice. *Diabetologia***6** 292-298.

Holland AM, Hale MA, Kagami H, Hammer RE & MacDonald RJ 2002 Experimental control of pancreatic development and maintenance. *Proc Natl Acad Sci***99** 12236-12241.

Kim JH, Stewart TP, Soltani-Bejnood M, Wang L, Fortuna JM, Mostafa OA, Moustaid-Moussa N, Shoieb AM, McEntee MF, Wang Y, et al. 2006 Phenotypic characterization of polygenic type 2 diabetes in TALLYHO/JngJ mice. *J Endocrinol***191** 437-446.

Kushner JA, Simpson L, Wartschow LM, Guo S, Rankin MM, Parsons R & White MF 2005 Phosphatase and tensin homolog regulation of islet growth and glucose homeostasis. *J Biol Chem***280** 39388-39393.

Matthaei S, Stumvoll M, Kellerer M & Häring HU 2000 Pathophysiology and pharmacological treatment of insulin resistance. *Endocr Rev***21** 585-618.

Missiaglia E, Dalai I, Barbi S, Beghelli S, Falconi M, della Peruta M, Piemonti L, Capurso G, Di Florio A, delle Fave G, et al. 2010 Pancreatic endocrine tumors: expression profiling evidences a role for AKT-mTOR pathway. *J Clin Oncol***28** 245-255.

Moon JS & Won KC 2015 Pancreatic α-Cell Dysfunction in Type 2 Diabetes: Old Kids on the Block. *Diabetes Metab J***39** 1-9.

Prentki M & Nolan CJ 2006 Islet beta cell failure in type 2 diabetes. *J Clin Invest***116** 1802-1812.

Reaven GM, Chen YD, Golay A, Swislocki AL & Jaspan JB 1987 Documentation of hyperglucagonemia throughout the day in nonobese and obese patients with noninsulin-dependent diabetes mellitus. *J Clin Endocrinol Metab***64** 106-110.

Rizza RA 2010 Pathogenesis of fasting and postprandial hyperglycemia in type 2 diabetes: implications for therapy. *Diabetes***59** 2697-2707.

Schlieman MG, Fahy BN, Ramsamooj R, Beckett L & Bold RJ 2003 Incidence, mechanism and prognostic value of activated AKT in pancreas cancer. *Br J Cancer***89** 2110-2115.

Song WJ, Mondal P, Wolfe A, Alonso LC, Stamateris R, Ong BW, Lim OC, Yang KS, Radovick S, Novaira HJ, et al. 2014 Glucagon regulates hepatic kisspeptin to impair insulin secretion. *Cell Metab***19** 667-681.

Stiles BL, Kuralwalla-Martinez C, Guo W, Gregorian C, Wang Y, Tian J, Magnuson MA & Wu H 2006 Selective deletion of Pten in pancreatic beta cells leads to increased islet mass and resistance to STZ-induced diabetes. *Mol Cell Biol***26** 2772-2781.

Tschopp O, Yang ZZ, Brodbeck D, Dummler BA, Hemmings-Mieszczak M, Watanabe T, Michaelis T, Frahm J, & Hemmings BA 2005 Essential role of protein kinase B gamma (PKB gamma/Akt3) in postnatal brain development but not in glucose homeostasis. *Development***132** 2943-2954.

Tuttle RL, Gill NS, Pugh W, Lee JP, Koeberlein B, Furth EE, Polonsky KS, Naji A & Birnbaum MJ 2001 Regulation of pancreatic beta-cell growth and survival by the serine/threonine protein kinase Akt1/PKBalpha. *Nat Med***7** 5-14.

Unger RH, Aguilar-Parada E, Müller WA & Eisentraut AM 1970 Studies of pancreatic alpha cell function in normal and diabetic subjects. *J Clin Invest***49** 837-848.

Wajngot A, Chandramouli V, Schumann WC, Efendic S & Landau BR 1991 Quantitation of glycogen/glucose-1-P cycling in liver. *Metabolism***40** 877-881.

Weir GC & Bonner-Weir S 2004 Five stages of evolving beta-cell dysfunction during progression to diabetes. *Diabetes***53** 16-21.

CHAPTER 4:
OVERT DIABETES IN TRANSGENIC MICE WITH CONSTITUTIVELY ACTIVE AKT1 AND MUTANT KRASG12D IN THE PANCREAS

Introduction

Pancreatic ductal adenocarcinoma (PDAC) is the most lethal common cancer largely due to late diagnosis. At diagnosis, which is typically 71 years of age, 85% of PDAC patients are inoperable due to local and distant metastasis. Drug treatments are typically ineffective at this advanced stage and the average survival rate is four to six months. Over the last 30 years PDAC incidence has been relatively stable (1 to 10 per 100,000 people). However, population changes, primarily the aging of 76.4 million baby boomers, are expected to thrust pancreatic cancer from the ninth to the second leading cause of cancer-related deaths within the next 15 years (Ryan et al. 2014). It is vital that we quickly identify an effective, noninvasive, and cost efficient early detection strategy, such as a biomarker, as clinical testing can take an estimated 7.9 years (Rahib et al. 2014).

As early as the 1900s a relationship between diabetes and pancreatic cancer has been proposed. Based upon experimental and clinical evidence, there are two prevailing theories: (1) long-term diabetes induces pancreatic cancer and (2) new onset diabetes is an early marker for pancreatic cancer. With 80% of PDAC patients suffering from hyperglycemia or diabetes prior to diagnosis, this has potential to serve as a viable early detection strategy (Wang et al. 2003). However, it is essential that the molecular mechanisms behind this association be understood. It would be difficult to study this association in humans, primarily because PDAC is asymptomatic until it reaches an advanced stage making it difficult to identify study participants. Moreover, it is challenging to perform retrospective studies as blood and/or tissue collections are needed up to

seven years prior to diagnosis. Additionally, we are currently unable to distinguish Type 2 Diabetes (T2D), which is common in the general population, from PDAC associated diabetes, which is less common. Despite these complications there are many unanswered questions and further basic research is required (Pannala et al. 2009; Bao et al. 2011).

Human PDAC progression is initiated by activation mutations of the KRas oncogene. This leads to additional molecular changes, such as activation of the AKT oncogene, which drives PDAC progression and tumor formation (Ryan et al. 2014). By mating transgenic mice with activation of KRas (Pdx- Cre;LSL-KRasG12D) and mice with activation of AKT1 (Pdx-tTA;TetO-MyrAKT1) we were able to produce mice with activation of both oncogenes ($AKT1^{Myr}$/KRasG12D). These mice accurately mimic the human PDA progression molecularly, structurally, and temporally. Additionally, they exhibit a pre-tumor diabetic phenotype at 3 weeks of age, including random and fasted hyperglycemia. By thoroughly studying our $AKT1^{Myr}$/KRasG12D mouse model we can identify key pre-tumor molecular events that induce metabolic changes, distinguish PDAC associated diabetes from T2D, and identify an early biomarker. This will ultimately lead to earlier pre-metastatic detection, effective drug treatment, and increased PDAC survival.

Materials and Methods

Genetically Engineered Mice

All mice were housed and handled according to protocols approved by the University of Central Florida (UCF) Institutional Animal Care and Use Committee at the AAALAC accredited UCF Lake Nona Animal Facility. Transgenic mice were mated, weaned, and tail snipped for DNA extraction and genotyping as previously described in chapter 2 and 3 materials and methods. Mice with TetO-MyrAKT1, but lacking the knock-in Pdx-tTA, were classified as normal or wild-type litter mates. Mice with Pdx-Cre;LSL-KRasG12D were classified as KRasG12D. Mice with Pdx-tTA, TetO-MyrAKT1, and Pdx-Cre;LSL-KRasG12D were classified as $AKT1^{Myr}$/KRasG12D. Litters were placed on a standard control diet or a doxycycline diet (BioServ, Frenchtown, NJ), which shuts off $AKT1^{Myr}$ transgene expression. All mice were euthanized according to American Veterinary Medical Association guidelines.

Blood Glucose Measurement

Blood glucose levels were measured, using a glucometer, as previously described in chapter 3 materials and methods.

Glucose and Insulin Tolerance Test

For glucose tolerance testing mice were fasted overnight, weighed (g), intraperitoneal (IP) injected with 2g/kg D-glucose and blood glucose tested with a glucometer before injection, 15-, 30-, 45-, 60-, and 120 minutes after injection. Blood was collected, via cheek bleeds, into serum collection tubes at 0 and 45 minutes after injection. The serum was separated and stored at -80°C

until analysis with Mercodia Glucagon and Ultrasensitive Mouse Insulin ELISAs. For insulin tolerance testing mice were fasted for 2 hours, weighed (g), IP injected with 2 IU/kg porcine insulin, and blood glucose tested with a glucometer before injection, 15-, 30-, 45-, and 60 minutes after injection. For both tests, GTT and ITT, blood glucose (mg/dL) versus time (minutes) was plotted and the area under the curve was calculated using GraphPad. Manufacturer information for all products were provided in chapter 3 materials and methods.

Statistical Analysis

All statistical analysis were described in chapter 3 materials and methods.

Results

Reversible, non-fasted and fasted hyperglycemia in AKT1^{Myr}/KRasG12D transgenic mice

At weaning, mice were tail snipped for genotyping and blood glucose tested. AKT1^{Myr}/KRasG12D (AKTRAS) mice (n=10), regardless of sex (Figure 22C), had significantly higher ($p<0.0001$) non-fasted blood glucose levels at weaning than wild-type littermates (Figure 22A). Non-fasted blood glucose levels were monitored biweekly for 9 weeks following weaning, and similarly, AKT1^{Myr}/KRasG12D mice had significantly higher ($p\leq0.0013$) non-fasted blood glucose levels at 12 weeks of age compared to wild-type mice (Figure 22A). There was no significant difference in non-fasted blood glucose levels, at any time point, when comparing KRasG12D (RAS) mice to wild type littermates.

Doxycycline was administered to mice in order to turn off the AKT1^{Myr} transgene. Mating cages were arranged, as described in chapter 3, for in utero exposure, feeding regimens were

continued at weaning, and non-fasted blood glucose levels were monitored biweekly for 9 weeks. At weaning, the non-fasted blood glucose levels for AKT1^{Myr}/KRasG12D mice on a standard diet were significantly higher ($p<0.0001$) than all other treatment groups. There was no significant difference between the AKT1^{Myr}/KRasG12D mice on doxycycline and the wild type or KRasG12D mice on either diet, and the same pattern was observed at 12 weeks (Figure 22B). At 12 weeks AKT1^{Myr}/KRasG12D mice also had significantly higher ($p\leq0.0002$) fasted blood glucose levels (Figure 22D), which is also reversible with doxycycline treatment ($p<0.0001$) (Figure 22E). Weight, measured at weaning, (Figure 22F) did not differ among genotypes. However, by 12 weeks of age AKT1^{Myr}/KRasG12D mice had significantly lower ($p\leq0.0002$) body weight than wildtype and KRasG12D littermates (Figure 22G). Food intake, measured at 12 weeks, (Figure 22H) did not differ among groups.

Glucose intolerance in AKT1^{Myr}/KRasG12D transgenic mice due to insulin-glucagon imbalance.

Glucose tolerance testing (GTT) was performed at 12 weeks (n=5 males) to analyze the ability of AKT1^{Myr}/KRasG12D (AKTRAS) and KRasG12D (RAS) mice to clear glucose from the blood. AKT1^{Myr}/KRasG12D mice had a significantly higher ($p=0.0003$) area under the curve (Figure 23B) compared to wild-type and KRasG12D mice, signifying glucose intolerance. The significantly elevated blood glucose levels began prior to the glucose injection when compared to wild type littermates and 15-minutes post injection compared to KRasG12D littermates. Blood glucose levels were significantly elevated for all but the last time point, 120 minutes post injection (Figure 23A).

Serum insulin and glucagon levels, collected via cheek bleeding, revealed significant differences between wild type, AKT1^{Myr}/KRasG12D, and KRasG12D mice. AKT1^{Myr}/KRasG12D mice had significantly ($p<0.02$) elevated insulin levels, which were evident 45 minutes after the glucose injection (Figure 23C/Table 4), but not prior to the injection. However, AKT1^{Myr}/KRasG12D mice had significantly ($p<0.05$) elevated fasted glucagon levels (0 min), and significantly ($p<0.003$) lower glucagon levels 45 minutes post injection (Figure 23D/Table 4). Serum insulin and glucagon levels did not significantly differ between wild type mice and KRasG12D littermates.

Insulin resistance in KRasG12D and AKT1^{Myr}/ KRasG12D mice.

One week following the GTT, an insulin tolerance test (n=5 males) was performed to analyze the sensitivity of insulin-responsive tissues in AKT1^{Myr}/KRasG12D and KRasG12D mice. Area under the curve was calculated (Figure 24A), blood glucose versus time, and was significantly higher in KRasG12D ($p=0.0357$) and AKT1^{Myr}/KRasG12D ($p=0.0463$) mice compared to wild type mice. KRasG12D mice had significantly ($p=0.006$) higher blood glucose levels at the 30 minute time point (Figure 24D). While AKT1^{Myr}/KRasG12D mice were significantly higher at the 15 ($p=0.01$) and 30 ($p=0.0328$) minute time points (Figures 24C and D).

Discussion

In chapter three we characterized the early onset, prediabetic phenotype observed in AKT1^{Myr} mice. We highlighted a novel mechanism by which AKT1 hyperactivation induces fasted hyperglucagonemia, leading to impaired glucose stimulated insulin secretion, glucose intolerance, hepatic insulin resistance, and hyperglycemia via increased hepatic glucose

production and decreased hepatic glucose storage. In this study, which is still in progress, our goal is to similarly characterize the diabetic phenotype observed in AKT1^{Myr}/KRasG12D transgenic mice, and better understand how the presence of two oncogenes (AKT1 and KRas) cooperate to affect glucose homeostasis.

AKT1^{Myr}/KRasG12D mice, as previously described (Albury et al. 2015) have bicistronic regulation of myristoylated AKT1 through a Pdx1-TetA and TetO-MyrAKT1 system, as well as Pdx-Cre–activated KRasG12D (Figure 12). As demonstrated in Chapter 3 Figure 17, this allows the expression of myristoylated, membrane-bound and thus activated, AKT1 in the pancreas except in the presence of doxycycline, while KRasG12D remains constitutively active within the pancreas. KRasG12D activation alone seemed to have no effect on fasted and non-fasted blood glucose levels. However, KRasG12D in cooperation with AKT1^{Myr} had a more severe effect on glucose homeostasis than AKT1^{Myr} alone. AKT1^{Myr}/KRasG12D (AKTRAS) mice, similar to AKT1^{Myr} mice, exhibited nonfasted hyperglycemia at weaning (3 weeks), regardless of sex or weight. Unlike AKT1^{Myr} mice, AKT1^{Myr}/KRasG12D mice had a more severe diabetic phenotype. This was evident by a significant increase in non-fasted blood glucose levels which averaged 309 mg/dl at 3 weeks of age and 449 mg/dl at 12 weeks of age. AKT1^{Myr}/KRasG12D mice also exhibited fasted hyperglycemia at 12 weeks, which was 2 months earlier than AKT1^{Myr} mice. The overall disease progression for AKT1^{Myr}/KRasG12D mice was faster than AKT1^{Myr} mice as polyuria, muscle wasting, and bloating often required euthanization with aging. Doxycycline treatment reduced AKT1^{Myr}/KRasG12D blood glucose levels to wild type and KRasG12D levels, confirming that KRasG12D alone had no effect on blood glucose levels and that the fasted and non-fasted hyperglycemia in AKT1^{Myr}/KRasG12D mice was largely due to AKT1 hyperactivation.

Doxycycline treatment, if provided at an early age, also prevented the diabetes associated symptoms (polyuria, muscle wasting, etc).

Glucose tolerance testing was performed at 12 weeks to compare the abilities of KRasG12D and AKT1^{Myr}/KRasG12D mice to clear glucose from the blood. AKT1^{Myr}/KRasG12D mice exhibited glucose intolerance, while KRasG12D activation alone had no effect on glucose tolerance. With the advanced disease progression noted in AKT1^{Myr}/KRasG12D mice, we hypothesized that they may more closely resemble the known, prediabetic AKT2 null mouse model (AKT2KO) characterized in chapter 3 and other studies (Garofalo et al. 2003; Cho H et al. 2001). While all three models (AKT2KO, AKT1^{Myr}/KRasG12D, AKT1^{Myr}) exhibit glucose intolerance, measurements of the area under the curve for AKT1^{Myr}/KRasG12D mice more closely resemble AKT1^{Myr} mice. Additionally, serum insulin and glucagon levels measured during the GTT also resemble AKT1^{Myr} mice, with fasted hyperglucagonemia and significantly elevated insulin secretion 45 minutes post injection. This increase in insulin secretion, along with the significant drop in glucagon levels, suggests that the pancreas is undergoing beta-cell compensation, an attempt to lower blood glucose levels by secreting insulin which inhibits glucagon secretion (Aronoff et al. 2004). Insulin and glucagon levels for KRasG12D mice did not differ from wild-type mice.

One week following the GTT, an insulin tolerance test was performed to analyze the sensitivity of insulin-responsive tissues in AKT1^{Myr}/KRasG12D and KRasG12D mice, since the elevated blood glucose levels were not due to a lack of insulin production or secretion. Surprisingly both KRasG12D and AKT1^{Myr}/KRasG12D mice appeared to have impaired insulin sensitivity. While the AKT1^{Myr}/KRasG12D impairment was more severe, the KRasG12D mice

did exhibit elevated blood glucose levels 30 minutes post insulin injection and a significantly higher area under the curve. Although statistically significant this impairment does not seem to cause hyperglycemia nor glucose intolerance. Further investigation into how the pancreas, or another insulin responsive tissue, is compensating for this impairment is necessary.

In this study we characterized the pre-tumor, diabetic phenotype of $AKT1^{Myr}$/KRasG12D mice in an attempt to better understand how KRasG12D and AKT1 oncogenes cooperate to affect glucose homeostasis. Similar to $AKT1^{Myr}$ mice, yet more severe, $AKT1^{Myr}$/KRasG12D mice exhibit non-fasted hyperglycemia as early as weaning and fasted hyperglycemia by 3 months of age, regardless of sex. Based upon previous findings, as described in chapter 3, this hyperglycemia is likely due to α-cell dysfunction, specifically fasted hyperglucagonemia, which induces glucose intolerance despite increased compensatory insulin secretion, impaired insulin sensitivity, increased hepatic glucose production, and decreased hepatic glucose storage. Collectively, this diabetic model provides an avenue to better distinguish Type 2 Diabetes and PDAC associated diabetes.

Figures and Tables

Table 4: The average insulin and glucagon serum levels in wild type, RAS, and AKTRAS mice during the glucose tolerance test.

* Indicates a significant difference. The data in this table corresponds to panels C and D in Figure 23.

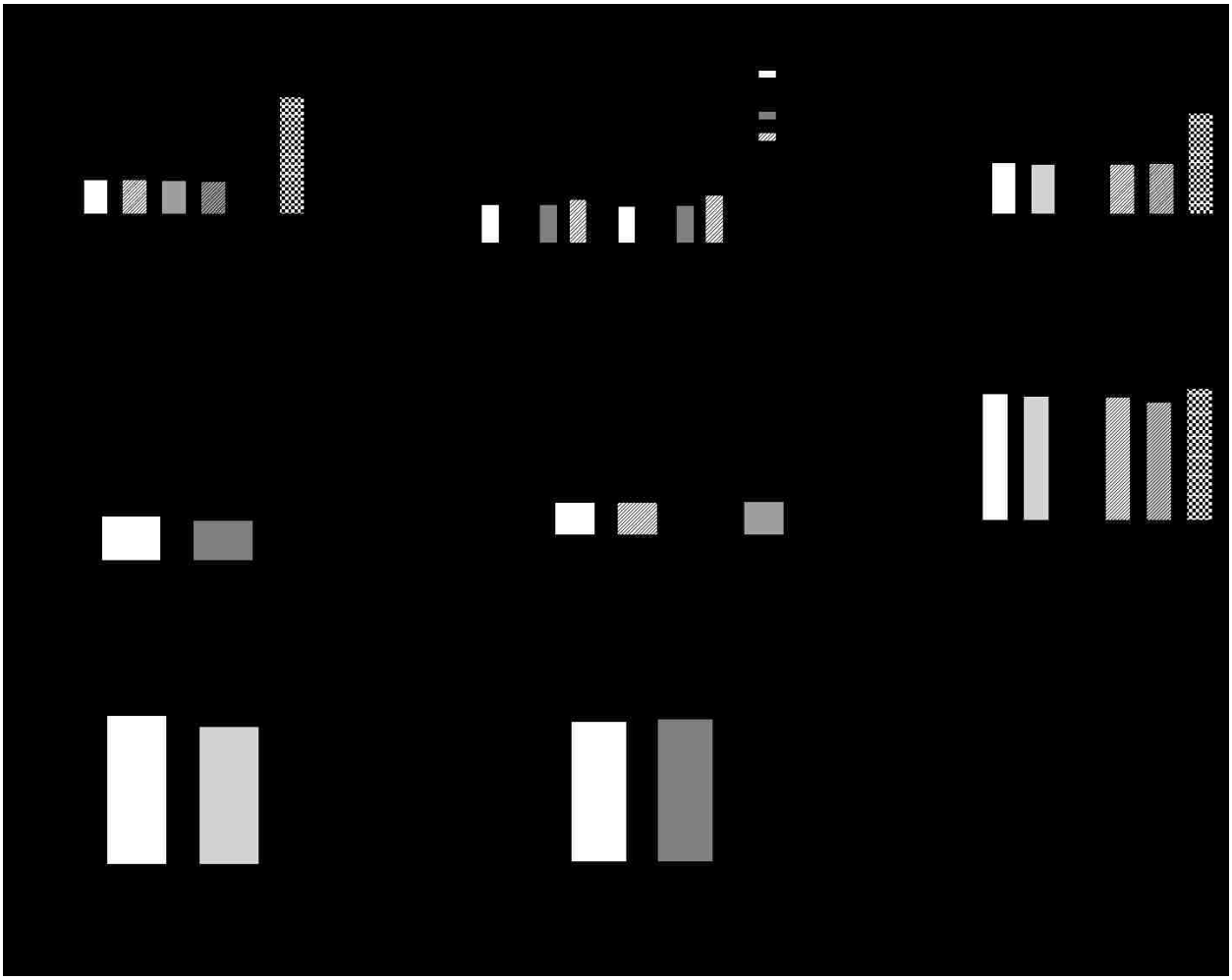

Figure 22: AKT1^{Myr}/KRasG12D mice have a reversible, fasted and non-fasted hyperglycemia.

Blood glucose levels were measured with a glucometer (A) at weaning ($p<0.0001$) and at 12 weeks ($p=0.0013$). Weaning occurred at 3 weeks of age. To determine if the hyperglycemia exhibited at weaning was reversible, breeder mice were placed on a doxycycline diet to expose the pups in utero. Blood glucose levels were then measured (B) at weaning ($p<0.0001$) and at 12 weeks ($p\leq0.0013$). Blood glucose levels, measured at weaning were also used to identify (C) sex differences. Mice were fasted overnight (16 hours) to determine fasted blood glucose levels (D) at 12 weeks ($p\leq0.0002$). Fasted blood glucose levels were also measured (E) at 12 weeks for the mice placed on a doxycycline diet ($p<0.0001$). Weight was measured (F) at weaning and (G) at 12 weeks ($p\leq0.0002$). At 12 weeks, mice were housed individually and (H) food intake was measured daily for four days by weighing the food in the cage. Two-way ANOVA followed by student's t-tests within groups were used to analyze the data for figures A-C and E-F. Unpaired student's t-test was used for figure D and G-H. N=10 for figures A-H except D and G (n=8). Abbreviations: Wks - week. Letters were used to illustrate significance as multiple groups are being compared (see materials and methods for explanation).

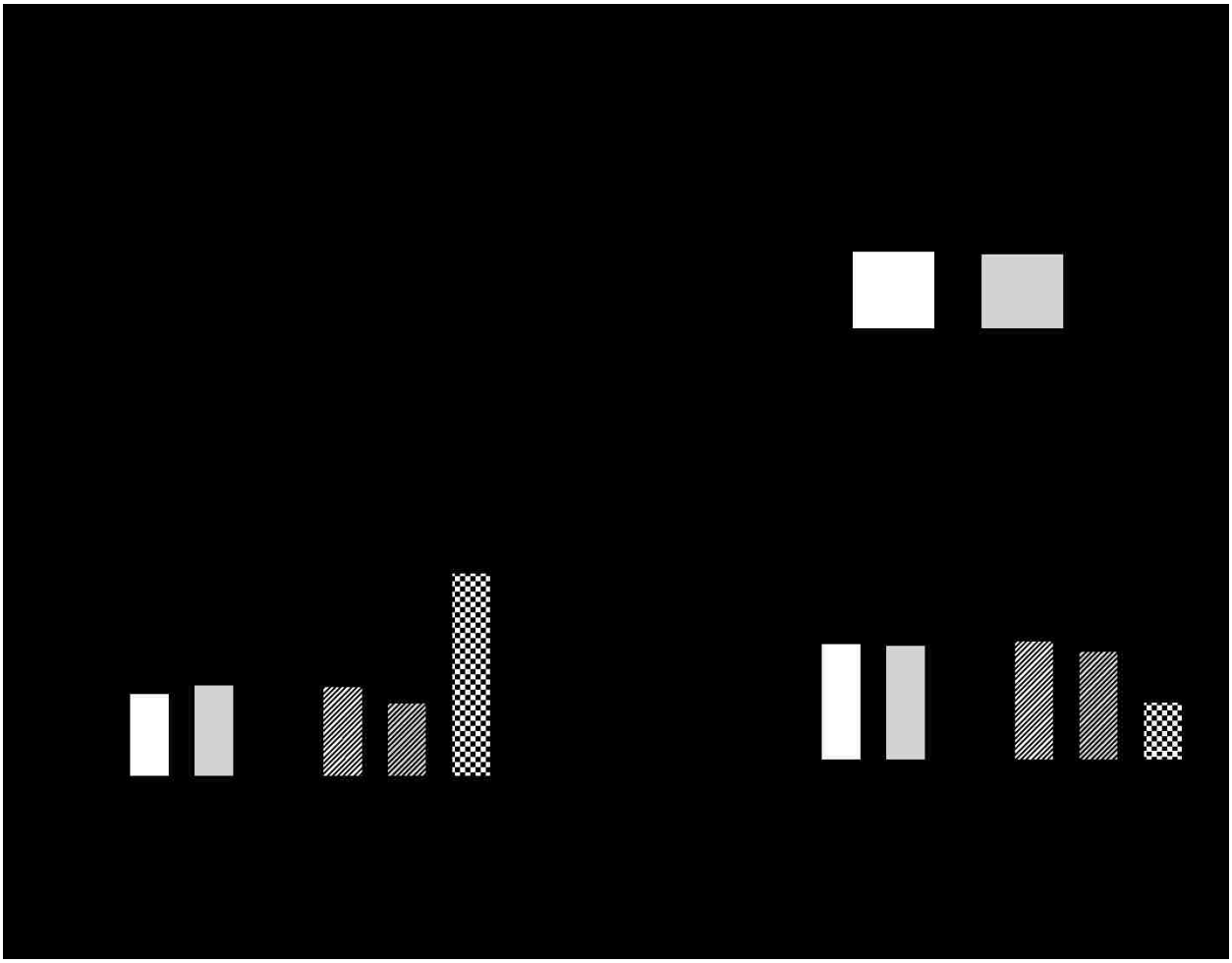

Figure 23: Glucose intolerance in AKT1^{Myr}/ KRasG12D mice due to insulin-glucagon imbalance.

Glucose tolerance testing (n=5) was performed at 12 weeks comparing: (A) wild type (WT), KRasG12D (RAS), and AKT1^{Myr}/KRasG12D (AKTRAS) mice. (B) Area under the curve. Data represented as mean ± SEM (p=0.0003). Blood was collected, via cheek bleeds, at the 0- and 45-minute time points to analyze serum (C) insulin and (D) glucagon levels using ELISAs. Insulin and glucagon values are also provided in Table 4. Unpaired student's t-tests were used to analyze differences in area under the curve. Two-way ANOVA followed by student's t-tests within groups were used to analyze the data for figures C-D. Letters were used to illustrate significance as multiple groups are being compared (see materials and methods for explanation).

Figure 24: Insulin resistance in KRas and AKT1^{Myr}/KRasG12D mice.

One week following the GTT, (B) an insulin tolerance test was performed (n=5). (A) Area under the curve. Data represented as mean ± SEM ($p<0.05$). Unpaired student's t-tests were used to analyze differences in the insulin tolerance tests time points. One-way ANOVA followed by student's t-tests within groups were used to analyze the data for figures A and C-D. Letters were used to illustrate significance as multiple groups are being compared (see materials and methods for explanation).

List of References

Albury TM, Pandey V, Gitto SB, Dominguez L, Spinel LP, Talarchek J, Klein-Szanto AJ, Testa JR, & Altomare DA 2015 Constitutive activation of Akt1 cooperates with KRasG12D to accelerate in vivo pancreatic tumor onset and progression. *Neoplasia***17** 175-183.

Aronoff SL, Berkowitz K, Shreiner B & Want L 2004 Glucose Metabolism and Regulation: Beyond Insulin and Glucagon. *Diabetes Spectrum***3** 183-190.

Bao B, Wang Z, Li Y, Kong D, Ali S, Banerjee S, Ahmad A & Sarkar FH 2011 The complexities of obesity and diabetes with the development and progression of pancreatic cancer. *Biochim Biophys Acta***1815** 135-146.

Cho H, Mu J, Kim JK, Thorvaldsen JL, Chu Q, Crenshaw EB, Kaestner KH, Bartolomei MS, Shulman GI & Birnbaum MJ 2001 Insulin resistance and a diabetes mellitus-like syndrome in mice lacking the protein kinase Akt2 (PKB beta). *Science***292** 1728-1731.

Garofalo RS, Orena SJ, Rafidi K, Torchia AJ, Stock JL, Hildebrandt AL, Coskran T, Black SC, Brees DJ, Wicks JR, et al. 2003 Severe diabetes, age-dependent loss of adipose tissue, and mild growth deficiency in mice lacking Akt2/PKB beta. *J Clin Invest***112** 197-208.

Pannala R, Basu A, Petersen GM & Chari ST 2009 New-onset diabetes: a potential clue to the early diagnosis of pancreatic cancer. *Lancet Oncol***10** 88-95.

Rahib L, Smith BD, Aizenberg R, Rosenzweig AB, Fleshman JM & Matrisian LM 2014 Projecting cancer incidence and deaths to 2030: the unexpected burden of thyroid, liver, and pancreas cancers in the United States. *Cancer Res***74** 2913-2921.

Ryan DP, Hong TS & Bardeesy N 2014 Pancreatic adenocarcinoma. *N Engl J Med***371** 1039-1049.

Wang F, Herrington M, Larsson J & Permert J 2003 The relationship between diabetes and pancreatic cancer. *Mol Cancer***2** 1-5.

CHAPTER 5: CONCLUSION

Merriam Webster's dictionary defines communication as, "the act or process of using words, sounds, signs, or behaviors to express or exchange information." It is important for the body, which works as a system to be able to "communicate" with its various parts, whether organ to organ or cell to cell. One way in which cells communicate is signal transduction, "a complex system of communication that allows external stimuli to alter molecular activities within a cell." This ability of cells to perceive changes in their microenvironment and correctly respond is vital for maintaining homeostasis, and errors in this communication system can lead to disease. Protein Kinase B, a serine threonine kinase in the phosphatidylinositol 3-kinase (PI3K) signaling pathway, is an important cell signaling protein, making its abnormal loss or gain of function the epicenter of a variety of diseases, including cancer and diabetes mellitus (Manning & Cantley 2007). The results described in this manuscript present previously unrecognized roles of AKT1 hyperactivation in the pathophysiology of pancreatic cancer and diabetes mellitus.

The hyperactivation of AKT has been conclusively linked to the development of various human cancers, including pancreatic ductal adenocarcinoma (PDAC). PDAC is the most lethal common cancer largely due to late diagnosis. At diagnosis, which is typically 71 years of age, 85% of PDAC patients are inoperable due to local and distant metastasis. Drug treatments are typically ineffective at this advanced stage and the average survival rate is four to six months, making early diagnosis a key therapeutic strategy. While it is known that activation mutations of Ras, present in 90% of PDACs, leads to AKT activation and loss of tumor suppressors (e.g., p16 and p19), further studies into the genetic changes that occur in early PanINs may provide an opportunity for early diagnosis and ultimately an increased survival rate (Ryan et al. 2014). .

However, the unavailability of early-stage tissue from patients has hampered the search for such genetic biomarkers, and made the use of pancreatic cancer mouse models of upmost importance.

By mating transgenic mice with activation of KRas (Pdx- Cre;LSL-KrasG12D) and mice with activation of AKT1 (Pdx- Tta;TetO-MyrAKT1) we were able to produce a PDAC mouse model with two activated oncogenes ($AKT1^{Myr}$/KRasG12D). Our objective was to characterize the incidence and frequency of histological and genetic alterations known to commonly occur in human pancreatic cancer, as well as delineate the role of AKT1 in pancreatic tumor progression and metastasis. We determined that AKT1 served as an accelerator increasing the frequency and incidence of PDACs in AKTRAS mice when compared to KRasG12D (RAS) mice. We also determined that $AKT1^{Myr}$/KRasG12D mice (AKTRAS), unlike other PDAC mouse models, accurately mimic the human PDAC progression molecularly (e.g., activation of PI3K/AKT pathway and loss of p16Ink4a and p19Arf), structurally (e.g., positive for tissue remodeling marker mucin-4 and fibrosis marker α-SMA), and most importantly temporally. Other PDAC models (mice with KRasG12D activation and Pten homozygous deletion) have rapid tumor development with mice dying at 3 weeks, while our model has a slower progression of about 54 weeks. This better mimics the human PDAC progression as the average time frame for progression from PanINs to PDAC is about 17 years. Ultimately, we were able to combine two oncogenic changes important for cancer progression to accelerate tumorigenesis, while maintaining a time frame that would align more closely with the physiological progression observed in the human disease. This will allow us to conduct therapeutic studies that can block tumor progression at the PanIN or early carcinoma stage, before there is excessive tissue damage.

Understanding that the hyperactivation of AKT1 is linked to PDAC and that 80% of PDAC patients suffer from hyperglycemia or diabetes prior to diagnosis, our next objective was to determine how AKT1 hyperactivation affects glucose homeostasis. We characterized the early onset, prediabetic phenotype observed in $AKT1^{Myr}$ mice and highlighted a novel mechanism by which AKT1 hyperactivation affects glucose homeostasis. Beginning at weaning, 3 weeks of age, the glucose intolerant $AKT1^{Myr}$ mice exhibited non-fasted hyperglycemia, which progressed to fasted hyperglycemia by 5 months of age. The glucose intolerance was attributed to a fasted hyperglucagonemia. Although the mechanisms behind hyperglucagonemia are still relatively unclear, we are proposing that $AKT1^{Myr}$ mice, with fasted hyperglucagonemia, have impaired GSIS, resulting in glucose intolerance despite increased compensatory insulin secretion. Hepatic insulin resistance, an additional factor, may exacerbate the problem, preventing normoglycemia via increased hepatic glucose production and decreased hepatic glucose storage.

$AKT1^{Myr}$/KRasG12D mice, which are currently being studied, appear to display a more severe diabetic phenotype, with fasted hyperglycemia noticeable at an earlier age (12 weeks), fasted hyperglucagonemia, polyuria, muscle wasting, and bloating. So, similar to the oncogenesis study, AKT1 hyperactivation appears to serve as an accelerator, increasing the severity while decreasing the average time required for disease progression. Treatment of both models with doxycycline diet, to turn-off the transgene, caused attenuation of the non-fasted and fasted hyperglycemia, thus affirming AKT1 hyperactivation as the trigger.

Over the last 30 years PDAC incidence has been relatively stable (1 to 10 per 100,000 people). However, population changes, primarily the aging of 76.4 million baby boomers, are expected to thrust pancreatic cancer from the ninth to the second leading cause of cancer-related

deaths within the next 15 years. These newly revealed effects of AKT1 hyperactivation, along with future studies of these mouse models, will help to better delineate the molecular mechanisms responsible for the individual and joint roles of AKT1 and KRas in pancreatic cancer oncogenesis, the initiation of cancer associated diabetes, and the association of these two diseases. By thoroughly studying our AKT1^{Myr}/KRasG12D mouse model we can identify key pre-tumor molecular events that induce metabolic changes, distinguish PDAC associated diabetes from T2D, and identify an early biomarker. This will ultimately lead to earlier pre-metastatic detection, effective drug treatment, and increased PDAC survival.

APPENDIX A: COPY RIGHT PERMISSION

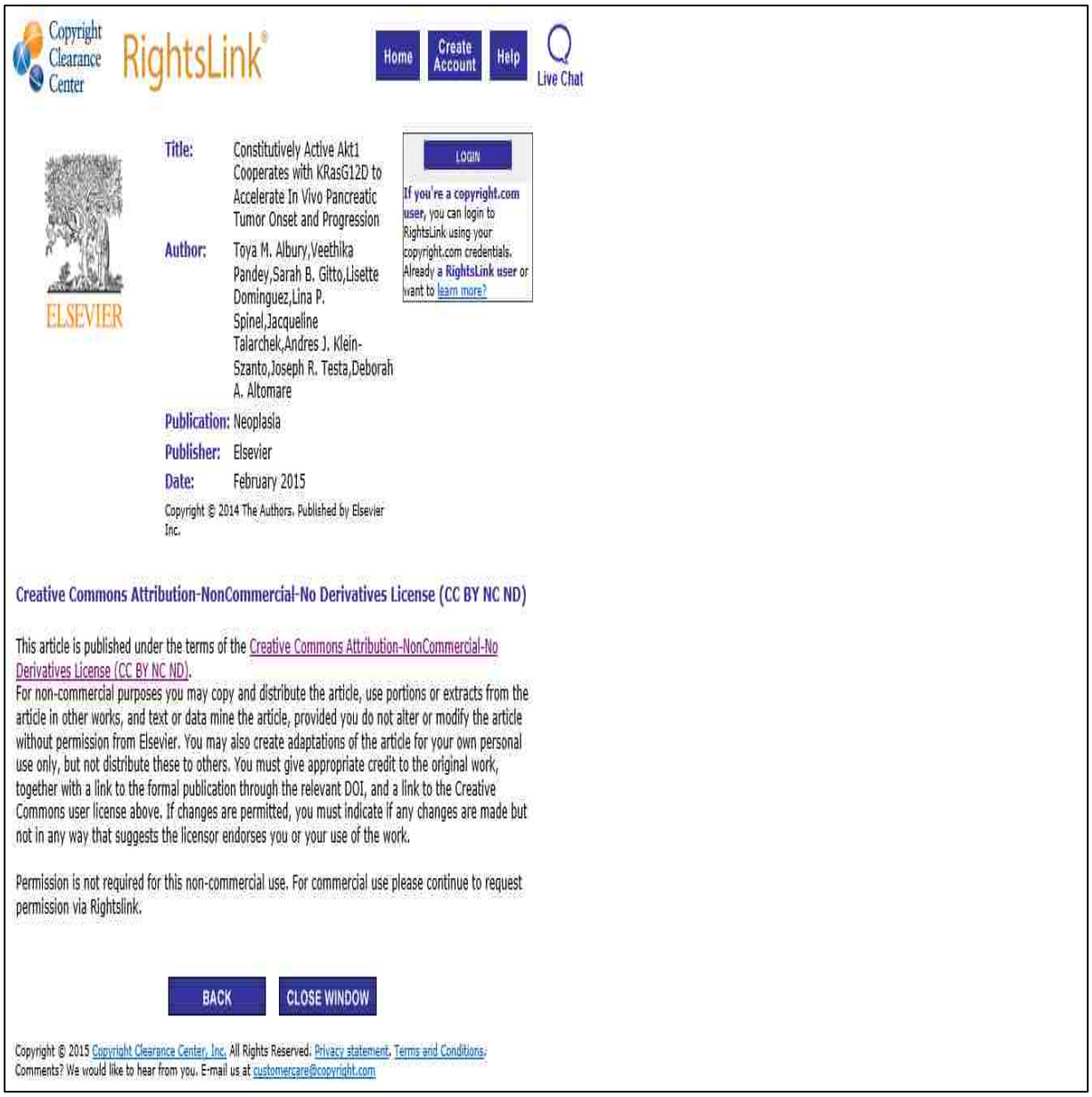

Copyright Clearance Center RightsLink

Home | Create Account | Help | Live Chat

ELSEVIER

Title: Constitutively Active Akt1 Cooperates with KRasG12D to Accelerate In Vivo Pancreatic Tumor Onset and Progression

Author: Toya M. Albury,Veethika Pandey,Sarah B. Gitto,Lisette Dominguez,Lina P. Spinel,Jacqueline Talarchek,Andres J. Klein-Szanto,Joseph R. Testa,Deborah A. Altomare

Publication: Neoplasia

Publisher: Elsevier

Date: February 2015

Copyright © 2014 The Authors. Published by Elsevier Inc.

LOGIN

If you're a copyright.com user, you can login to RightsLink using your copyright.com credentials. Already a RightsLink user or want to learn more?

Creative Commons Attribution-NonCommercial-No Derivatives License (CC BY NC ND)

This article is published under the terms of the Creative Commons Attribution-NonCommercial-No Derivatives License (CC BY NC ND).
For non-commercial purposes you may copy and distribute the article, use portions or extracts from the article in other works, and text or data mine the article, provided you do not alter or modify the article without permission from Elsevier. You may also create adaptations of the article for your own personal use only, but not distribute these to others. You must give appropriate credit to the original work, together with a link to the formal publication through the relevant DOI, and a link to the Creative Commons user license above. If changes are permitted, you must indicate if any changes are made but not in any way that suggests the licensor endorses you or your use of the work.

Permission is not required for this non-commercial use. For commercial use please continue to request permission via Rightslink.

BACK | CLOSE WINDOW

Copyright © 2015 Copyright Clearance Center, Inc. All Rights Reserved. Privacy statement. Terms and Conditions.
Comments? We would like to hear from you. E-mail us at customercare@copyright.com

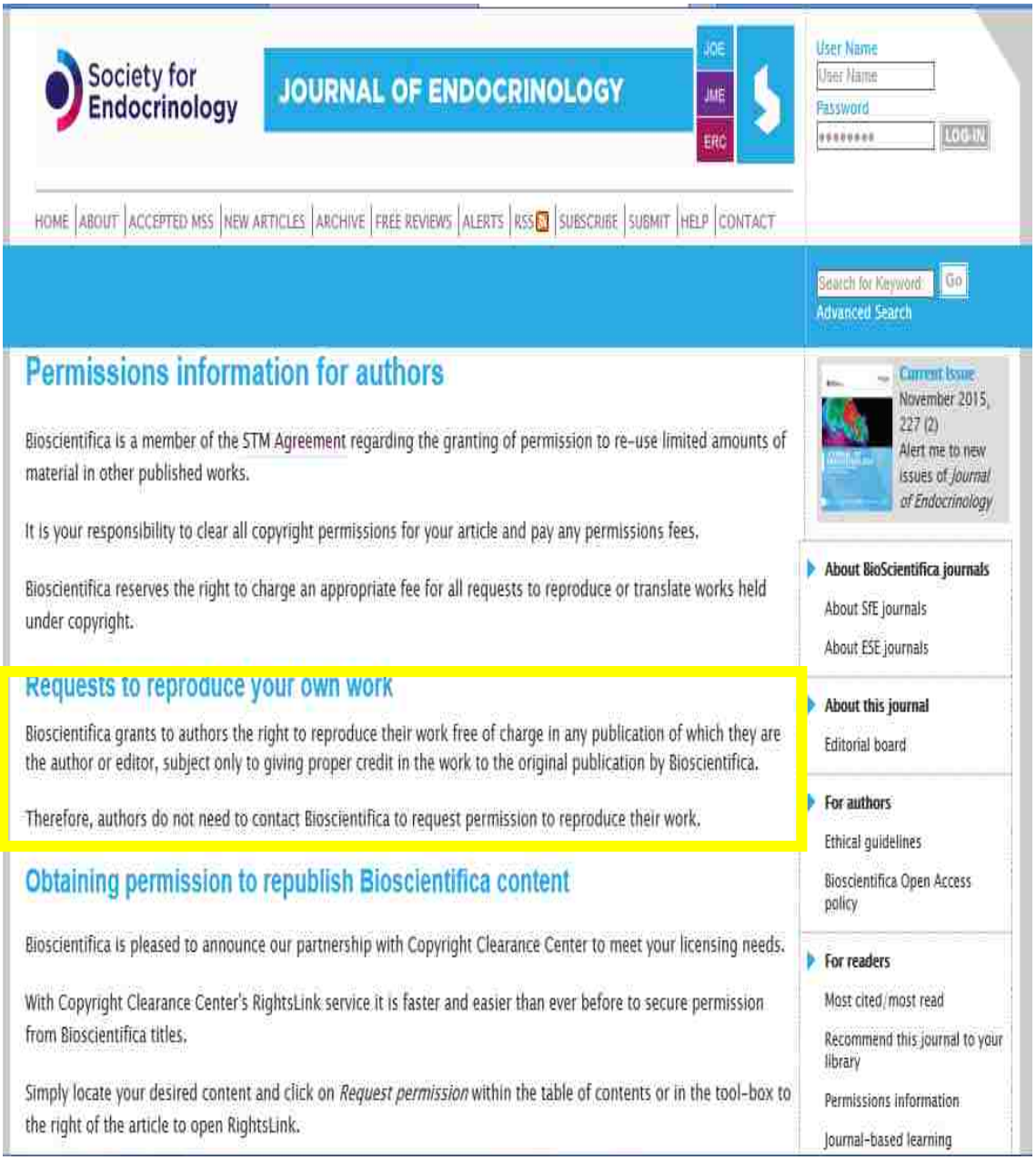
Society for Endocrinology
JOURNAL OF ENDOCRINOLOGY
JOE
JME
ERC
User Name
Password
LOG-IN
HOME | ABOUT | ACCEPTED MSS | NEW ARTICLES | ARCHIVE | FREE REVIEWS | ALERTS | RSS | SUBSCRIBE | SUBMIT | HELP | CONTACT
Search for Keyword
Go
Advanced Search
Permissions information for authors
Bioscientifica is a member of the STM Agreement regarding the granting of permission to re-use limited amounts of material in other published works.
It is your responsibility to clear all copyright permissions for your article and pay any permissions fees.
Bioscientifica reserves the right to charge an appropriate fee for all requests to reproduce or translate works held under copyright.
Requests to reproduce your own work
Bioscientifica grants to authors the right to reproduce their work free of charge in any publication of which they are the author or editor, subject only to giving proper credit in the work to the original publication by Bioscientifica.
Therefore, authors do not need to contact Bioscientifica to request permission to reproduce their work.
Obtaining permission to republish Bioscientifica content
Bioscientifica is pleased to announce our partnership with Copyright Clearance Center to meet your licensing needs.
With Copyright Clearance Center's RightsLink service it is faster and easier than ever before to secure permission from Bioscientifica titles.
Simply locate your desired content and click on Request permission within the table of contents or in the tool-box to the right of the article to open RightsLink.
Current Issue
November 2015, 227 (2)
Alert me to new issues of Journal of Endocrinology
About BioScientifica journals
About SfE journals
About ESE journals
About this journal
Editorial board
For authors
Ethical guidelines
Bioscientifica Open Access policy
For readers
Most cited/most read
Recommend this journal to your library
Permissions information
Journal-based learning

Brown, Carol <brown@cshl.edu>

Mon 10/19/2015 4:27 PM

To:alburyt83 <alburyt83@knights.ucf.edu>;

Permission is granted for the use of Figs 1&2 in the article detailed below in your PhD thesis only. Please cite this article as Cold Spring Harb Perspect Biol 2012;4:a011189, with copyright to Cold Spring Harbor Laboratory Press.

Best wishes for success with your thesis,

Carol C. Brown
Books Development, Marketing and Sales
Cold Spring Harbor Laboratory Press
500 Sunnyside Blvd
Woodbury, New York 11797
516 422 4038 ph.
516 422 4095 fx.
brown@cshl.edu

Permission letter for figures 1 and 2.

NATURE PUBLISHING GROUP LICENSE
TERMS AND CONDITIONS

Oct 18, 2015

This is a License Agreement between Toya Albury ("You") and Nature Publishing Group ("Nature Publishing Group") provided by Copyright Clearance Center ("CCC"). The license consists of your order details, the terms and conditions provided by Nature Publishing Group, and the payment terms and conditions.

All payments must be made in full to CCC. For payment instructions, please see information listed at the bottom of this form.

License Number	3732240779094
License date	Oct 18, 2015
Licensed content publisher	Nature Publishing Group
Licensed content publication	Oncogene
Licensed content title	AKT crystal structure and AKT-specific inhibitors
Licensed content author	Chandra C Kumar and Vincent Madison
Licensed content date	Nov 14, 2005
Volume number	24
Issue number	50
Type of Use	reuse in a dissertation / thesis
Requestor type	academic/educational
Format	print and electronic
Portion	figures/tables/illustrations
Number of figures/tables/illustrations	1
High-res required	no
Figures	Table 1 - Pairwise % identity in AKT domains
Author of this NPG article	no
Your reference number	None
Title of your thesis / dissertation	DIABETES PHENOTYPES IN TRANSGENIC PANCREATIC CANCER MOUSE MODELS
Expected completion date	Nov 2015
Estimated size (number of	125

Permission letter for figure 3.

NATURE PUBLISHING GROUP LICENSE
TERMS AND CONDITIONS

Oct 28, 2015

This is a License Agreement between Toya Albury ("You") and Nature Publishing Group ("Nature Publishing Group") provided by Copyright Clearance Center ("CCC"). The license consists of your order details, the terms and conditions provided by Nature Publishing Group, and the payment terms and conditions.

All payments must be made in full to CCC. For payment instructions, please see information listed at the bottom of this form.

License Number	3733170288832
License date	Oct 20, 2015
Licensed content publisher	Nature Publishing Group
Licensed content publication	Oncogene
Licensed content title	Perturbations of the AKT signaling pathway in human cancer
Licensed content author	Deborah A Altomare and Joseph R Testa
Licensed content date	Nov 14, 2005
Volume number	24
Issue number	50
Type of Use	reuse in a dissertation / thesis
Requestor type	academic/educational
Format	print and electronic
Portion	figures/tables/illustrations
Number of figures/tables/illustrations	1
High-res required	no
Figures	Table 1 AKT activation in human cancers
Author of this NPG article	no

Permission letter for figure 5

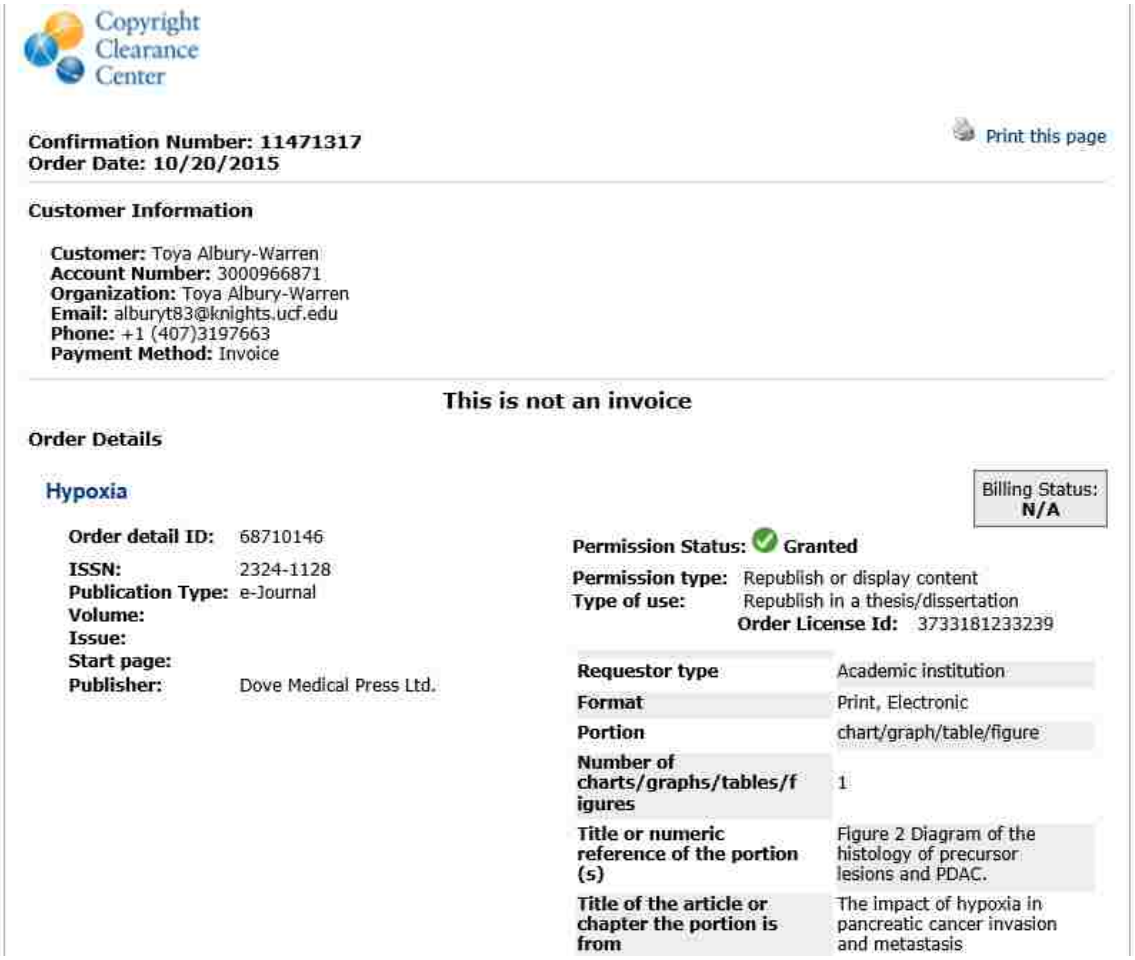

Copyright Clearance Center

Print this page

Confirmation Number: 11471317
Order Date: 10/20/2015

Customer Information

Customer: Toya Albury-Warren
Account Number: 3000966871
Organization: Toya Albury-Warren
Email: alburyt83@knights.ucf.edu
Phone: +1 (407)3197663
Payment Method: Invoice

This is not an invoice

Order Details

Hypoxia

Billing Status: **N/A**

Order detail ID: 68710146
ISSN: 2324-1128
Publication Type: e-Journal
Volume:
Issue:
Start page:
Publisher: Dove Medical Press Ltd.

Permission Status: Granted
Permission type: Republish or display content
Type of use: Republish in a thesis/dissertation
Order License Id: 3733181233239

Requestor type	Academic institution
Format	Print, Electronic
Portion	chart/graph/table/figure
Number of charts/graphs/tables/figures	1
Title or numeric reference of the portion (s)	Figure 2 Diagram of the histology of precursor lesions and PDAC.
Title of the article or chapter the portion is from	The impact of hypoxia in pancreatic cancer invasion and metastasis

Permission letter for figure 6

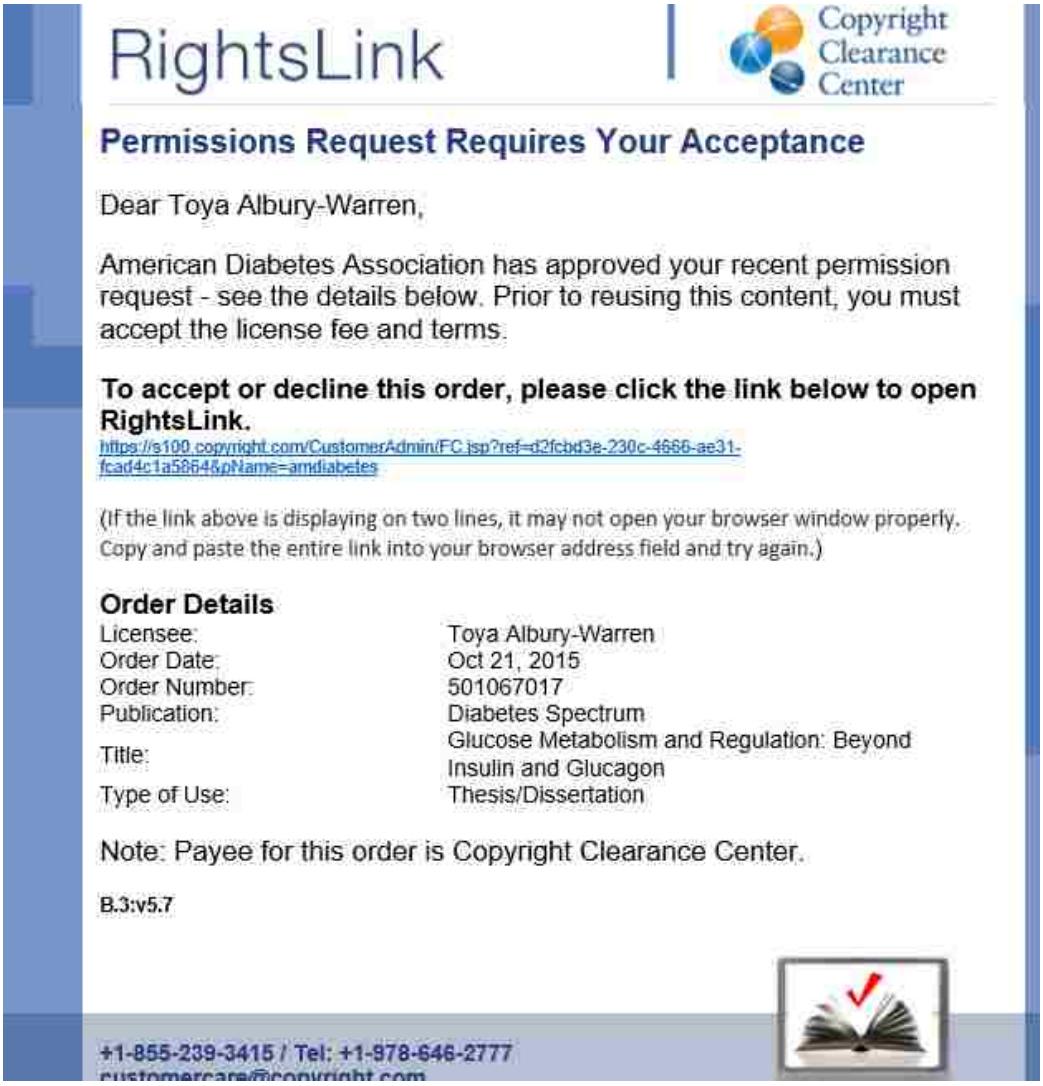

RightsLink | Copyright Clearance Center

Permissions Request Requires Your Acceptance

Dear Toya Albury-Warren,

American Diabetes Association has approved your recent permission request - see the details below. Prior to reusing this content, you must accept the license fee and terms.

To accept or decline this order, please click the link below to open RightsLink.

https://s100.copyright.com/CustomerAdmin/FC.jsp?ref=d2fcbd3e-230c-4666-ae31-fcad4c1a5864&pName=amdiabetes

(If the link above is displaying on two lines, it may not open your browser window properly. Copy and paste the entire link into your browser address field and try again.)

Order Details

Licensee:	Toya Albury-Warren
Order Date:	Oct 21, 2015
Order Number:	501067017
Publication:	Diabetes Spectrum
Title:	Glucose Metabolism and Regulation: Beyond Insulin and Glucagon
Type of Use:	Thesis/Dissertation

Note: Payee for this order is Copyright Clearance Center.

B.3:v5.7

+1-855-239-3415 / Tel: +1-978-646-2777

Permission letter for figure 7.

APPENDIX B: IACUC APPROVAL LETTERS

University of Central Florida

Office of Research & Commercialization

12/21/2012

Dr Deborah Altomare
Burnett School of Biomedical Sciences
Lake Nona
6900 Lake Nona Blvd
Orlando, FL 32827

Subject: Institutional Animal Care and Use Committee (IACUC) Protocol Submission

Dear Dr Deborah Altomare:

This letter is to inform you that your following animal protocol was approved by the IACUC. The IACUC Use Approval Form is attached for your records.

Animal Project #:	12-51
Title:	AKT Function in Pancreatic Tumor Cell Invasiveness and In Vivo Pathogenesis.
First Approval Date:	12/21/2012

Please be advised that IACUC approvals are limited to one year maximum. Should there be any technical or administrative changes to the approved protocol, they must be submitted in writing to the IACUC for approval. Changes should not be initiated until written IACUC approval is received. Adverse events should be reported to the IACUC as they occur. Furthermore, should there be a need to extend this protocol, a renewal must be submitted for approval at least three months prior to the anniversary date of the most recent approval. If the protocol is over three years old, it must be rewritten and submitted for IACUC review.

Should you have any questions, please do not hesitate to call me at (407) 882-1164.

Please accept our best wishes for the success of your endeavors.

Best Regards,

University of Central Florida

Office of Research & Commercialization

September 9, 2013

Dr. Deborah Altomare
Burnett School of Biomedical Sciences
6900 Lake Nona Blvd.
Orlando, FL 32827

Subject: Institutional Animal Care Use Committee (IACUC) Addendum Submission.

Dear Dr. Altomare,

This letter is to inform you that the following addendum submitted was approved by the IACUC.

Animal Project:	12-51
Title:	AKT Function in Pancreatic Tumor Cell Invasiveness and In Vivo Pathogenesis. (Addendum #1)
Approval Date:	9/7/2013

Please see the attached copy of the approved addendum and please keep a copy for your records. Should you have any questions, please do not hesitate to call me at (407) 822-1164.

Sincerely,

Cristina Caamaño
Assistant Director, Research Program Services

University of Central Florida

Office of Research & Commercialization

April 24th, 2014

Dr. Deborah Altomare
Burnett School of Biomedical Sciences
6900 Lake Nona Blvd.
Orlando, FL 32827

Subject: Institutional Animal Care Use Committee (IACUC) Addendum Submission.

Dear Dr. Altomare,

This letter is to inform you that the following addendum submitted was approved by the IACUC.

Animal Project:	12-51
Title:	AKT Function in Pancreatic Tumor Cell Invasiveness and In Vivo Pathogenesis. (Addendum #2)
Approval Date:	04/23/2014

Please see the attached copy of the approved addendum and please keep a copy for your records. Should you have any questions, please do not hesitate to call me at (407) 822-1164.

Sincerely,

Cristina Caamaño

Cristina Caamaño
Associate Director, Research Program Services